

Cooperative Resource Allocation in Wireless Communication Networks

Vom Fachbereich 18
Elektrotechnik und Informationstechnik
der Technischen Universität Darmstadt
zur Erlangung der Würde eines
Doktor-Ingenieurs (Dr.-Ing.)
genehmigte Dissertation

von
M.Sc. Oscar Dario Ramos Cantor
geboren am 15.05.1986 in Ibagué - Kolumbien

Referent:	Prof. Dr.-Ing. Marius Pesavento
Korreferent:	Prof. Dr.-Ing. Constantinos B. Papadias
Tag der Einreichung:	09.05.2017
Tag der mündlichen Prüfung:	18.07.2017

D 17
Darmstädter Dissertation
2017

*To my uncle,
my mother
and the rest of my family*

Acknowledgments

I would like to sincerely thank Prof. Marius Pesavento and Dr. Gerhard Kadel, from Technische Universität Darmstadt and Deutsche Telekom AG, respectively, for believing in the benefits of the close cooperation between academia and industry. Their constant support made this work possible.

I would like to acknowledge the cooperation and support of the simulation team from the Technology Innovation Division (Deutsche Telekom AG) in developing and providing the system-level simulator, whose functionality has been extended in the realization of this work.

I also would like to thank all my colleagues at both, the Communication Systems Group (TU Darmstadt) and the Wireless Technologies and Innovation Division (former Telekom Innovation Laboratories), for the valuable discussions and lessons throughout the realization of this thesis. I have not only improved my technical skills, but I have had also the chance to come to know new cultures and to broaden my perspectives about life.

Furthermore, thanks to Marlis Gorecki and Heike Kaffenberger for all their support on the administrative related issues. You have been always attentive and ready to give any guidance when needed.

Finally, I would like to thank my family and friends for all their love, patience and support. To make you proud is my main motivation to work hard towards the achievement of my goals.

Kurzfassung

Das Konzept der Kooperation, in dem zwei oder mehr Parteien zusammenarbeiten, um ein gemeinsames Ziel zu verfolgen, ist auf fast jeden Aspekt des heutigen Lebens anwendbar. Zum Beispiel, in der kommenden Fahrzeug-zu-Fahrzeug (eng. *car-to-car*) Kommunikation Szenarien tauschen die Fahrzeuge Informationen über ihren aktuellen Status sowie potenzielle Bedrohungen auf der Straße aus, um Unfälle zu vermeiden. Mit der Entwicklung drahtloser Kommunikationssysteme, dem Aufkommen neuer Dienste sowie Geräten mit zusätzlichen Fähigkeiten steigt die Nachfrage nach höheren Datenraten an.

In zellularen Mobilfunknetzen werden die erreichbaren Datenraten der Nutzer beschränkt durch die Inter-Zell-Interferenz, welche durch die gleichzeitige Nutzung von Zeit/Frequenz Ressourcen verursacht wird. Besonders die Datenraten derjenigen Nutzer werden beschränkt, die sich in der näheren Umgebung anderer Basisstationen befinden. Das ist der Ausgangspunkt dieser Arbeit, in der die Kooperation in zellularen Mobilfunknetzen für die Datenübertragung von Basis- zu Mobilstationen untersucht wird, insbesondere, um den Einfluss der Gleichkanal-Inter-Zell-Interferenz zu reduzieren, wodurch der ständig ansteigende Nutzerbedarf erfüllt werden kann. Kooperative Ressourcen-Zuteilungsverfahren werden hergeleitet, wobei praktische Gegebenheiten und Einschränkungen bezüglich der verfügbaren Kanalinformation an den Basisstationen berücksichtigt werden.

Hauptsächlich wird dabei die Kooperation in der Form der Sendeleistungskontrolle und der gemeinsamen Zeit-/Frequenzplanung untersucht. In der ersten Art der Kooperation regeln die Basisstationen dynamisch ihre eigene Sendeleistung, um weniger Inter-Zell-Interferenz für Nutzer, die mit Nachbarbasisstationen verbunden sind, zu erzeugen. Im Fall der kooperativen Ressourcenzuweisung werden die Zeit-/Frequenzressourcen durch die Basisstationen gemeinsam zugeteilt um einen Kompromiss zwischen erreichbaren Nutzerdatenraten und Inter-Zell-Interferenzen zu erreichen. Die kooperativen Ressourcenzuweisungsverfahren wenden zwei Sonderfälle des Leistungskontrollverfahrens an. Hierbei bedienen die Basisstationen entweder ihre verbundenen Nutzer mit maximaler Sendeleistung, oder eine Datenübertragung wird unterdrückt (engl. *muting*), um die Interferenz für Nutzer, die durch benachbarte Basisstationen bedient werden, zu reduzieren. Ein Hauptbeitrag dieser Arbeit ist die mathematische Formulierung der kooperativen Ressourcenzuteilungsprobleme unter Zuhilfenahme der verfügbaren Kanalinformation am Sender, in Form von Kontrollinformationen über die erreichbaren Datenraten, welche auf den Standardprozeduren der aktuellen Mobilfunkstandards wie LTE und LTE-Advanced basieren.

Aus einer Systemperspektive werden in dieser Dissertation zwei Parameter betrachtet, um die vorgeschlagenen kooperativen Verfahren abzuleiten. Diese Parameter sind die Kooperationsarchitektur und das Verkehrsmodell zur Charakterisierung des Nutzerbedarfs. Im Falle der Kooperationsarchitektur werden zentralisierte und dezentralisierte Verfahren untersucht. In ersterer führt ein zentraler Controller die kooperativen Verfahren, basierend auf der Kenntnis der globalen Kanalinformation, aus und in

letzterer werden die kooperativen Entscheidungen von den Basisstationen unabhängig gefällt, basierend auf lokalen Informationen, die mit den angrenzenden Basisstationen ausgetauscht werden. Es wird erwartet, dass eine zentralisierte Architektur die beste Leistungsfähigkeit bereitstellt, trotzdem reduziert sich der Unterschied signifikant in Bezug auf dezentralisierte Verfahren bei Berücksichtigung von Annahmen über praktische Netze, wie in dieser Arbeit basierend auf numerischen Simulationen gezeigt wird. Dabei wird der Nutzerbedarf durch Modelle mit voller und teilweiser Auslastung des Netzes charakterisiert. Das erste Modell wird angewandt, um die Leistungsfähigkeit des vorgeschlagenen kooperativen Verfahrens aus Netzwerkkapazitätsperspektive einzuschätzen, wobei alle Nutzer gleichbleibend so viele Daten wie möglich anfordern. Im Gegensatz dazu repräsentieren die Modelle mit teilweiser, dynamischer Auslastung des Netzes ein eher realistisches Netzwerkszenario. Hier werden Verfahren abgeleitet, um die Linkanpassungsprozeduren durch die Basisstationen zu verbessern, die Nutzer mit ungleichmäßigem (engl. *bursty*) Verkehr bedienen. Die Linkanpassungsprozeduren konfigurieren die Übertragungsparameter pro bedientem Link, z. B. die Sendeleistung, die Modulationsverfahren und die Kodierungsverfahren.

Im Detail wird ein kooperatives Leistungskontrollverfahren mit einer geschlossenen Form hergeleitet, wobei die Basisstationen ihre eigene Sendeleistung dynamisch anpassen, um die geforderten Datenraten der Nutzer, die mit den Nachbar-Basisstationen verbunden sind, zu erreichen. Außerdem wird zur Erhöhung der Datenraten der Nutzer eine zentralisierte und eine dezentralisierte koordinierte Ressourcenzuweisung inklusive möglicher Unterdrückung der Übertragung untersucht. Für den zentralisierten Fall wird die Formulierung eines ganzzahlig linearen Optimierungsproblems vorgeschlagen, welches durch die Benutzung kommerzieller Löser optimal gelöst wird. Die optimale Lösung wird als Maßstab zur Bewertung heuristischer Algorithmen genutzt. Im Fall der dezentralisierten koordinierten Planung mit möglicher Unterdrückung der Übertragung wird ein heuristisches Verfahren hergeleitet, welches nur einen geringen Nachrichtenaustausch zwischen den Basisstationen benötigt, um die Kooperation zu koordinieren. Weiterhin wird ein ganzzahliges lineares Optimierungsproblem formuliert, um die Linkanpassungsprozeduren für Netzwerke mit dynamischem Verkehr zu verbessern. Das Ergebnis ist eine Reduzierung der fehlerhaft übertragenen Datenblöcke und ein Anstieg der von den Nutzern erfahrenen Datenraten. Im Vergleich zu unkoordinierten Systemen und Koordinationsverfahren nach dem Stand der Technik werden unter Anwendung des vorgeschlagenen kooperativen Verfahrens signifikante Verbesserungen der erreichbaren Datenraten der Nutzer erzielt, insbesondere für die Nutzer, die schwerwiegender Inter-Zell-Interferenz ausgesetzt sind.

Abstract

The concept of cooperation where two or more parties work together to pursue a common goal, is applicable in almost every aspect of today's life. For instance, in the upcoming car-to-car communications, the vehicles exchange information regarding their current status and potential threats on the road in order to avoid accidents. With the evolution of the wireless communication systems and the advent of new services and devices with more capabilities, the demand for higher data rates is ever increasing.

In cellular networks, the achievable data rates of the users are limited by the inter-cell interference, which is caused by the simultaneous utilization of the time/frequency resources. Especially, the data rates of the users located at the vicinity of neighboring base stations is affected by the inter-cell interference. Hence, in this dissertation, cooperation in cellular communication downlink networks is investigated, where the base stations coordinate their operation in order to mitigate the impact of co-channel inter-cell interference. Thus, the constantly increasing user demand can be satisfied. Cooperative resource allocation schemes are derived, where practical conditions and side constraints regarding the available channel state information at the base stations are taken into account.

Cooperation in the form of power control and joint time/frequency scheduling is mainly studied. In the former type of cooperation, the base stations dynamically adjust their own transmit powers to cause less inter-cell interference to the users connected to neighboring base stations. In the case of cooperative scheduling, the available time/frequency resources are jointly allocated by the base stations in order to trade off user throughput and inter-cell interference. The cooperative scheduling schemes apply two special cases of the power control approach, where the base stations either serve their connected users with maximum transmit power, or abstain from transmitting data, i.e., muting, in order to reduce the interference caused to users served by neighboring base stations. One major contribution of this work is the formulation of the cooperative resource allocation problems by considering the availability of channel state information at the transmitter in form of data rate measurement reports, which follows standard compliant procedures of current mobile networks such as LTE and LTE-Advanced.

From a system perspective, two parameters are considered throughout this dissertation in order to derive the proposed cooperative schemes. These parameters are the cooperation architecture and the traffic model characterizing the demand of the connected users. In the case of the cooperation architecture, centralized and decentralized schemes are studied. In the former, a central controller performs the cooperative schemes based on global knowledge of the channel state information, and in the latter, the cooperative decisions are carried out independently per base station based on local information exchanged with adjacent base stations. It is expected that the centralized architecture provides the best performance, however, the gap with respect to the decentralized approaches reduces significantly under practical network assumptions, as demonstrated

in this work based on numerical simulations. With respect to the traffic model, the user demand is characterized by full-buffer and non-full-buffer models. The first model is applied in order to assess the performance of the proposed cooperative schemes from a capacity enhancement perspective, where all users constantly demand as much data as possible. On the other hand, the non-full-buffer model represents a more practical network scenario with a dynamic utilization of the network resources. In the non-full-buffer model case, the proposed schemes are derived in order to improve the link adaptation procedures at the base stations serving users with bursty traffic. These link adaptation procedures, establish the transmission parameters used per serving link, e.g., the transmit power, the modulation and the coding schemes.

Specifically, a cooperative power control scheme with closed-form solution is derived, where base stations dynamically control their own transmit powers to satisfy the data rate requirements of the users connected to neighboring base stations. Moreover, centralized and decentralized coordinated scheduling with muting is studied to improve the user throughput. For the centralized case, an integer linear problem formulation is proposed which is solved optimally by using commercial solvers. The optimal solution is used as a benchmark to evaluate heuristic algorithms. In the case of decentralized coordinated scheduling with muting, a heuristic approach is derived which requires a low number of messages exchanged between the base stations in order to coordinate the cooperation. Finally, an integer linear problem is formulated to improve the link adaptation procedures of networks with user demand characterized by bursty traffic. This improvement results in a reduction of the transmission error rates and an increase of the experienced data rates. With respect to non-cooperative approaches and state-of-the-art solutions, significant performance improvement of the achievable user throughput is obtained as the result of applying the proposed cooperative schemes, especially for the users experiencing severe inter-cell interference.

Contents

1	Introduction	1
1.1	Aims, Contributions and Overview	3
2	Theoretical Background	5
2.1	LTE-Advanced Networks	5
2.1.1	Network deployments	6
2.1.2	Physical resources	7
2.1.3	CSI estimation and reporting	9
2.2	Interference Management Schemes	12
2.2.1	ICIC and enhanced-ICIC	13
2.2.2	CoMP transmission	14
2.3	Integer Linear Programming	17
2.4	System-Level Simulations	17
3	Mobile Communication Networks	19
3.1	CSI Reports for non-Cooperative and Cooperative Schemes	22
3.2	Scheduling Strategy	24
4	Cooperative Power Control for Hierarchical Mobile Communication Networks	27
4.1	State-of-the-art and Contributions	27
4.2	System Model	29
4.2.1	Available CSI reports	32
4.2.2	Scheduling strategy	34
4.3	Power Control Scheme	35
4.4	Simulation Results	37
4.4.1	Impact of the transmit power reduction schemes	38
4.4.2	Performance of the proposed cooperative power control scheme	40
4.5	Summary	43
5	Centralized Coordinated Scheduling in Mobile Communication Networks	45
5.1	State-of-the-art and Contributions	45
5.2	System Model	47
5.2.1	CSI reporting for centralized CS with muting	50
5.3	Centralized CS with Muting	52
5.3.1	Proposed INLP - Problem formulation	53
5.3.2	Proposed ILP - Parallelized sub-problem formulation	56
5.3.3	State-of-the-art greedy heuristic algorithm	59
5.3.4	Generalized greedy heuristic algorithm	61
5.4	Simulation Results	62
5.4.1	Performance analysis	63
5.4.2	Potential gains	67
5.5	Summary	70

6	Decentralized Coordinated Scheduling in Mobile Communication Networks	73
6.1	State-of-the-art and Contributions	73
6.2	System Model	74
6.2.1	Decentralized cooperation clusters	75
6.2.2	CSI reporting for decentralized CS with muting	76
6.3	Decentralized CS with Muting	77
6.3.1	State-of-the-art decentralized CS with muting scheme	78
6.3.2	Proposed decentralized CS with muting scheme	79
6.4	Simulation Results	82
6.5	Summary	84
7	Coordinated Scheduling under Bursty Traffic	87
7.1	State-of-the-art and Contributions	87
7.2	System Model	89
7.2.1	Traffic modeling	89
7.2.2	CSI feedback and uncertainty	91
7.3	Coordinated Scheduling for Link Adaptation	92
7.3.1	Non-cooperative scheduling	93
7.3.2	Cooperative scheduling	95
7.4	Simulation Results	97
7.5	Summary	101
8	Conclusions and Outlook	103
	Appendix	107
A	Proof of Proposition 5.1	107
B	Proof of Proposition 5.2	107
C	Proof of Proposition 5.3	108
D	Proof of Theorem 5.1	108
	List of Abbreviations	111
	List of Symbols	115
	Bibliography	117
	Curriculum Vitae	127
	List of Publications	129

Chapter 1

Introduction

In cellular communication networks, the simultaneous utilization by the transmitters of the available time/frequency resources cause two opposite effects. On the one hand, high spectral efficiency is achieved, which describes the average amount of bits per second per channel use supported by the network. On the other hand, co-channel interference is generated, which represents one of the main limiting factors of the user throughput. This co-channel interference particularly affects the users located at the cell-edge, in the following referred to as the *cell-edge users* [BPG⁺09, KG08, KOG07, YZSL14]. In contemporary and future cellular communication networks, a constantly increasing demand for high data rates of new services and devices with more capabilities is expected. It is foreseen that by 2021 more than 11.5 billion connected devices generate a global mobile data traffic reaching 49 exabytes per month, which represents a sevenfold increase with respect to the global mobile data traffic from 2016 [Cis17]. Therefore, the networks are planned to operate with full frequency reuse in order to achieve high spectral efficiencies. Moreover, all users expect to enjoy excellent network performance irrespective of their geographic location and the load conditions of the network. In order to fulfill the ever increasing requirements, new solutions are required in particular for the cell-edge users suffering from large path loss and strong inter-cell interference. Promising advances in this aspect have been made with multi-antenna technology [GS05, LHZ09, PNG03, ZT03], network densification with interference management schemes [And13, LCLV14, LHAL11], and Coordinated Multi-Point (CoMP) transceiver techniques [IDM⁺11, LKL⁺12, SKM⁺10].

To enhance the network capacity, Multiple-Input-Multiple-Output (MIMO) technology has been introduced that increases the throughput and reliability of the transmissions by means of multiplexing and diversity, respectively [LHZ09, LJ10, ZT03]. Additionally, MIMO technology is used for beamforming in order to reduce interference towards co-channel users [GS05, PNG03]. Another sound alternative corresponds to network densification, i.e., the deployment of a larger number of base stations (BSs) per unit area, which boosts the network capacity due to an increase in the cell-splitting gain and a reduction in the path loss [And13, LCLV14, LHAL11]. Nevertheless, the increase in the network capacity due to the introduction of small cells, depends on the ability to counteract high inter-cell interference caused by the significant difference of transmit power levels among the distinct serving points. In particular, the cell-edge users experience high interference from neighboring BSs that heavily impact the achievable data rates. In order to increase the user data rates, especially of the cell-edge users, interference management schemes are proposed to diminish or completely cancel the interference at the user equipment (UE) [CJ08, LPVdlRZ09, RY10, RYW09]. In Long Term Evolution (LTE)-Advanced networks [DPS14, GRM⁺10, SBT11], the enhanced-Inter-Cell Interference Cancellation (ICIC) scheme establishes a muting pattern for the BSs over time/frequency resources, where the BSs are requested to suspend transmission in order

to reduce the interference to UEs located in neighboring cells [LPGdlR⁺11]. Additionally, cooperation between BSs, known as CoMP, improves the UEs' channel conditions through the coordination of the interfering BSs [IDM⁺11, LKL⁺12, SKM⁺10].

In this dissertation, CoMP network operation is studied, where the BSs connected within a cooperation cluster are prompted to cooperate with each other with the objective of improving the cell-edge network performance, even at the expense of their individual cell or user throughputs [LJ08]. In the literature and in LTE-Advanced networks, four main CoMP schemes are considered for the downlink scenario [BBB14, BO16, rGPP11]. These are: *i*) Joint Transmission (JT), where multiple BSs simultaneously transmit a common message to a UE usually located at the cell-edge, *ii*) Dynamic Point Selection (DPS), where the UEs can be served by different BSs at each transmission time, *iii*) Dynamic Point Blanking (DPB), where the BSs abstain from transmitting data on specific time/frequency resources, and *iv*) Coordinated Scheduling (CS), where the BSs jointly make scheduling decisions to manage the available time/frequency resources.

The performance of the above mentioned CoMP schemes heavily depends on the quality of the channel state information (CSI) available at the transmitter. This CSI can be of different types, e.g., in form of instantaneous channel values or user's average achievable downlink data rates, where the former represents the deepest level of detail and finest granularity, while the latter has the highest abstraction and aggregation levels. In practical downlink networks, where perfect global knowledge of the instantaneous channel values is generally not available at the BSs, CSI is typically obtained in form of data rate measurement reports generated by the UEs. These data rate measurement reports are averaged over multiple time/frequency/space dimensions and quantized to reduce the signaling overhead. Moreover, in order to limit the processing and transmission overheads, the CSI estimation process is only periodically carried out by the UEs. Thus, energy consumption is reduced at the expense of outdated CSI. In this work, the CoMP problem formulation is based on practical considerations of the CSI in form of periodic data rate measurement reports, in the following referred to as *CSI reports*.

The network architecture in which the CoMP schemes are implemented, also influences the performance of such schemes. Two main CoMP network architectures are typically defined, namely, the centralized and the decentralized ones [SYH13]. In the case of centralized CoMP, a central entity, also known as central processing unit or central controller, is connected to multiple BSs via backhaul links. This central controller is in charge of gathering and using the CSI reports to make a coordinated decision among the connected BSs. For the decentralized CoMP case, no central processing unit to control the coordination is available. Instead, decisions are individually made by each BS based on the information exchanged with neighboring BSs. A trade-off between coordination gains and system requirements, such as signaling overhead and computational complexity, needs to be found when designing a proper CoMP solution. In the case of centralized CoMP, high coordination gains are achievable at the expense of high computational complexity and large signaling overheads. Moreover, decentralized CoMP requires significantly less information exchange with lower coordination gains.

1.1 Aims, Contributions and Overview

The objective of this dissertation is to study and develop new techniques to improve the user throughput, especially for the cell-edge users, by applying cooperative resource allocation schemes on wireless mobile communication downlink systems. The focus relies on cooperative power control and CoMP CS schemes, where one special case of the former approach corresponds to the CoMP DPB scheme. One major contribution of this thesis is the consideration of practical restrictions related to the usage of CSI reports in the derivation of the proposed cooperative schemes. The used CSI reports are standardized in the 3rd Generation Partnership Project (3GPP) LTE and LTE-Advanced networks. Therefore, a deeper understanding of the potential gains and expected performance of the studied cooperative schemes is achieved under practical network conditions.

Additionally, the proposed cooperative schemes take into account practical network considerations with respect to the network architecture and the traffic models characterizing the users' demand. Hence, cooperative schemes are derived for centralized and decentralized CoMP architectures, and for user demands resembling full-buffer and bursty traffic. The problem formulations, the corresponding derived solutions and the numerical evaluations constitute valuable information to support the design and deployment of current and future generations of mobile communication networks.

The detailed outline of this dissertation is as follows.

In **Chapter 2**, the theoretical background utilized throughout the thesis is presented. The focus relies on the description of standardized procedures in LTE and LTE-Advanced networks, where among others, the available time/frequency resources are described in detail together with the process to estimate and report CSI. These standardized procedures are of significant relevance since they determine the formulation of the cooperation problems, as well as the derivation of their corresponding solutions in the proceeding chapters.

In **Chapter 3**, the general system model of cellular communication networks is presented, which is used throughout this work in order to introduce and evaluate the studied cooperative schemes. In each of the remaining chapters, this general system model is adjusted and extended accordingly to the particular conditions of the studied scenarios.

In **Chapter 4**, a cooperative power control scheme is presented for heterogeneous networks, where cooperation between a macro BS and the small cells located within the coverage area of the macro BS is considered [RCBP14]. After the scheduling decisions have been independently made by the BSs, the macro BS can adjust its transmit power on the available time/frequency resources in order to reduce the inter-cell interference caused to the UEs served by the small cells. If a cell-edge user is served by a small cell,

the macro BS can reduce its transmit power to the point that the macro BS avoids transmitting on a particular time/frequency resource. In this particular case, the macro BS is called *muted*, and the cooperative control approach is equivalent to the CoMP DPB scheme.

In **Chapter 5**, centralized CS with muting is studied for macro-only and heterogeneous networks, where a central controller is in charge of making the scheduling and muting decisions to be carried out by the connected BSs [RCBHP17]. The central controller decides whether the BSs serve their connected UEs on particular time/frequency resources, or if the BSs are muted to reduce the inter-cell interference experienced by the UEs served by neighboring BSs. Since the proposed centralized CS with muting scheme includes the scheduling and muting decisions in the cooperation, the CS approach extends the cooperative power control scheme studied in Chapter 4. Nevertheless, the CS scheme is restricted to only two power control scenarios corresponding to the BSs transmitting with maximum transmit power, or muted. Hence, the number of CSI reports required to support the operation of the proposed CoMP CS with muting scheme is limited. This restriction to only two power control scenarios is introduced by following the standardized procedures of LTE-Advanced networks.

In **Chapter 6**, a decentralized CS with muting scheme is proposed for macro-only and heterogeneous networks [RCP17]. The derived decentralized scheme aims to reduce the amount of information exchanged between adjacent BSs, by making muting decisions based on the altruistic behavior of the BSs. Thus, the BSs independently decide to avoid transmitting on particular time/frequency resources, based on their current knowledge of the CSI reports from their own UEs and limited feedback from adjacent BSs describing the impact of muting decisions made on previous transmission times. Compared to its centralized counterpart from Chapter 5, the decentralized CS with muting scheme achieves a lower performance in terms of cell-edge user throughput. Nevertheless, the simplicity of the derived scheme and its decentralized nature, make it applicable for large-scale networks where the implementation of real-time centralized cooperation is restricted due to its high computational complexity. Furthermore, the performance gap between the centralized and the decentralized schemes is marginal under current practical network considerations.

In **Chapter 7**, centralized CS is studied for a network under bursty traffic conditions [RCBP16]. In chapters 4 to 6, the proposed schemes are derived from a capacity enhancement perspective, thus, full-buffer systems are assumed, where the UEs constantly demand as much data as possible. However, in many practical networks, such a full-buffer system assumption generally does not hold true. Therefore, the proposed scheme in Chapter 7 is derived with the aim to improve the performance of the link adaptation procedures under bursty traffic conditions, i.e., in non-full-buffer systems. These link adaptation procedures, establish the transmission parameters used per serving link, e.g., the transmit power, the modulation and the coding schemes.

Finally, conclusions are drawn and future work is discussed in **Chapter 8**.

Chapter 2

Theoretical Background

A revision of the main theoretical concepts applied throughout this thesis are presented in the following. Along this work, the proposed cooperative schemes are designed and investigated by taking into account their implementation in LTE-Advanced networks. Therefore, in Section 2.1 relevant aspects of LTE-Advanced networks such as the deployment of BSs and UEs, the definition of physical resources in time/frequency/space, and the estimation and reporting of CSI are revised. Furthermore, an overview of interference management schemes is given in Section 2.2, where implicit and/or explicit cooperation among the BSs is exploited in order to improve the downlink network performance in terms of the average user throughput. Specifically, CoMP operation is introduced, from which the practically relevant DPB and CS schemes are studied in this work. As previously mentioned in Chapter 1, the investigated cooperative schemes are derived with restrictions on the available CSI at the transmitter, which is in form of standardized CSI reports from LTE and LTE-Advanced networks. In the case of the proposed CS schemes, such a restriction on the CSI implies that the resulting CS problem formulations are integer linear programs (ILPs), where the selection of a particular CSI report corresponds to an integer, or even binary, decision. Hence, a short description of integer linear programming with focus on its combinatorial nature is provided in Section 2.3. Finally, system-level simulations are used to evaluate the studied algorithms. For that purpose, a system-level simulator has been extended to support such simulations. In Section 2.4, the main modules of the system-level simulator are presented and briefly explained.

2.1 LTE-Advanced Networks

LTE-Advanced [DPS14, GRM⁺10, SBT11] standardized by 3GPP (www.3gpp.org) is the most recognized technology of the fourth generation of mobile communications. The first release of LTE, i.e., Release-8, was published in December 2008 with the introduction of Orthogonal Frequency Division Multiple Access (OFDMA) as the radio access scheme, in contrast to Wideband Code Division Multiple Access (WCDMA) used in the previous generation. Additional features of LTE Release-8 are the usage of MIMO technology, variable bandwidth and ICIC procedures, among others. The latter feature, i.e., ICIC, is explained in Section 2.2.1. Extensions to the LTE standard have been further brought in later releases, with the Release-10 introducing LTE-Advanced in March 2011 [DPS14, GRM⁺10, SBT11]. LTE-Advanced was proposed to fulfill the International Mobile Telecommunications (IMT)-Advanced requirements of the International Telecommunications Union (ITU) for the fourth generation of mobile communications [Int15]. Some of the new features in LTE-Advanced correspond

to the usage of additional number of antenna ports at the transmitter and at the receiver, where LTE-Advanced supports up to eight antenna ports in contrast to the four ports supported by LTE Release-8 [GS05,LHZ09,PNG03,ZT03], the deployment of heterogeneous networks with interference management schemes [And13,LCLV14,LHAL11], and the aggregation of multiple frequency bands for transmission, known as *carrier aggregation* [PFR⁺11,SPM⁺12,YZWY10].

This work is mainly based on the features of LTE-Advanced networks. Therefore, the main aspects of the LTE-Advanced standard, related to this dissertation, are briefly described in the following.

2.1.1 Network deployments

Cellular communication networks are considered where UEs are deployed in the coverage area of the BSs. The BSs are usually classified based on their transmit power. Hence, the so called *macro* cells correspond to BSs with a high transmit power, e.g., 46 dBm, and the *small* cells correspond to BSs with lower transmit power than the macro BSs. Some examples of small cells are the pico BSs with a typical transmit power of 30 dBm and the femto BSs, which usually transmit with a total power of 24 dBm [rGPP10]. Due to the difference in the transmit powers and the resulting coverage area of the above mentioned BSs, the macro and pico cells are typically used for outdoor coverage, while the femto BSs are deployed indoors. Throughout this thesis, the performance of the proposed cooperative schemes is studied for outdoor deployments of BSs and UEs, where the mobile communication network is classified into a homogeneous or heterogeneous cellular network depending on the type of deployed BSs.

A homogeneous cellular network implies that all deployed BSs are of the same type, where a well-known example corresponds to a macro-only network with all the cells consisting of macro BSs. This macro-only network has been commonly used in previous generations of mobile communications, including LTE Release-8. A macro-only network is illustrated in Figure 2.1a with seven cells composed of three macro BSs each. In Chapter 1, it has been mentioned that the networks typically operate with full frequency reuse, i.e., all BSs simultaneously transmit over the same time/frequency resources in order to achieve high spectral efficiency [BPG⁺09,KG08,KOG07]. However, when operating with full frequency reuse, the UEs served by one BS, and especially the cell-edge UEs, are affected by considerable inter-cell interference caused by the neighboring BSs. One alternative to cope with the inter-cell interference is to restrict the minimum separation distance between neighboring BSs, such that the interference caused to the neighboring cells is below a threshold. The minimum separation distance is then a function of the transmit power of the BSs and the propagation parameters such as path loss and shadow fading. For the macro-only network in Figure 2.1a, the minimum separation distance between BSs can be large due to the high transmit power of the macro cells. In such a case, each BS needs to cover a large area with a non-uniform distribution of the signal strength due to fading. Thus, the performance experienced

by the UEs depends on their locations in the cell, where the cell-edge UEs which are located far away from the serving BS, usually experience lower user throughputs than the UEs located closer to the BS. Additionally, as a result of the large coverage area the BSs need to serve more UEs. Due to the fact that the time/frequency resources are limited, serving more UEs per unit area reduces the average amount of time/frequency resources that each UE receives. One solution to cope with the above mentioned disadvantages of the macro-only networks is to deploy homogeneous networks with smaller coverage areas and lower transmit power per BS, e.g., pico-only networks. However, the requirements regarding the number of small cells, the backhaul connectivity, i.e., connectivity to the core network, and the deployment costs, make the implementation of such a homogeneous network infeasible in practice. Therefore, solutions to cope with the inter-cell interference are favored such as ICIC, explained in Section 2.2.1.

Heterogeneous networks are proposed as a trade-off between inter-cell interference and cell size, where small cells are located within the coverage area of the macro BSs. More specifically, the small cells are typically located in regions where the signal strength of the macro BS is low in comparison to the maximum signal strength observed in the macro cell, due to fading or path loss. In this manner, a more uniform distribution of the signal strength experienced by the UEs is achieved in the geographical area. Furthermore, because the UEs can connect to additional BSs in the same area, and assuming that all BSs use the same time/frequency resources, it is possible to increase the average amount of resources per UE, i.e., *cell-splitting gain* is achieved [Don79, GMD13]. However, due to the difference in transmit powers of the macro BSs and the small cells lying on the coverage areas of the former, the UEs connected to the small cells suffer from high inter-cell interference coming from the macro BSs. If the inter-cell interference is not kept sufficiently low, the cell-splitting gain might be counteracted by the effects of the interference. Mechanisms to manage the inter-cell interference such as ICIC and enhanced-ICIC are explained in Section 2.2.1. Figure 2.1b illustrates an example of a heterogeneous network, where one small cell is located in the coverage area of a macro BS.

2.1.2 Physical resources

LTE downlink and uplink transmissions are based on the Orthogonal Frequency Division Multiplexing (OFDM) transmission scheme, where narrow-band subcarriers are combined over the time/frequency domains in order to achieve wider-band transmissions [rGPP04,rGPP06]. Due to the narrowness of the subcarriers and the large number of them, the OFDM systems successfully counteract the negative effects of frequency selective channels by increasing the frequency diversity. Thus, it is typically possible to find *favorable* subcarriers to transmit. However, OFDM transmissions have some associated drawbacks, such as the reduction of the spectral efficiency due to the utilization of a cyclic prefix and the low power amplifier efficiency caused by the high peak-to-average-power ratio [LS06,Pra04]. The cyclic prefix is used to make the OFDM transmission less sensitive to time dispersion and thus, to avoid inter-symbol-

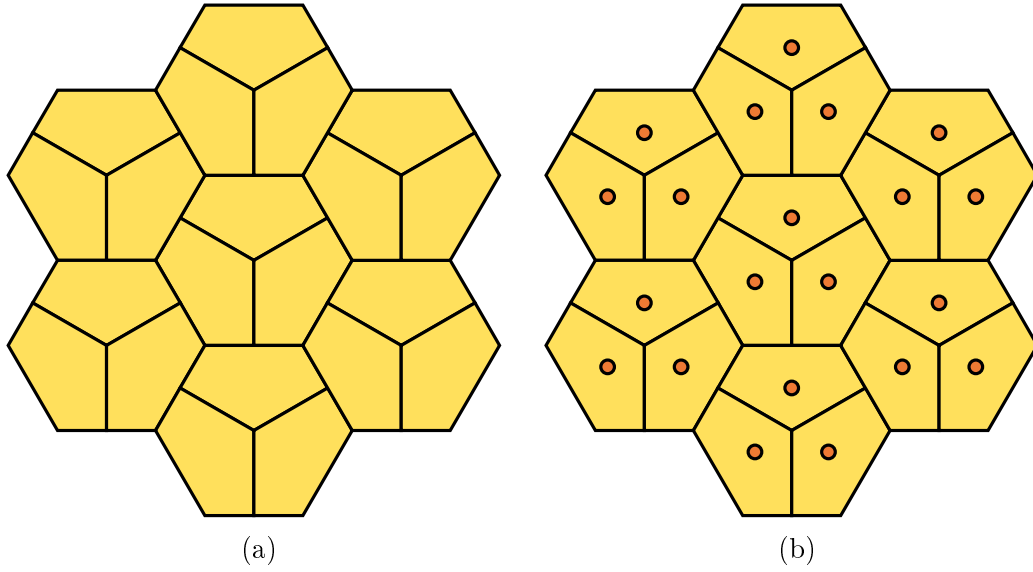


Figure 2.1. Illustration of network deployments. (a) Homogeneous network of macro BSs. (b) Heterogeneous network with small cells (circles) within the coverage area of the macro BSs

and inter-subcarrier-interference by inserting a copy of the last part of the OFDM symbol, right before the symbol starts. Since a fraction of the transmitted OFDM symbols is redundant, the spectral efficiency decreases, i.e., lower throughput per channel use is obtained. Moreover, due to the high variations between the peak and the average powers of the transmitted OFDM symbols, the power amplifiers require a large operational dynamic range, which reduces their efficiency and increases the implementation costs [DPS14].

In the time domain, the OFDM symbols are grouped into time-slots with a duration of 0.5 ms. The number of OFDM symbols per time-slot depends on the length of the cyclic prefix. Hence, when a normal cyclic prefix is used, one time-slot is formed by seven OFDM symbols, while in the case of an extended cyclic prefix, the time-slot contains only six OFDM symbols. Two time-slots constitute one subframe with a duration of 1 ms, and one radio frame consists of ten subframes. Figure 2.2 illustrates the time domain configuration of the LTE resources when using the normal cyclic prefix [DPS14]. In the frequency domain, the OFDM subcarrier spacing is equivalent to 15 kHz. Thus, the total amount of subcarriers in the system depends on the available bandwidth. As an example, a 20 MHz LTE system has 1200 subcarriers without including the carrier center frequency, i.e., the Direct Current (DC) subcarrier which remains unused.

A Resource Element (RE) corresponds to one subcarrier in the frequency domain with a duration of one OFDM symbol in the time domain. Furthermore, a Physical Resource Block (PRB) is formed by 12 subcarriers in the frequency domain, and one time-slot in the time domain. Therefore, if the normal cyclic prefix is used, a total of 84 REs represent one PRB. The time/frequency representation of a PRB is illustrated

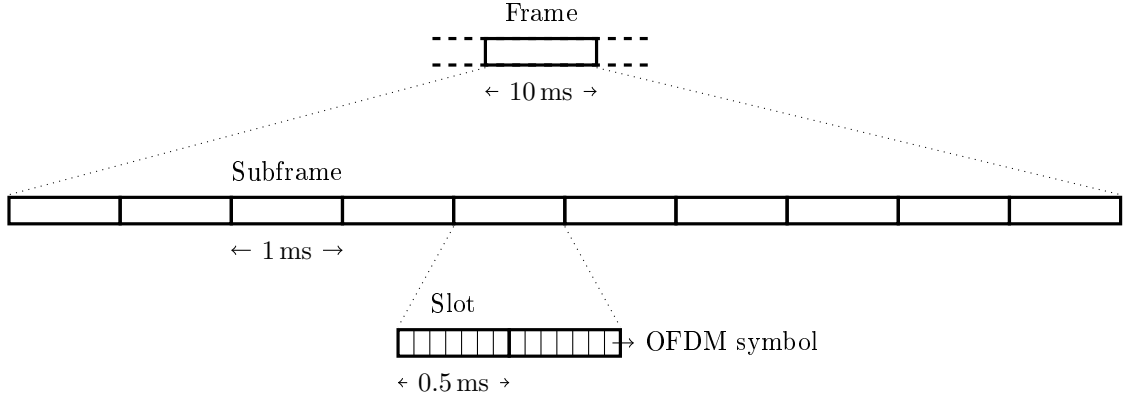


Figure 2.2. Configuration of the LTE resources in the time domain when using normal cyclic prefix

in Figure 2.3. Regarding the scheduling process, the minimum scheduling unit that can be assigned to a UE corresponds to a *resource block pair*. Thus, the scheduling decisions are given in a time span of one subframe in the time domain, i.e., 1 ms. In this dissertation, the term PRB is used in association to the scheduling decisions. Therefore, in the following, a PRB refers to a resource block pair.

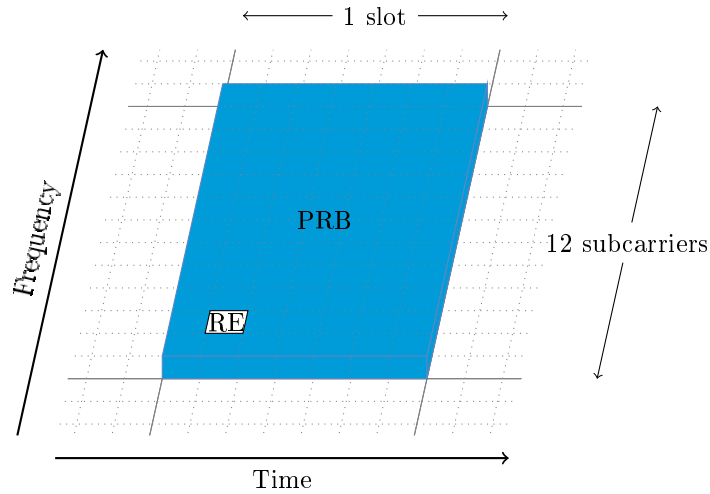


Figure 2.3. Definition of a PRB in the time and the frequency domains

2.1.3 CSI estimation and reporting

In order to support opportunistic scheduling, CSI knowledge at the transmitters is required. In this dissertation, the cooperative schemes are studied for downlink transmissions. Thus, the BSs require CSI knowledge to serve the connected UEs in the downlink. In systems operating in Time Division Duplexing (TDD) mode, where the

uplink and downlink transmissions make use of the same frequency resources, channel reciprocity can be exploited, enabling the BSs to estimate the downlink channel from the incoming uplink reference signals transmitted by the UEs [Bal29, Car29]. Nevertheless, in several cases assuming the reciprocity of the channel is not realistic due to e.g., the usage of different antennas for transmission and reception [GL14, HYW⁺13]. In the case of non-reciprocal channels when operating in TDD mode, or in the case of Frequency Division Duplexing (FDD) mode operation, where the downlink and uplink transmissions take place in different frequency bands, alternative mechanisms are required in the network to acquire CSI. In LTE systems, the UEs estimate the channel in the downlink and report this information back to the serving BSs to support the scheduling and link adaptation procedures for the upcoming downlink transmissions [KW15].

In LTE networks, the CSI reported by the UEs is typically composed of a Channel Quality Indicator (CQI), a Precoding Matrix Index (PMI) and a Rank Indication (RI) [3rd13]. The CQI reflects the estimated signal-to-interference-plus-noise ratio (SINR) and the corresponding achievable data rate of a UE, when assuming a downlink transmission of rank indicated by the RI and transmit precoding vector taken from a finite-length codebook and indexed by the PMI. In the selection of the CQI, lookup tables are typically used by the UEs depending on the device capabilities. These lookup tables indicate the modulation and coding scheme (MCS) with the highest achievable data rate that the UE can decode for a maximum Block Error Rate (BLER) of 10 % [SBT11, SMR10]. Examples of such lookup tables are available in [CPP12, FYL⁺11]. Throughout this thesis, a similar lookup table is used based on proprietary link-level simulations.

In order to estimate the downlink channel, the BSs transmit *known* training pilots to the UEs. In the case of LTE networks, these training pilots are referred to as downlink reference signals (RSs). In this work, two kinds of RSs used by the UEs for CSI estimation are considered as follows [DPS14, SBT11].

Cell-Specific Reference Signal (CRS): in order to estimate the CSI, CRSs have been introduced in the first LTE release, i.e., Release-8. Each BS can transmit one to four different CRSs, corresponding to an equal number of antenna ports, with the port numbers indexed by $\{0, 1, 2, 3\}$. The CRSs are transmitted on every time subframe on specific REs, where the selectable REs are illustrated in Figure 2.4. In the case of the first two antenna ports, i.e., antenna ports P0 and P1, a total of 16 REs are available for the transmission of the CRSs, while for the additional antenna ports, i.e., antenna ports P2 and P3, only eight REs can be used for the CSI estimation. The reason for such a reduction in the number of REs is to limit the signaling overhead, thus, more REs are available for data transmission.

CSI Reference Signal (CSI-RS): in LTE-Advanced, i.e., Release-10, the CSI-RSs were included as a complement of the already existing CRSs. The available REs to be used for the transmission of CSI-RSs are illustrated in Figure 2.4, where 40

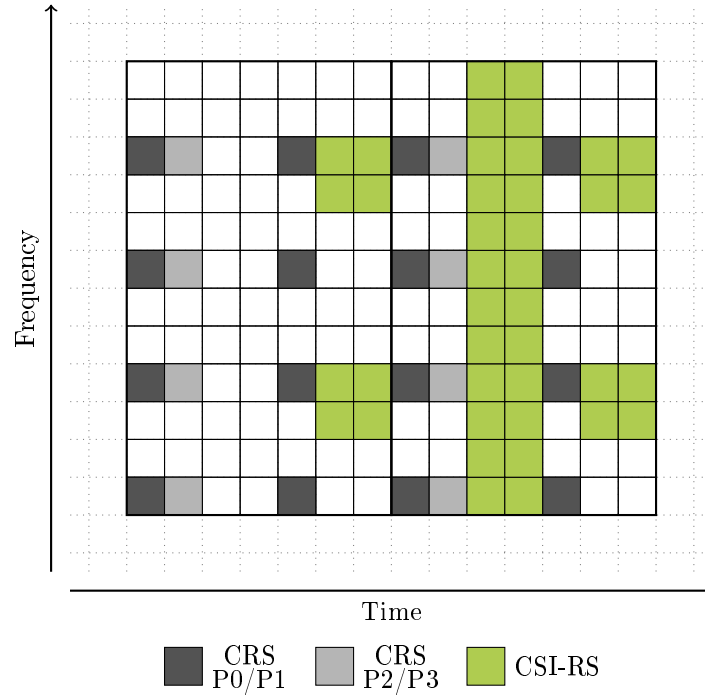


Figure 2.4. Possible REs to be used for CRS and CSI-RS within a PRB

possible positions can be selected. Each BS can transmit CSI-RSs for one, two, four or eight antenna ports. Therefore, MIMO transmissions with more than four antenna ports are possible in comparison to LTE Release-8. A main difference between the CSI-RSs and the CRSs, is that the transmission of the former is not expected at every time-slot. Thus, in the case of slowly varying channels, the overall signaling overhead can be reduced by sporadically transmitting the CSI-RSs. Moreover, in order to ease the estimation of CSI from neighboring cells, it is possible to configure *muted* CSI-RSs, which implies the lack of any transmission from a specific cell on given REs. These muted CSI-RSs are further exploited in the cooperative schemes studied in this work and introduced in LTE Release-11.

By using the above described reference signals, the UEs can estimate the CSI either in the time or the frequency domains by applying e.g., the maximum likelihood approach. The CSI estimation mechanisms are beyond the scope of this thesis. Interested readers are referred to [ABB⁺07, ABS07, MM01] for more information on CSI estimation approaches. After the CSI estimation is performed, the UEs report the CQI, PMI and RI values to the BSs to support the downlink transmissions. Moreover, the CSI estimation can be based on CRSs or CSI-RSs, where the latter support the estimation for *muted* antenna ports. In order to distinguish between the CSI based on the different reference signals, the notation $\text{CSI}^{\text{R-8}}$ and $\text{CSI}^{\text{R-11}}$ is used, where the former corresponds to the CSI generated based on CRSs, as introduced in LTE Release-8, and the latter refers to the CSI obtained by using the CSI-RSs, to support the cooperative schemes from the LTE Release-11.

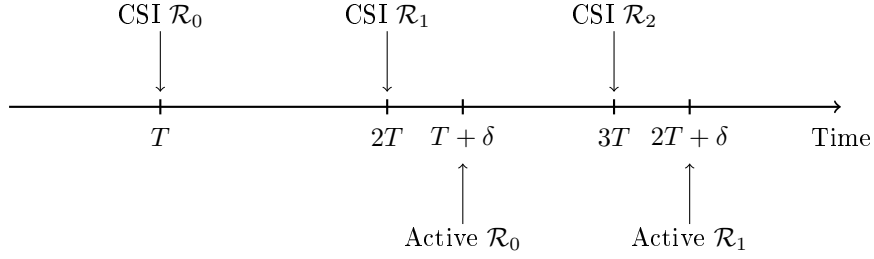


Figure 2.5. Periodic CSI estimation and reporting process. The CSI reports are generated by the UE with periodicity T and get active at the serving BS after a time δ

Regarding the timing for reporting CSI, Figure 2.5 illustrates the periodic CSI estimation and reporting process of a UE. The UE reports CSI to the serving BS every time T , where the reported CSI gets *active*, i.e., is used for the scheduling process, after a time δ . The reported CSI remains active for the periodicity T . Typical values for T and δ in LTE networks correspond to a periodic reporting of $T = 5$ ms and an activation delay of $\delta = 6$ ms.

2.2 Interference Management Schemes

In a multi-cell scenario as depicted in Figure 2.1, inter-cell interference represents a limiting factor in the achievable user throughput. As mentioned in Section 2.1.1, this inter-cell interference is caused by the simultaneous utilization of the time/frequency resources by neighboring BSs. In the heterogeneous network case, the negative effect of such an inter-cell interference is even higher due to the significant difference in transmit powers between the macro and small cells. Hence, interference mitigation techniques target to reduce the inter-cell interference by applying different approaches as follows [CJ08, RY10, RYW09].

Interference cancellation: in this technique, coherent, phase synchronous signal processing at the receiver is performed in order to estimate and subtract the interference from the desired signal.

Interference averaging: in this approach, the BSs transmit data to the UEs by hopping over the time/frequency dimensions in order to average the effect of interference.

Interference avoidance: this scheme concentrates on reducing the simultaneous utilization of the time/frequency resources in order to find a good trade-off between achievable data rates and inter-cell interference.

In this work, interference avoidance schemes are investigated. Thus, two main interference avoidance approaches are presented in more detail in the following.

2.2.1 ICIC and enhanced-ICIC

In homogeneous networks, e.g., macro-only networks, ICIC is applied in order to reduce, or completely avoid, the inter-cell interference over time/frequency resources [DPS14, SBT11]. When decreasing the interference, ICIC specifies transmissions over a pattern of time/frequency resources with reduced transmit power. In that manner, the cell-edge UEs can be served while experiencing a lower received interference power level. Hence, increasing the achievable data rates of the cell-edge UEs. Moreover, due to the reduced transmit power, the neighboring BSs schedule transmissions to cell-center UEs, i.e., UEs located at the vicinity of the serving BSs, with low impact on their achievable data rates. This ICIC option is also known as Fractional Frequency Reuse [LHXQ13, RYW09]. However, in some scenarios the cell-edge UEs experience such a high inter-cell interference, that a limited reduction of the interference power does not improve their achievable data rates. Therefore, a complete avoidance of the inter-cell interference is required. In those cases, the frequency reuse factor, defined as the number of BSs that do not transmit on a certain frequency band¹, is larger than one and the BSs abstain from transmitting on certain time/frequency resources [RY10, RYW09]. Since the neighboring BSs do not transmit on all the available time/frequency resources, a reduction of the spectral efficiency typically occurs, with respect to a system operating with full frequency reuse.

In the heterogeneous network case, the deployment of small cells attempts to achieve cell-splitting gains, as mentioned in Section 2.1.1. For that purpose, *load balancing* is required among the macro and small cells, implying that each type of BS serves a similar number of UEs. A typical strategy to select the serving BS for a UE corresponds to the selection of the BS providing the highest total received power. However, due to the significant difference of transmit powers between the macro and small cells, such a selection strategy of the serving BS causes that most of the UEs are served by the macro BSs despite of their proximity to the small cells. Thus, the load balancing is negatively affected. In order to balance the load among the BSs, techniques like cell-range expansion (CRE) are applied, e.g., in LTE-Advanced, where the UEs are instructed to add a constant off-set in the computation of the total received powers of the small cells for the purpose of selecting the serving cell [DMW⁺11, GLBC17, YRC⁺13]. For UEs located in the cell-range extended region, the interference level of the macro BSs is higher than the received power from the serving small cell, thus, these UEs experience a negative SINR in dB. In order to improve the achievable data rates of these cell-edge UEs, ICIC with complete interference avoidance in the time domain is applied, known as enhanced-ICIC [LPGdlR⁺11, OH12]. An example of the enhanced-ICIC operation is illustrated in Figure 2.6, where two subframe types are configured, namely, normal and Almost Blank Subframe (ABS) [CWW⁺13, KPRA15]. In the normal subframe, the macro BS, i.e., BS m , transmits with maximum transmit

¹In the literature, two definitions of the frequency reuse factor can be found. In the second definition, the factor corresponds to the inverse of the number of BSs that do not transmit. Thus, the maximum frequency reuse factor is one. In this work, the commonly used definition related to LTE and LTE-Advanced networks is adopted.

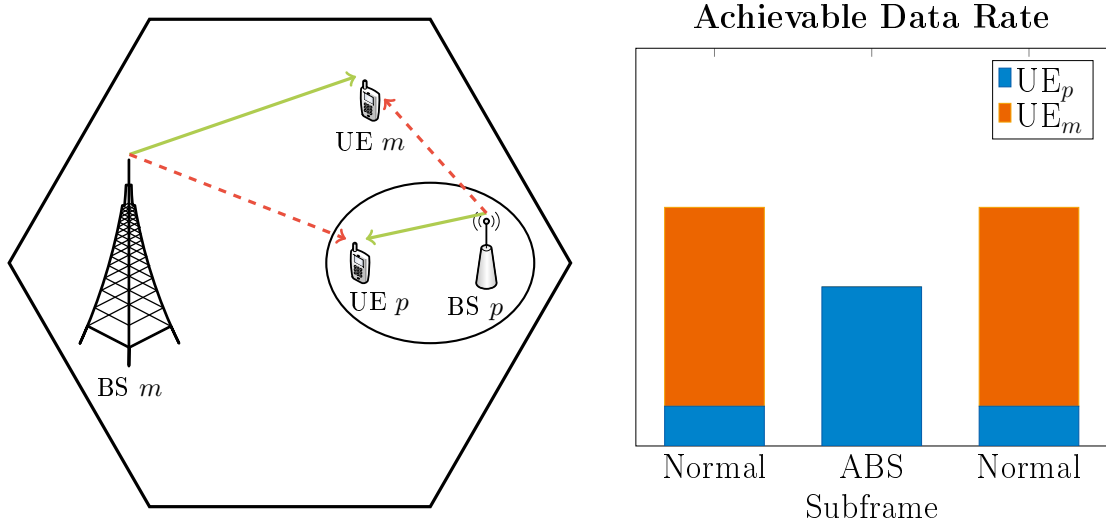


Figure 2.6. Enhanced-ICIC mechanism. The macro BS m does not transmit during the ABS to avoid interfering UE p , located in the CRE region of the small cell BS p

power, thus, causing severe interference to a UE located in the CRE region of the pico cell BS p , i.e., UE p . As a consequence, the achievable data rate of UE p is very low, or even equal to zero, during the normal subframes as illustrated in the right-hand side of Figure 2.6. During the ABS, the macro cell BS m is muted, i.e., it does not transmit data. Therefore, the interference level experienced by UE p decreases and its achievable data rate increases. Although the spectral efficiency is negatively affected by the introduction of the ABSs, this negative effect can be compensated by the cell-splitting gains achieved by the deployment of the small cells.

The benefits of ICIC and enhanced-ICIC have been studied in e.g., [BGG⁺12, DMBP13], especially in fully-loaded systems, i.e., the UEs constantly demand as much data as possible. However, when the load conditions in the network vary, the static patterns usually configured in ICIC and enhanced-ICIC operation potentially reduce the network performance. Therefore, more dynamic algorithms based on the ICIC operational principle have been proposed in different works such as [OH12, SPK⁺13].

2.2.2 CoMP transmission

In order to improve the network performance, the concept of BS cooperation has been subject of study in recent years [LJ08]. In CoMP transmission, the BSs are prompted to cooperate with each other even at the expense of their individual cell or user throughputs, so that the performance of the cell-edge users is enhanced. As mentioned in Chapter 1, four main CoMP schemes are considered in the literature, as follows [BBB14, BO16, MHV⁺12].

Joint Transmission (JT): in this CoMP scheme, the BSs simultaneously transmit a common message to a UE usually located at the cell-edge. Therefore, the interference experienced by the UE from the neighboring BSs is converted into useful signal and the UE's SINR is increased. From another perspective, in CoMP JT the cooperative BSs behave as a single BS with widely separated antennas. The potential gains of CoMP JT are the highest among the CoMP schemes because the schemes described below are special cases of JT. However, the practical implementation of CoMP JT heavily depends on the quality of the available CSI at the BSs. If the quality of the CSI is low, the correct reception of the transmitted symbols is affected by the imperfect combination of the signals transmitted from the cooperative BSs. Additionally, the CoMP JT scheme requires the availability of the UE data at each of the cooperative BSs, which represents a strict requirement in backhaul capacity and connectivity.

Dynamic Point Selection (DPS): for the cell-edge UEs, small modifications of the channel conditions can trigger handover procedures, where the serving BS changes from the current BS to the neighboring cell. Such handover procedures represent signaling overheads and the possibility of *ping-pong* effects if the channel conditions again vary in favor of the previously serving BS [KBL⁺14]. The CoMP DPS scheme, enables the quick change per transmission time of serving BS without triggering any handover procedures. In this way, the UE is served at each transmission time by the BS providing the best SINR. Since the serving BS can change per transmission time, the UE data needs to be simultaneously available at each potential serving BS.

Dynamic Point Blanking (DPB): this scheme prompts the BSs to abstain from transmitting data on specific time/frequency resources to reduce the inter-cell interference caused to the UEs connected to neighboring BSs. If a BS does not transmit on a particular time/frequency resource, the BS is called muted. Similar to DPS, in DPB the BSs can be muted at each transmission time. Thus, the UE's achievable data rate can be improved according to the current channel conditions.

Coordinated Scheduling (CS): another alternative of cooperation is to allow the BSs to jointly make the scheduling decisions. In CoMP CS, the BSs manage the interference experienced by the UEs in either one of the following approaches: *i*) designing the beamformers in a coordinated manner, i.e., coordinated beamforming, *ii*) assigning orthogonal resources to the BSs, i.e., muted BSs, or *iii*) keeping stable interference conditions under highly varying traffic in order to improve the effectiveness of radio link adaptation procedures which select the transmit power, modulation and coding, among others. Although the potential gains of CoMP CS are lower than CoMP JT, the dependency of the former scheme on the CSI is limited. Moreover, since the transmissions to each UE take place only from its serving BS, the cooperative BSs do not need to share UE data. Thus, the requirements on the network's backhaul are relaxed.

An illustration of the above mentioned CoMP schemes is presented in Figure 2.7, together with the case where no cooperation takes place among the BSs. If the BSs do

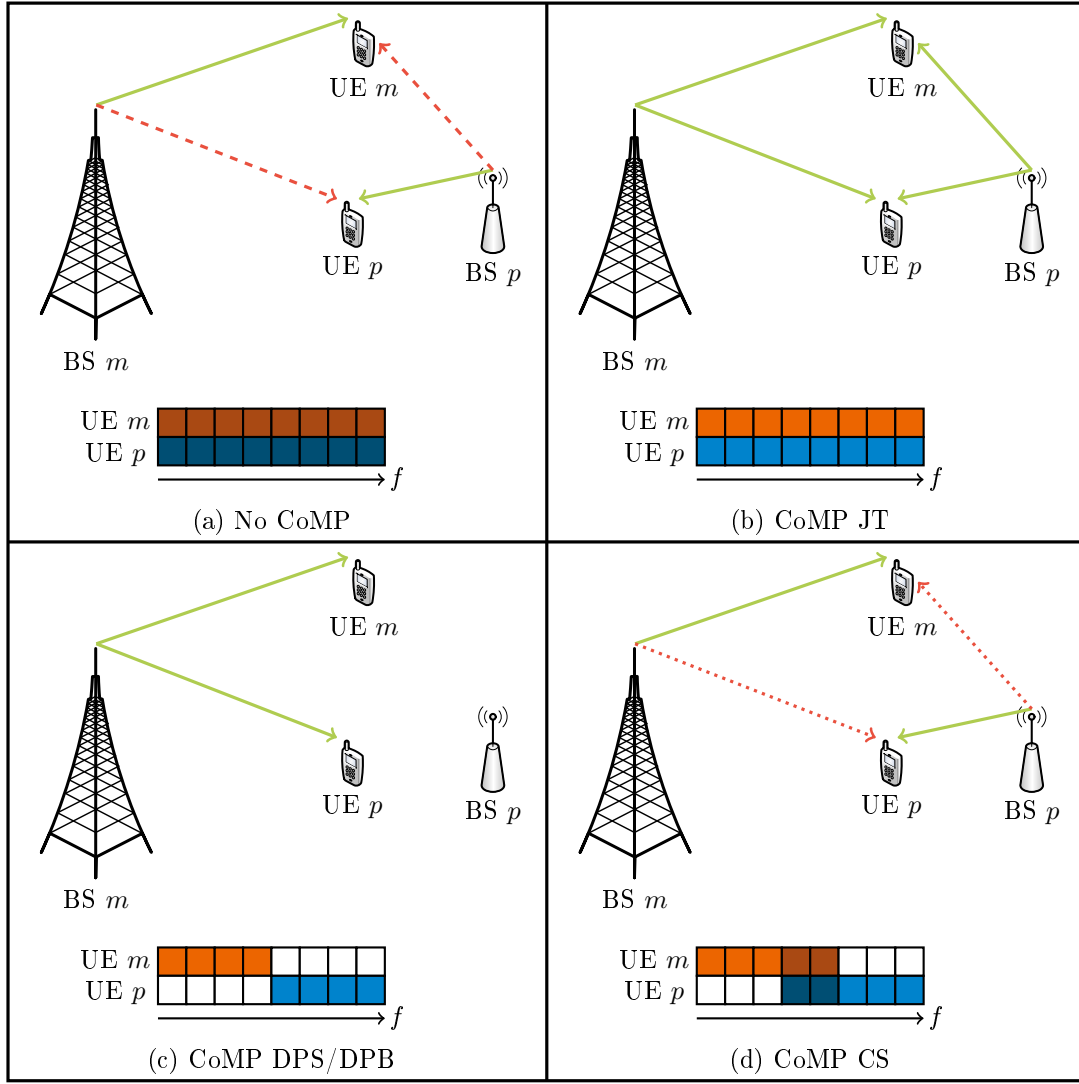


Figure 2.7. Comparison of non-cooperative and cooperative schemes. The solid arrow represents the serving link, the dashed/dotted arrows represent the interfering links

not cooperate with each other, all the available time/frequency resources are used for simultaneous transmissions. Thus, inter-cell interference is experienced, as illustrated in the case (a) No CoMP. However, if CoMP JT is applied, both BSs transmit useful signals to both connected UEs over all available time/frequency resources. Therefore, no inter-cell interference is present and the UEs are served with maximum achievable data rates. In the case (c) CoMP DPS/DPB, the serving BS that provides the best SINR conditions for each UE is selected. Additionally, the BSs are muted on specific time/frequency resources to avoid interference. Nevertheless, the spectral efficiency is negatively affected by the reduction of the available time/frequency resources. Finally, CoMP CS achieves a trade-off between spectral efficiency loss and inter-cell interference reduction, by jointly making scheduling decisions among the BSs, including muting on time/frequency resources.

In the following chapters, CoMP DPB and CS with muting schemes are studied, with the main focus relying on the latter CoMP approach.

2.3 Integer Linear Programming

One type of linear programming problems corresponds to the ILP, where one or more variables are restricted to take only integer values. If all the variables are integers, the problem is known as a *pure-ILP*. On the other hand, if some of the variables can take continuous values, then the problem is said to be a *mixed-ILP*. Moreover, in the case that the variables can only take the values in the set $\{0, 1\}$, the problem is known as a *binary-LP* [BHM77]. The scheduling problem is a typical example of an ILP, where the resources to be distributed can only take integer values, e.g., only an integer number of PRBs can be scheduled to a UE. Moreover, from a different perspective, the scheduling problem can be modeled as a binary-LP, where the decision variable states whether a given PRB is assigned or not, to a specific UE. In this work, the centralized CoMP CS problems studied in chapters 5 and 7 are classified as binary-LPs.

The problems classified as ILP are generally considered to be purely combinatorial in nature. Thus, they are typically classified as non-deterministic polynomial-time (NP)-hard. Hence, the ILP problems are known to be difficult to solve optimally and the computational complexity generally scales poorly with the problem size. For ILP problems of small- to moderate-size, the commercial solvers such as CPLEX [Flo95] or MATLAB Optimization Toolbox [Mes15] can efficiently find optimal solutions. For larger-size ILP problems, however, approximate solutions need to be found by using fast heuristics [Wol98]. In this dissertation, commercial solvers are used to find optimal solutions of the formulated problems in medium- to large-scale networks, and these solutions are used as benchmarks to compare with state-of-the-art and proposed fast heuristics.

2.4 System-Level Simulations

In order to evaluate the performance of the cooperative schemes proposed in this work, system-level simulations are performed. For that purpose, an LTE-compliant system-level simulator has been jointly extended in collaboration with the Technology Innovation Division of Deutsche Telekom AG, to introduce the cooperative schemes proposed in this thesis. From a system-level perspective, the evaluations are focused on the network performance mainly in terms of average UE and BS throughputs.

A simplified block diagram description of a system-level simulator is illustrated in Figure 2.8 for a single iteration, where the following four modules are considered.

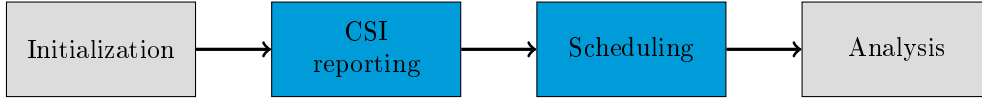


Figure 2.8. Simplified block diagram of a system-level simulator. In this thesis, the main focus relies on the CSI reporting and Scheduling modules, where the proposed cooperative schemes are implemented

Initialization: the configuration of the system-level simulation is performed in this module, where some of the main procedures are described as follows: *i)* BSs and UEs are deployed in the studied area, *ii)* the parameters for determining the channel coefficients between BSs and UEs are generated based on the network's geometry, e.g., the location of the BSs, UEs and scatterers; where two main channel models are typically used, such as the Spatial Channel Model (SCM) [rGPP12] and WINNER Phase I model [SGS⁺05], *iii)* mobility and traffic models are defined and associated to the deployed UEs, and *iv)* initial serving relations between the BSs and the UEs are established.

CSI reporting: in this module, the estimation and reporting process of CSI is carried out at the UEs, as explained in Section 2.1.3. Once the CSI is available at the BSs, it is used to support the scheduling and link adaptation procedures.

Scheduling: in this module, the available PRBs are distributed by the BSs among the UEs for uplink/downlink transmissions. For that purpose, different scheduling approaches can be applied such as Round-Robin (RR) or Proportional Fair (PF) schedulers [TV05, WMMZ11, ZH07]. In the following chapters, different scheduling strategies are proposed based on cooperative schemes as introduced in Section 2.2.2. After making the scheduling decisions, the data transmission takes place as configured by the CSI reports, where parameters such as the MCS are specified.

Analysis: finally, the evaluation of the scheduling and link adaptation procedures is performed in this module by means of calculating the resulting BLER and average user throughput of the deployed UEs. Some of the key performance parameters recommended to be evaluated in [rGPP10] are the average UE and BS throughputs and spectral efficiency, among others. In this thesis, the main performance parameters are the long-term average user throughput of the cell-edge UEs, and the mean and geometric mean of the long-term average user throughput of all UEs.

This work is focused on the study of cooperative schemes under practical considerations of available CSI at the transmitter. Therefore, the CSI reporting and Scheduling modules were modified with regard to the guidelines in [rGPP10], in order to support the system-level evaluation of the proposed schemes.

Chapter 3

Mobile Communication Networks

A general mobile communication network is considered as illustrated in Figure 3.1, where M BSs operating in FDD mode serve N UEs in the downlink. OFDMA is assumed with frequency reuse one, where at each transmission time all BSs can make use of the same L PRBs for transmission, with the PRBs as defined in Section 2.1.2. Thus, inter-cell interference affects the SINR and the achievable data rates of the UEs, especially of those located at the cell-edge. Two network types are considered throughout this work, namely, macro-only and heterogeneous networks, as introduced in Section 2.1.1, where connectivity between the BSs is assumed through the implementation of backhaul links. Moreover, depending on the particular scenario, the presence of a central controller is considered as explicitly mentioned in the upcoming chapters. In the following, the sets of indices $\mathcal{M} = \{1, \dots, M\}$, $\mathcal{N} = \{1, \dots, N\}$ and $\mathcal{L} = \{1, \dots, L\}$ are used to address the BSs, UEs and PRBs, respectively.

The received power at UE $n \in \mathcal{N}$ from BS $m \in \mathcal{M}$ on PRB $l \in \mathcal{L}$ is denoted as $p_{n,m,l}$. Hence, for Single-Input-Single-Output (SISO) transmission,

$$p_{n,m,l} = |q_n h_{n,m,l}|^2 \Phi_{m,l}, \quad (3.1)$$

where $\Phi_{m,l}$ corresponds to the maximum transmit power of BS m on PRB l , the complex coefficient $h_{n,m,l}$ represents the downlink channel gain between BS m and UE n on PRB l , aggregated over all subcarriers of PRB l , and q_n is the receiver processing gain of UE n after applying receiving processing methods such as Maximum Ratio Combining (MRC) or Zero-forcing (ZF) [Gol05, K 6]. In (3.1) the transmitted symbols are assumed to exhibit unit average power. Moreover, in the case of multiple antennas at the transmitter and at the receiver, i.e., MIMO transmissions, $p_{n,m,l}$ as in (3.1) can be straightforwardly extended as in [MHV⁺12]. The total received power at UE n from BS m , denoted as $p_{n,m}$, is obtained as the sum over all PRBs such that

$$p_{n,m} = \sum_{l=1}^L p_{n,m,l}. \quad (3.2)$$

Generally, the serving BS for UE $n \in \mathcal{N}$ is selected as the BS from which the highest total received power, as defined in (3.2), is obtained. In Section 2.1.1, it has been explained that in the case of heterogeneous networks, the difference in transmit powers between the macro BSs and the small cells is significant. Thus, the total received powers at the UEs from the macro BSs are typically larger than the received powers from the small cells, which are deployed in the coverage area of the macro BSs. Hence, the above mentioned selection strategy of the serving BS implies that the UEs attempt to connect to the macro BSs despite their proximity to the small cells. As a consequence, the macro

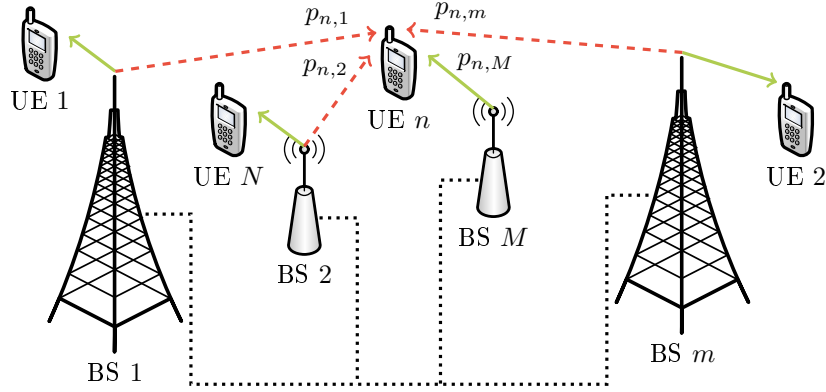


Figure 3.1. Mobile communication network of M BSs and N UEs in the downlink. For UE n , the solid arrow represents the serving link while the dashed arrows correspond to the interfering links. Connectivity between the BSs is achieved through backhaul links (dotted lines)

BSs need to serve a larger number of UEs while the available time/frequency/space resources at the small cells are underutilized. In order to achieve cell-splitting gain, an alternative serving BS selection method for heterogeneous networks is based on CRE techniques as mentioned in Section 2.2.1. In this work, both homogeneous macro-only and heterogeneous networks are studied, where for the latter case, CRE is applied. The $N \times M$ connection matrix \mathbf{C} is defined, with elements

$$c_{n,m} = \begin{cases} 1 & \text{if UE } n \text{ is served by BS } m \in \mathcal{M} \\ 0 & \text{otherwise,} \end{cases} \quad (3.3)$$

characterizing the serving conditions between BSs and UEs. It is assumed that only one BS serves UE n over all PRBs. Hence, it is worth noting that the PRB index is not considered in \mathbf{C} , and that

$$\sum_{m \in \mathcal{M}} c_{n,m} = 1 \quad \forall n \in \mathcal{N}. \quad (3.4)$$

It is further assumed for simplicity, that the UEs are quasi-static, such that no handover procedures are triggered between the BSs. Therefore, the connection matrix \mathbf{C} is assumed to be updated periodically at a much lower rate than the scheduling time and it is, thus, assumed to be constant during the considered operation time.

The set of indices of BSs within the cooperation cluster, that interfere with UE $n \in \mathcal{N}$ is defined as $\mathcal{I}_n = \{m \mid c_{n,m} = 0, \forall m \in \mathcal{M}\}$, with cardinality $|\mathcal{I}_n| = M - 1$. Moreover, since UE n experiences different interfering power levels from the interfering BSs indexed by \mathcal{I}_n , the set of indices of the M' *strongest interfering BSs* of UE n , denoted as \mathcal{I}'_n , with $\mathcal{I}'_n \subseteq \mathcal{I}_n$, $|\mathcal{I}'_n| = M'$, is defined such that

$$\min_{m' \in \mathcal{I}'_n} p_{n,m'} \geq \max_{m \in \mathcal{I}_n \setminus \mathcal{I}'_n} p_{n,m}, \quad (3.5)$$

i.e., the set \mathcal{I}'_n contains the indices of the M' interfering BSs with the highest total received powers at UE n , as calculated in (3.2). The number of strongest interfering BSs is bounded as $0 \leq M' \leq M - 1$, where the sets \mathcal{I}'_n and \mathcal{I}_n are identical if $M' = M - 1$. The sets \mathcal{I}_n and \mathcal{I}'_n apply for all PRBs in the reporting period.

One of the aspects of the cooperative schemes studied in this thesis, considers the cooperation between the BSs in form of power control, where the BSs reduce their own transmit powers in order to improve the interference conditions experienced by the UEs connected to neighboring BSs. As explained in Section 2.2.2, in some of the cooperative schemes the transmit power reduction method even mutes the BSs if it is considered beneficial for the network. At transmission time t , the transmit power of BS $m \in \mathcal{M}$ on PRB $l \in \mathcal{L}$ is controlled by the transmit power control parameter $\bar{\alpha}_{m,l}(t)$, with $0 \leq \bar{\alpha}_{m,l}(t) \leq 1$. Therefore, the transmit power of BS m on PRB l , denoted as $\phi_{m,l}$, is given by

$$\phi_{m,l}(t) = (1 - \bar{\alpha}_{m,l}(t)) \Phi_{m,l}, \quad (3.6)$$

with $\Phi_{m,l}$ corresponding to the maximum transmit power of BS m on PRB l , as introduced in (3.1). At the boundaries of $\bar{\alpha}_{m,l}(t)$, i.e., $\bar{\alpha}_{m,l}(t) = 0$ or $\bar{\alpha}_{m,l}(t) = 1$, BS m transmits with maximum transmit power $\Phi_{m,l}$ or, BS m is muted, respectively. In order to simplify the notation in the remainder of this document, the dependency of $\bar{\alpha}_{m,l}(t)$ on the transmission time t is ignored, except for the cases where differentiation between transmission times is required. Based on (3.1) and (3.6), the SINR on PRB l of UE n , which is served by BS $k \in \mathcal{M}$, is defined as the ratio between the average received signal power and the average received interference and noise powers, and it is given by

$$\gamma_{n,l}(\bar{\alpha}_l) = \frac{(1 - \bar{\alpha}_{k,l}) p_{n,k,l}}{I_{n,l}(\bar{\alpha}_l) + \sigma^2}, \quad (3.7)$$

where the $M \times 1$ vector $\bar{\alpha}_l = [\bar{\alpha}_{1,l}, \dots, \bar{\alpha}_{M,l}]^T$, with $[\cdot]^T$ denoting the transpose operation, contains the transmit power control parameters of all the M BSs on PRB l . The numerator corresponds to the average received power at UE n from the serving BS k on PRB l , with $p_{n,k,l}$ as defined in (3.1). The first term in the denominator, i.e., $I_{n,l}(\bar{\alpha}_l)$, corresponds to the average inter-cell interference power experienced by UE n on PRB l from the remaining BSs in the network, with

$$\begin{aligned} I_{n,l}(\bar{\alpha}_l) &= \sum_{m \in \mathcal{I}_n} (1 - \bar{\alpha}_{m,l}) p_{n,m,l} \\ &= \sum_{m' \in \mathcal{I}'_n} (1 - \bar{\alpha}_{m',l}) p_{n,m',l} + \sum_{m \in \mathcal{I}_n \setminus \mathcal{I}'_n} (1 - \bar{\alpha}_{m,l}) p_{n,m,l}. \end{aligned} \quad (3.8)$$

The second term in the denominator, i.e., σ^2 , is the additive white Gaussian noise (AWGN) power level assumed, without loss of generality, to be constant for all UEs over all PRBs.

The achievable data rate on PRB $l \in \mathcal{L}$ of UE $n \in \mathcal{N}$, denoted as $r_{n,l}$, is modeled as a function of the UE's SINR, as defined in (3.7). Hence,

$$r_{n,l} = f(\gamma_{n,l}), \quad (3.9)$$

where $f(\gamma_{n,l})$ denotes a mapping from the SINR on PRB l of UE n , to the achievable data rate.

Example 3.1. A widely used mapping based on Shannon's capacity bound is

$$f(\gamma_{n,l}) = D \log_2(1 + \gamma_{n,l}), \quad (3.10)$$

where the scaling factor D represents the PRB bandwidth and the selected MCS [FYL⁺11, rGPP16], and $\gamma_{n,l}$ is defined in (3.7). In (3.10), it is assumed without loss of generality, that all PRBs correspond to the same time-bandwidth product.

3.1 CSI Reports for non-Cooperative and Cooperative Schemes

In order to support the scheduling schemes for both, non-cooperative and cooperative approaches, knowledge about the achievable data rates of the UEs, i.e., $r_{n,l}$, $\forall n \in \mathcal{N}$, $\forall l \in \mathcal{L}$, as defined in (3.9) is required at the BSs. These achievable data rates depend on the values of the transmit power control parameters of all M BSs on PRB l , as expressed in $\bar{\alpha}_l$. Therefore, the BSs need to know the achievable data rates of their connected UEs for specific combinations of the transmit power control parameters, referred to as *interference scenarios*. For that purpose, CSI is estimated and reported by the UEs to the serving BSs. The CSI can be of different types, such as instantaneous channel coefficients, received powers from BSs, SINR values and average achievable data rates. In the following, a brief description of the main characteristics of the above mentioned CSI types is presented.

Instantaneous channel coefficients: this typically complex-valued type of CSI represents the channels between the BSs and UEs. In the case of SISO transmission, if CSI is available in form of the instantaneous channel coefficients $h_{n,m,l}$, $\forall n \in \mathcal{N}$, $\forall m \in \mathcal{M}$, $\forall l \in \mathcal{L}$, as introduced in (3.1), then the computation of the SINR, $\gamma_{n,l}(\bar{\alpha}_l)$, and the achievable data rates, $r_{n,l}$, as defined in (3.7) and (3.9), respectively, can be carried out in a straightforward manner for any possible interference scenario. Despite the great flexibility associated to the knowledge of CSI in form of instantaneous channel coefficients, the reporting process of such CSI represents a significant overhead. Each UE needs to report complex quantities per PRB, per BS, and per antenna link in the case of MIMO transmission.

Received powers: CSI in form of real-valued received powers at the UEs as defined in (3.1), is aggregated over the multiple antennas in the case of MIMO transmission. Thus, the signaling overhead is reduced in comparison to CSI in form of instantaneous channel coefficients. Nevertheless, in order to compute the achievable data rates, $r_{n,l}$, $\forall n \in \mathcal{N}$, $\forall l \in \mathcal{L}$, information related to each of the BSs in the network is still required in order to support the scheduling process for any possible interference scenario. Therefore, if the size of the network is large, the amount of CSI to be reported still represents a significant signaling overhead.

SINR values: this continuous real-valued type of CSI is calculated as given by (3.7) for a specific interference scenario. Therefore, the amount of SINR values that need to be reported per UE is equivalent to the number of interference scenarios under investigation. If the number of interference scenarios considered for CoMP operation is large, and taking into account the continuous nature of the SINR values, the signaling overhead in terms of bits can still be prohibitive.

Average achievable data rates: CSI in form of achievable data rates as defined in (3.9), can be calculated for any level of granularity, starting from a single subcarrier and ending in a wide-band achievable data rate value. As mentioned in Example 3.1, the achievable data rates are typically calculated with the logarithmic function of the SINR according to the Shannon's capacity bound. Therefore, similar to the case of CSI in form of SINR values, multiple achievable data rates need to be reported as the number of interference scenarios under investigation. However, in contrast to the continuous real-valued SINR information, these achievable data rates generally correspond to a finite MCS in practical networks. Thus, the achievable data rates are characterized by discrete indices which can be reported with less bits as compared to the CSI in form of SINR values.

In the literature it is common to assume perfect CSI knowledge in form of the instantaneous channel coefficients as described above. In this dissertation, one of the major contributions is to study the mobile communication networks from a more practical perspective. Therefore, in this work it is assumed that the CSI is reported as standardized for LTE and LTE-Advanced networks, as described in Section 2.1.3. Thus, CSI is considered to be in form of average achievable data rates, in the following referred to as CSI reports, where each CSI report describes the average achievable data rates for a specific interference scenario. Furthermore, the CSI reports are differentiated according to the type of reference signals used for their calculation. Hence, the $\text{CSI}^{\text{R-8}}$ reports refer to CSI reports generated from LTE Release-8 CRSs, while the $\text{CSI}^{\text{R-11}}$ reports are generated based on LTE-Advanced CSI-RSs. The information provided by the $\text{CSI}^{\text{R-8}}$ reports supports one particular interference scenario corresponding to the non-cooperative case, where all BSs constantly transmit with maximum transmit power over all PRBs. The information provided by multiple $\text{CSI}^{\text{R-11}}$ reports reflects different interference scenarios, including the non-cooperative case. In the following chapters, it is assumed that a total of J interference scenarios are signaled by the $\text{CSI}^{\text{R-11}}$ reports, with each interference scenario addressed by the index set $\mathcal{J} = \{1, \dots, J\}$. For interference scenario $j \in \mathcal{J}$, the $\text{CSI}^{\text{R-11}}$ report contains the information of the SINR and achievable data rate on PRB $l \in \mathcal{L}$ of UE $n \in \mathcal{N}$, denoted as $\gamma_{n,l,j}$ and $r_{n,l,j}$, respectively, which follow the definitions in (3.7) and (3.9).

In Section 2.1.3, the timing of the CSI reports has been depicted in Figure 2.5, where the CSI report \mathcal{R}_0 is generated at the transmission time T and it is used at the transmission times $T + \delta \leq t \leq 2T + \delta$. It is possible that the transmit power control parameters, and hence, the interference scenario, vary from the time when the CSI report is generated, to the moment when the CSI report is actually used. Moreover, some CSI reports can even represent hypothetical interference scenarios. Therefore, the transmit power

control parameters used for transmission, and for the generation of the CSI reports, are distinguished as follows. The variable $\alpha_{m,l}$ describes the transmit power control parameter of BS $m \in \mathcal{M}$ on PRB $l \in \mathcal{L}$, as *assumed* in the generation of the CSI report. On the other hand, the variable $\bar{\alpha}_{m,l}$ refers to the transmit power control parameter used at the current transmission time, as a result of the implementation of the cooperative schemes under investigation.

Example 3.2. *The CSI^{R-8} reports support only one interference scenario, i.e., $J = 1$, where $\alpha = \bar{\alpha} = \mathbf{0}_{M \times L}$, where $\mathbf{0}_{M \times L}$ is an $M \times L$ matrix with zero elements. Therefore, in the non-cooperative case, all BSs transmit with maximum transmit power $\Phi_{m,l}$, $\forall m \in \mathcal{M}$, $\forall l \in \mathcal{L}$, as introduced in (3.1).*

Example 3.3. *In a specific CSI-RS configuration, BS $m \in \mathcal{M}$ can be defined as not transmitting, i.e., muted, so that the CSI^{R-11} report provides information regarding the achievable data rates for CS with muting. In that case, the CSI^{R-11} report assumes the transmit power control parameters to be $\alpha = \mathbf{0}_{M \times L}^m$, where $\mathbf{0}_{M \times L}^m$ is an $M \times L$ matrix with zero elements in all but the m -th row, which contains one elements. If at the time of generating the CSI^{R-11} report, the set $\tilde{\mathcal{M}}$ of BSs such that $\phi_{\tilde{m},l} < \Phi_{\tilde{m},l}$, $\tilde{m} \neq m$, $\forall \tilde{m} \in \tilde{\mathcal{M}}$, $\forall l \in \mathcal{L}$, is not empty, then $\alpha \neq \bar{\alpha}$.*

In order to reduce the signaling overhead and the number of studied interference scenarios, as denoted by J , the proposed schemes consider the cooperation of a subset of interfering BSs per UE $n \in \mathcal{N}$. The set of indices of cooperative interfering BSs of UE n is denoted by \mathcal{I}_n^c , with $\mathcal{I}_n^c \subseteq \mathcal{I}_n' \subseteq \mathcal{I}_n$. In the following chapters, a detailed description of the BSs that belong to the set \mathcal{I}_n^c is given according to the studied cooperative scheme.

3.2 Scheduling Strategy

In downlink transmissions, the BSs can apply different scheduling strategies in order to serve the connected UEs such as RR or PF scheduling [TV05, WMMZ11, ZH07]. In the former scheduling strategy, the BSs attempt to distribute the time/frequency resources in a fair fashion among the served UEs. Although the RR scheduler is fair in terms of scheduled time/frequency resources, this strategy negatively affects the spectral efficiency of the network since the opportunity to exploit *favorable* channel conditions is limited by the fairness constraint. In the case of the opportunistic PF scheduler, a trade-off between user throughput and fairness is pursued, where the objective is to maximize the sum over all UEs, of the PF metrics given by

$$\Omega_n = \frac{r_n}{R_n} \quad \forall n \in \mathcal{N}. \quad (3.11)$$

For UE $n \in \mathcal{N}$, the ratio between the total instantaneous achievable data rate and the average user throughput over time, denoted by r_n and R_n , respectively, is considered in (3.11). The total instantaneous achievable data rate of UE n is calculated as

$$r_n = g(r_{n,l,j}, \bar{\alpha}) \quad \forall l \in \tilde{\mathcal{L}}_n, \forall j \in \mathcal{J}, \quad (3.12)$$

where $g(\cdot)$ denotes a function of the achievable data rates of UE n , as defined in (3.9), over the PRBs scheduled to UE n as described by the index set $\check{\mathcal{L}}_n$, and the matrix $\bar{\alpha}$ of transmit power control parameters. The average user throughput over time of UE n at transmission time t is defined by an averaging window and it is updated based on the scheduling decisions made at the previous transmission time $t - 1$. Therefore,

$$R_n(t) = \kappa R_n(t - 1) + (1 - \kappa) r_n(t - 1), \quad (3.13)$$

with $\kappa = 0.97$, denoting the forgetting factor parameter used to trade off user throughput and fairness [Mot06]. The total instantaneous achievable data rate of UE n , at the previous transmission time, denoted by $r_n(t - 1)$, is calculated as given by e.g., (3.12). Hence, the PF scheduler serves the UEs experiencing favorable channel conditions, and thus, having high total instantaneous achievable data rates, together with the UEs that have not been served for a certain period, which have a low average user throughput over time.

In this dissertation, both, non-cooperative and cooperative schemes are based on a PF scheduler, where it is assumed without loss of generality that single-user transmissions are carried out, i.e., each available PRB is scheduled to only one UE per BS.

Chapter 4

Cooperative Power Control for Hierarchical Mobile Communication Networks

In this chapter, cooperative power control is studied in a heterogeneous network operating under the License Shared Access (LSA) principle [Rad11]. The incumbent network, corresponding to the small cells, owns the available time/frequency resources. The licensee system is represented by the macro BSs which are allowed to transmit on the same time/frequency resources as the small cells, if minimum requirements regarding the SINR and the equivalent achievable data rates of the UEs connected to the small cells are satisfied. As explained in Section 2.1.1, the difference in the transmit powers of the macro and small cells is significant. Therefore, the cooperative scheme investigated in this chapter, dynamically applies a power control procedure which decreases the transmit power of the macro BS in order to reduce the interference experienced by the UEs connected to the small cells. If required, the macro BSs can even mute transmissions on particular time/frequency resources, which resembles the CoMP DPB scheme as described in Section 2.2.2.

In order to support the cooperative power control method, a minimum number of $\text{CSI}^{\text{R-11}}$ reports as explained in Section 2.1.3 is required. These $\text{CSI}^{\text{R-11}}$ reports, reflect the behavior of the incumbent network with and without the interference caused by the licensee system. Thus, the derived cooperative scheme calculates the required transmit power reduction of the macro BSs to fulfill the achievable data rate requirements of the UEs connected to the small cells.

One major difference of the cooperative scheme investigated in this chapter, with respect to the cooperative schemes derived in the remaining chapters, is the separation between the scheduling and the power control procedures. Given the assumption of an LSA framework in this chapter, the macro and small cells make independent scheduling decisions based on their individual objectives of maximizing their PF metrics as introduced in Section 3.2. Once the scheduling decisions are made, the macro BSs apply the cooperative power control procedure. In contrast, the remaining chapters focus on CoMP CS, where the scheduling and power control decisions are jointly made by the cooperative BSs in the network.

4.1 State-of-the-art and Contributions

In order to reduce the inter-cell interference, power control is one of the most studied approaches in cellular communication networks. In the specific case of heterogeneous

networks, a plethora of schemes are available in the literature for uplink and downlink transmissions with some examples described as follows.

In [MBS⁺10], joint cell association and power control is studied in order to enhance the user throughput of the heterogeneous networks. With regard to the power control, semi-static and dynamic approaches are considered. In the semi-static approaches, frequency reuse patterns are defined which are used for a long time span, while in the dynamic case, the transmit powers of the BSs are calculated on a transmission time basis. Due to the complexity of the optimization problem, iterative algorithms are used to solve the joint formulation in [MBS⁺10]. A similar problem is studied by the authors in [CHS⁺14], where the macro BSs vary their own transmit powers in order to adapt the user association and the inter-cell interference. The power control only applies for a predefined set of frequency resources, named the *capacity band*, while on the remaining frequency resources the macro BSs transmit with maximum transmit power. Moreover, the power reduction is equally applied for all the frequency resources in the capacity band. Another approach that applies fractional frequency reuse, i.e., less than the maximum transmit power is applied on certain frequency bands, is proposed in [LHXQ13] for a heterogeneous network with predefined user association. In order to maximize the long-term log-scale user throughput, the proposed optimal fractional frequency reuse scheme determines then, the size of the frequency bands and the transmit power on each of them. With respect to the scheduling, the served UEs are pre-assigned to the corresponding frequency bands. Thus, the flexibility of the applied scheduler is limited to these pre-assigned frequency bands per UE. With respect to CoMP, the discussion in [CKL⁺11] considers a different deployment scenario, where the small cells are part of the macro BS in the form of Remote Radio Heads (RRHs). In order to reduce the interference in the resulting Distributed Antenna System (DAS), great flexibility on the selection of the serving cells and the possibility to apply power control for specific RRHs is ensured. Nevertheless, high demanding requirements on the backhaul connections and the complexity imposed to the algorithms applied by the macro BSs, represent a challenge for the implementation of such DASs. Furthermore, the schemes proposed in [FSCK10] study CoMP DPS/DPB, where the power control consists of binary decisions on whether to transmit with maximum transmit power or to mute the BSs on particular time/frequency resources. With exception of the approach in [FSCK10], the above mentioned schemes do not consider limitations on the knowledge of CSI. Thus, it is assumed that instantaneous channel coefficients are available at a central entity to carry out the power control schemes.

The cooperative power control scheme studied in this chapter is derived in relation to a heterogeneous network operating under the LSA principle. In that case, the objective of the cooperation is to ensure that the simultaneous transmissions of the licensee system, i.e., the macro BSs, have a limited impact on the performance in terms of user throughput of the incumbent users, i.e., the UEs connected to the small cells. In [NTP15], a coordinated beamforming scheme is proposed, where in contrast to the scheme investigated in this dissertation, the licensee system corresponds to the small cells deployed within the coverage area of a macro BS, which is considered to be the incumbent transmitter.

The major contributions of this chapter are summarized as follows.

- In order to enhance the user throughput of the UEs connected to the small cells, which are located within the coverage area of the macro BSs, a cooperative power control scheme is proposed where the macro BSs reduce their own transmit powers to reduce the interference in the small cells.
- The studied cooperative power control scheme requires a minimum exchange of CSI^{R-11} reports between the macro and small cells, in order to dynamically select the transmit power of the macro BSs on a PRB basis.
- The formulated problem is solved by close-form expressions with low computational complexity. Thus, the proposed method is applicable for large-size heterogeneous networks and/or for networks with limited backhaul and computation capabilities.

4.2 System Model

In this section, the system model of Chapter 3 is extended to the particular scenario under investigation, which consists of a heterogeneous cellular network where M macro BSs and S small cells operating in FDD mode, serve N UEs in the downlink. At each transmission time, all BSs, i.e., macro and small cells, can make use of the same L PRBs for transmission, provided that the UEs connected to the small cells achieve a certain user throughput under the inter-cell interference caused by the macro BSs. The set of indices $\mathcal{M} = \{1, \dots, M\}$, $\mathcal{S} = \{1, \dots, S\}$, $\mathcal{N} = \{1, \dots, N\}$ and $\mathcal{L} = \{1, \dots, L\}$ are used to address the macro BSs, the small cells, the UEs and the PRBs, respectively. Moreover, the set of indices $\mathcal{S}_m \subsetneq \mathcal{S}, \forall m \in \mathcal{M}$ is defined to indicate the indices of the small cells located within the coverage area of the macro BS m , where it is assumed that each small cell is associated to only one macro BS. Thus,

$$\mathcal{S}_b \cap \mathcal{S}_k = \emptyset \quad \forall b, k \in \mathcal{M} \mid b \neq k, \quad (4.1)$$

where \emptyset denotes the empty set.

A cooperation cluster is formed by one macro BS $m \in \mathcal{M}$, in the following referred to as the *cooperative macro BS*, and the small cells located within its coverage area, i.e., BS $k, \forall k \in \mathcal{S}$ such that $k \in \mathcal{S}_m$. In order to reduce the interference caused to the UEs connected to the small cells in the cooperation cluster, a cooperative power control scheme is carried out by the cooperative macro BS. A cooperation cluster is illustrated in Figure 4.1, where it is assumed that the cooperative macro BS m is connected through an ideal backhaul link to the small cell BS k . In the following, the discussion is focused on a single cooperation cluster as illustrated in Figure 4.1, with the remaining cooperation clusters in the heterogeneous network behaving similarly.

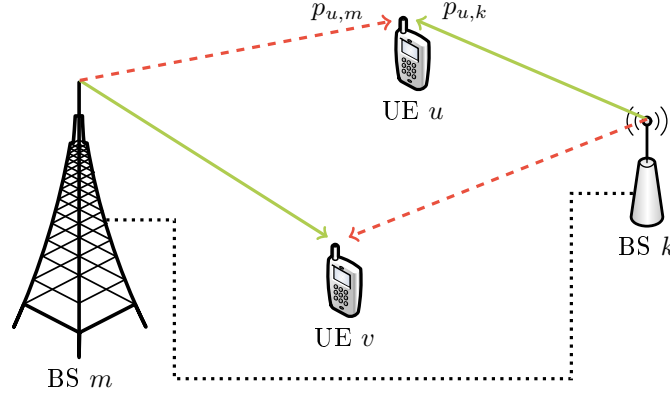


Figure 4.1. Cooperation cluster consisting of one cooperative macro BS m and a small cell BS k to improve the performance of the UE u , connected to the BS k . The solid arrows represent the serving links, while the dashed arrows correspond to the interfering links. Connectivity between the BSs is achieved through backhaul links (dotted lines)

The received powers at UE $n \in \mathcal{N}$ from macro BS $m \in \mathcal{M}$ on PRB $l \in \mathcal{L}$, denoted as $p_{n,m,l}$, and from small cell BS $k, \forall k \in \mathcal{S}$ such that $k \in \mathcal{S}_m$, denoted as $p_{n,k,l}$, are defined according to (3.1), where $\Phi_{m,l}$ and $\Phi_{k,l}$ correspond to the maximum transmit powers of macro BS m and small cell BS k , respectively. Furthermore, the total received powers at UE n from BS m and BS k , denoted as $p_{n,m}$ and $p_{n,k}$, respectively, are calculated as in (3.2). As previously discussed in Sections 2.1.1 and 2.2.1, one of the benefits of implementing heterogeneous networks is the possibility of achieving cell-splitting gains, where additional PRBs are in average available per UE. However, in order to achieve these cell-splitting gains, load balancing is necessary, i.e., a *fair* distribution of served UEs among the macro BSs and the small cells. Due to the significant difference between the transmit powers from the macro BSs and the small cells, where $\Phi_{m,l} > \Phi_{k,l}, \forall m \in \mathcal{M}, \forall k \in \mathcal{S}$, the load balancing is negatively affected. Thus, in this chapter it is assumed that CRE is applied, where the serving BS for UE n is selected as the BS providing the maximum received power after adding a constant off-set to the received power from the small cells. Mathematically, the serving BS for UE n is defined as

$$\arg \max_{b \in \mathcal{M} \cup \mathcal{S}} p_{n,b} + \varphi_b, \quad (4.2)$$

where $p_{n,b}$ is calculated as in (3.2), and the CRE off-set parameter, denoted as φ_b , is given by

$$\varphi_b = \begin{cases} 0 & \text{if BS } b \in \mathcal{M} \\ \tilde{\Phi} & \text{if BS } b \in \mathcal{S}, \end{cases} \quad (4.3)$$

with $\tilde{\Phi}$ a constant value. Thus, the connection matrix \mathbf{C} of size $N \times M + S$ is defined similarly to (3.3), with elements

$$c_{n,b} = \begin{cases} 1 & \text{if UE } n \text{ is served by BS } b \in \mathcal{M} \cup \mathcal{S} \\ 0 & \text{otherwise,} \end{cases} \quad (4.4)$$

characterizing the serving conditions between BSs and UEs. Given that the cooperation takes place between the macro BS m and the small cells located within its coverage area, the set of indices of cooperative interfering BSs of UE n , introduced in Chapter 3, is given by

$$\mathcal{I}_n^c = \begin{cases} \{m\} & \text{if } c_{n,k} = 1, \forall m \in \mathcal{M}, \forall k \in \mathcal{S} \mid k \in \mathcal{S}_m \\ \emptyset & \text{otherwise.} \end{cases} \quad (4.5)$$

Therefore, the macro BS m is considered as the cooperative interfering BS of the UEs served by the small cells, located within the coverage area of BS m . On the other hand, the UEs connected to the macro BSs do not require cooperation, since these UEs belong to the licensee system, and thus, the index set of cooperative interfering BSs is empty.

Example 4.1. In Figure 4.1 an exemplary cooperation cluster is illustrated, where UE u is served by the small cell BS k as depicted by the solid green arrow, i.e., $c_{u,k} = 1$. Therefore, UE u experiences interference from BS m as illustrated by the dashed red arrow, with $c_{u,m} = 0$. Similarly, UE v is served by BS m , i.e., $c_{v,m} = 1$ and experiences interference from the small cell BS k , i.e., $c_{v,k} = 0$. Furthermore, the sets of indices of cooperative interfering BSs of UE u and UE v are $\mathcal{I}_u^c = \{m\}$ and $\mathcal{I}_v^c = \emptyset$, respectively.

The objective of the cooperative power control scheme carried out at the macro BS $m \in \mathcal{M}$, is to reduce the interference experienced by the UEs connected to the small cells located within its coverage area. For that purpose, the cooperative macro BS m scales its maximum transmit power on PRB $l \in \mathcal{L}$, according to the transmit power control parameter $\bar{\alpha}_{m,l}$, with $0 \leq \bar{\alpha}_{m,l} \leq 1$, as introduced in Chapter 3. In the following, the transmit power control parameter is referred to as the *transmit power scaling factor*. Based on (3.7), the SINR on PRB l of UE $u \in \mathcal{N}$, connected to the small cell BS $k, \forall k \in \mathcal{S}$ such that $k \in \mathcal{S}_m$, is defined as

$$\gamma_{u,l}^{\text{sc}}(\bar{\alpha}_l) = \frac{p_{u,k,l}}{I_{u,l}^c(\bar{\alpha}_l) + I_{u,l}^{\text{nc-sc}}(\bar{\alpha}_l) + \sigma^2}, \quad (4.6)$$

where the $M \times 1$ vector $\bar{\alpha}_l$ contains the transmit power scaling factors of all the macro BSs in the network on PRB l . It is assumed, without loss of generality, that the small cells always transmit with maximum transmit power, i.e., $\Phi_{k,l}, \forall k \in \mathcal{S}, \forall l \in \mathcal{L}$. Thus, the numerator of (4.6) describes the average received power at UE u from the serving BS k on PRB l , without any transmit power scaling factor or, in other words, $\alpha_{k,l} = 0, \forall k \in \mathcal{S}, \forall l \in \mathcal{L}$. The denominator in (4.6) consists of the inter-cell interference and the noise powers at UE u on PRB l . The first term in the denominator corresponds to the interference from the cooperative macro BS m , denoted by $I_{u,l}^c$ and defined as

$$I_{u,l}^c(\bar{\alpha}_l) = (1 - \bar{\alpha}_{m,l}) p_{u,m,l}, \quad (4.7)$$

where the dependency on the transmit power scaling factor $\bar{\alpha}_{m,l}$ is highlighted. The interference from the remaining BSs in the network is given by

$$I_{u,l}^{\text{nc-sc}}(\bar{\alpha}_l) = \sum_{b \in \mathcal{M} \setminus \mathcal{I}_u^c} (1 - \bar{\alpha}_{b,l}) p_{u,b,l} + \sum_{k' \in \mathcal{S} \mid k' \neq k} p_{u,k',l}, \quad (4.8)$$

with the first term corresponding to the interference from the additional macro BSs in the network, and the second, representing the interference from the remaining small cells. Again, the dependency on the transmit power scaling factor is highlighted for the interference caused by the remaining macro BSs. The AWGN power is denoted by σ^2 , which is assumed without loss of generality to be constant for all UEs over all PRBs. Similarly, the SINR on PRB l of UE $v \in \mathcal{N}$, connected to the cooperative macro BS m , is defined as

$$\gamma_{v,l}^{\text{mc}}(\bar{\alpha}_l) = \frac{(1 - \bar{\alpha}_{m,l}) p_{v,m,l}}{I_{v,l}^{\text{nc-mc}}(\bar{\alpha}_l) + \sigma^2}, \quad (4.9)$$

where the numerator corresponds to the average received power at UE v from the serving macro BS m on PRB l , which depends on the transmit power scaling factor $\bar{\alpha}_{m,l}$. The denominator is composed by the inter-cell interference at UE v on PRB l , given by

$$I_{v,l}^{\text{nc-mc}}(\bar{\alpha}_l) = \sum_{b \in \mathcal{M} \mid b \neq m} (1 - \bar{\alpha}_{b,l}) p_{v,b,l} + \sum_{k' \in \mathcal{S}} p_{v,k',l}, \quad (4.10)$$

and the noise power σ^2 . Furthermore, the achievable data rate on PRB l of UE $n \in \mathcal{N}$ is defined as in (3.9), where the SINR on PRB l of UE n depends on the serving BS for UE n , such that

$$\gamma_{n,l} = \begin{cases} \gamma_{n,l}^{\text{sc}} & \text{if UE } n \text{ is served by BS } k \in \mathcal{S} \\ \gamma_{n,l}^{\text{mc}} & \text{if UE } n \text{ is served by BS } m \in \mathcal{M}, \end{cases} \quad (4.11)$$

with $\gamma_{n,l}^{\text{sc}}$ and $\gamma_{n,l}^{\text{mc}}$ defined in (4.6) and (4.9), respectively.

Definition 4.1. *In this chapter, the achievable data rate on PRB $l \in \mathcal{L}$ of UE $n \in \mathcal{N}$ is calculated with the function $f(\gamma_{n,l})$, as given by (3.10) in Example 3.1, where the SINR on PRB l of UE n is calculated as in (4.11).*

4.2.1 Available CSI reports

In order to support the scheduling and cooperative power control procedures, CSI at the transmitters, i.e., at the BSs, is required. In this section, it is assumed that CSI is available at the BSs in form of the CSI^{R-11} reports as explained in Section 3.1. In the following, a description of the different CSI^{R-11} reports generated by the UEs and used by the BSs is presented, where the $M \times L$ matrix α is employed in order to refer to the assumed transmit power scaling factors of all M macro BSs over all L PRBs, associated to a specific CSI^{R-11} report.

CSI reports for scheduling and link adaptation

From a network perspective, all the N UEs generate CSI^{R-11} reports to support the scheduling and link adaptation procedures, which are carried out at the serving BSs.

In order to calculate the achievable data rates of UE n , denoted by $r_{n,l}$, as given in Definition 4.1, the UEs use the SINR values, $\gamma_{n,l}$, $\forall n \in \mathcal{N}$, $\forall l \in \mathcal{L}$, as defined in (4.11), in the generation of the CSI^{R-11} reports. Thus, the achievable data rates $r_{n,l}$, signaled in the CSI^{R-11} reports, reflect the values of the transmit power scaling factors $\bar{\alpha}$, for the M macro BSs, which were used at the time of generating such CSI^{R-11} reports. Therefore, $\alpha = \bar{\alpha}$.

CSI reports for cooperative power control scheme

At each cooperation cluster with cooperative macro BS $m \in \mathcal{M}$ and small cells indexed by \mathcal{S}_m , the UEs connected to the small cells, i.e., UE n , $\forall n \in \mathcal{N}$, $\forall k \in \mathcal{S}_m \mid c_{n,k} = 1$, generate additional CSI^{R-11} reports to support the cooperative power control scheme carried out at the cooperative macro BS m . As explained in Section 3.1, the additional CSI^{R-11} reports reflect different interference scenarios with respect to the transmit power of the cooperative macro BS m . A total of $J = 2$ additional interference scenarios are considered as follows.

In a first interference scenario, the cooperative macro BS $m \in \mathcal{M}$ is assumed to transmit with maximum transmit power $\Phi_{m,l}$, $\forall l \in \mathcal{L}$, i.e., the macro BS does not cooperate with the small cells located within its coverage area. Thus, from (4.6), the SINR on PRB l of UE $n \in \mathcal{N}$, connected to the small cell BS $k \in \mathcal{S}$, located within the coverage area of the macro BS m such that $k \in \mathcal{S}_m$, is defined as

$$\gamma_{n,l,j_m^0} = \frac{p_{n,k,l}}{p_{n,m,l} + z_{n,l}}. \quad (4.12)$$

In (4.12), the index j_m^0 is used to indicate the interference scenario with the transmit power scaling factor of the cooperative macro BS m considered to be $\alpha_{m,l} = 0$, $\forall l \in \mathcal{L}$, and the term $z_{n,l}$, contains the inter-cell interference from the remaining BSs and the noise power on PRB l . A second interference scenario considered in the CSI^{R-11} reports, denoted as j_m^1 , assumes the cooperative macro BS m to abstain from transmitting, i.e., $\alpha_{m,l} = 1$, $\forall l \in \mathcal{L}$. Therefore, the SINR on PRB l of UE n under the assumption of no interference from the cooperative macro BS m , is given by

$$\gamma_{n,l,j_m^1} = \frac{p_{n,k,l}}{z_{n,l}}. \quad (4.13)$$

It is worth noting that given the definition of the cooperation cluster with cooperative interfering BSs as in (4.5), the UEs connected to the small cells located within the coverage area of the cooperative macro BS m , are not aware of the transmit power scaling factors applied by the remaining macro BSs in the network. Therefore, it is assumed that the inter-cell interference from the remaining BSs in the network, i.e., $z_{n,l}$, is constant in the calculation of the different CSI^{R-11} reports used to support the cooperative power control scheme as defined in (4.12) and (4.13). Thus, based on (4.8),

$$z_{n,l} = \sum_{b \in \mathcal{M} \setminus \mathcal{I}_n^c} p_{n,b,l} + \sum_{k' \in \mathcal{S} \mid k' \neq k} p_{n,k',l} + \sigma^2, \quad (4.14)$$

Table 4.1. Summary of the $\text{CSI}^{\text{R-11}}$ reports generated by UE u , served by the small cell BS k on PRB l

$\text{CSI}^{\text{R-11}}$ report index	Data rate	SINR	$\alpha_{m,l}$	$\alpha_{b,l}$ $\forall b \in \mathcal{M} \mid b \neq m$	Description
1	$r_{u,l}$	$\gamma_{n,l}^{\text{sc}}$	$\bar{\alpha}_{m,l}$	$\bar{\alpha}_{b,l}$	Used for scheduling
2	r_{u,l,j_m^0}	γ_{n,l,j_m^0}	0	1	Macro BS m transmits
3	r_{u,l,j_m^1}	γ_{n,l,j_m^1}	1	1	Macro BS m muted

where it is assumed without loss of generality, that all the remaining macro BSs transmit with maximum transmit power, i.e., $\alpha_{b,l} = 0, \forall b \in \mathcal{M} \mid b \neq m$, in order to generate conservative $\text{CSI}^{\text{R-11}}$ reports. Based on the assumption on the inter-cell interference from (4.14), the interference scenarios defined in (4.12) and (4.13) represent the lower and upper bounds, respectively, of the SINR on PRB l of UE n , with respect to the interference caused by the cooperative macro BS m .

As explained in Section 2.1.3, in order to reduce signaling overhead, the $\text{CSI}^{\text{R-11}}$ reports supported in LTE-Advanced contain information of the achievable data rates as given in Definition 4.1. As previously mentioned, the UEs connected to the small cell BS $k \in \mathcal{S}$ located within the coverage area of the macro BS $m \in \mathcal{M}$, such that $k \in \mathcal{S}_m$, generate two additional $\text{CSI}^{\text{R-11}}$ reports to support the cooperative power control scheme. Therefore, the additional $\text{CSI}^{\text{R-11}}$ reports correspond to the interference scenarios with the cooperative macro BS m either transmitting with maximum transmit power, or muted. These two interference scenarios are then described by the achievable data rates, denoted as r_{n,l,j_m^0} and r_{n,l,j_m^1} , $\forall n \in \mathcal{N} \mid c_{n,k} = 1, \forall l \in \mathcal{L}$, respectively. In order to support the cooperative power control scheme, it is assumed that the BSs are able to translate the reported achievable data rates into the corresponding experienced SINRs by applying Definition 4.1.

Example 4.2. *Continuing with the exemplary cooperation cluster from Example 4.1, Table 4.1 summarizes the $\text{CSI}^{\text{R-11}}$ reports generated by UE u , which is served by the small cell BS k on PRB $l \in \mathcal{L}$. It is assumed that BS m corresponds to the cooperative macro BS, i.e., $\mathcal{I}_u^c = \{m\}$.*

4.2.2 Scheduling strategy

Supported by the $\text{CSI}^{\text{R-11}}$ reports, the BSs in the cooperation cluster, i.e., the macro BS and the small cells located within its coverage area, independently perform the scheduling procedure. In Section 3.2, the PF scheduler has been introduced, where the BSs pursue a trade-off between user throughput and fairness. In this chapter, it is assumed without loss of generality, that the BSs apply the PF scheduling strategy,

where single-user transmissions are carried out. That is, each BS assigns one UE per available PRB.

After the scheduling decisions are made, these decisions are transmitted from the small cells to the cooperative macro BS, together with the CSI^{R-11} reports of the UEs to be served, in order for the cooperative macro BS to perform the cooperative power control scheme.

4.3 Power Control Scheme

The description of the cooperative power control scheme is focused on a single cooperation cluster with cooperative macro BS $m \in \mathcal{M}$ and small cells BS $k, \forall k \in \mathcal{S}$ such that $k \in \mathcal{S}_m$. It is assumed that the remaining cooperation clusters in the network behave similarly. For the UE $n \in \mathcal{N}$ to be served by the small cell BS k on PRB $l \in \mathcal{L}$, the impact of the interference caused by the cooperative macro BS m , with respect to the additional interference and noise $z_{n,l}$, as introduced in (4.14), is defined as

$$\bar{\gamma}_{n,l} = \frac{p_{n,m,l}}{z_{n,l}} = \frac{\gamma_{n,l,j_m^1}}{\gamma_{n,l,j_m^0}} - 1, \quad (4.15)$$

where the information from the CSI^{R-11} reports, for the interference scenarios with and without interference from the cooperative macro BS m , denoted as j_m^0 and j_m^1 as given in (4.12) and (4.13), respectively, has been used. The impact coefficient $\bar{\gamma}_{n,l}$, as defined in (4.15), indicates the influence of the cooperative macro BS m on UE n to be served on PRB l . That is, if $\bar{\gamma}_{n,l} = 0$, UE n does not experience interference from the cooperative macro BS m , and if $\bar{\gamma}_{n,l}$ is large, the interference experienced by UE n from the cooperative macro BS m on PRB l is significant, and thus, UE n can benefit from any reduction on the transmit power of the cooperative macro BS m .

With respect to the interference scenario where the cooperative macro BS $m \in \mathcal{M}$ transmits with maximum transmit power $\Phi_{m,l}$ on PRB $l \in \mathcal{L}$, denoted by j_m^0 , the achievable data rate gain on PRB l of UE $n \in \mathcal{N}$, to be served by the small cell BS $k \in \mathcal{S}$ such that $k \in \mathcal{S}_m$, is defined as

$$\eta_{n,l} = \frac{r_{n,l}(\bar{\alpha}_{m,l}^n)}{r_{n,l,j_m^0}} = \frac{D \log_2(1 + \gamma_{n,l})}{D \log_2(1 + \gamma_{n,l,j_m^0})}, \quad (4.16)$$

where the numerator corresponds to the achievable data rate on PRB l of UE n , with the cooperative macro BS m transmitting with transmit power scaling factor $\bar{\alpha}_{m,l}^n$. For the calculation of the achievable data rates in (4.16), Definition 4.1 with scaling factor D is used under the assumption of the remaining interference and noise being defined as in (4.14). The achievable data rate gain of UE n to be served on PRB l , i.e., $\eta_{n,l}$, is considered to be a design parameter and it is therefore, known by the cooperative

macro BS m . Hence, in order to obtain the design achievable data rate gain $\eta_{n,l}$, the required SINR of UE n to be served on PRB l , is given by

$$\gamma_{n,l} = (1 + \gamma_{n,l,j_m^0})^{\eta_{n,l}} - 1, \quad (4.17)$$

where the property of logarithms

$$\log_x(a^y) = y \log_x(a), \quad (4.18)$$

has been used in (4.16).

Furthermore, the SINR gain of UE $n \in \mathcal{N}$ to be served on PRB $l \in \mathcal{L}$, required to obtain the design achievable data rate gain $\eta_{n,l}$, is defined as

$$\Gamma_{n,l} = \frac{\gamma_{n,l}}{\gamma_{n,l,j_m^0}}, \quad (4.19)$$

where $\gamma_{n,l}$ is calculated according to (4.17), and γ_{n,l,j_m^0} is obtained from the CSI^{R-11} reports as defined in (4.12). Similar to the design achievable data rate gain $\eta_{n,l}$, the SINR gain of UE n to be served on PRB l is considered to be known by the cooperative macro BS $m \in \mathcal{M}$. The goal of the cooperative power control scheme is to determine the transmit power scaling factor of the cooperative macro BS m , in order to enhance the achievable data rate on PRB l of UE n , to be served by the small cell BS $k \in \mathcal{S}$ such that $k \in \mathcal{S}_m$, denoted as $\bar{\alpha}_{m,l}^n$. For that purpose, the SINR gain of UE n to be served on PRB l , $\Gamma_{n,l}$, is redefined based on the calculation of $\gamma_{n,l}$ as in (4.6), such that

$$\Gamma_{n,l} = \frac{p_{n,m,l} + z_{n,l}}{(1 - \bar{\alpha}_{m,l}^n) p_{n,m,l} + z_{m,l}}, \quad (4.20)$$

with the additional interference and noise powers given in (4.14). Based on the definition in (4.15) of the impact coefficient $\bar{\gamma}_{n,l}$, and by solving from the SINR gain $\Gamma_{n,l}$, given in (4.20), the required transmit power scaling factor of the cooperative macro BS m , to obtain the design achievable data rate gain $\eta_{n,l}$, is defined as

$$\bar{\alpha}_{m,l}^n(\eta_{n,l}) = 1 - \frac{\bar{\gamma}_{n,l} - \Gamma_{n,l} + 1}{\bar{\gamma}_{n,l} \Gamma_{n,l}}. \quad (4.21)$$

Moreover, in the case that multiple small cells are located within the coverage area of the cooperative macro BS m , the transmit power scaling factor of the cooperative macro BS m corresponds to the maximum required value, among the UEs to be served by the small cells on PRB l . Therefore, by denoting the set of UEs to be served on PRB l by the small cells, which are located within the coverage area of the cooperative macro BS m , as $\mathcal{N}_{m,l}^{\text{sc}}$, the selected transmit power scaling factor of the cooperative macro BS m is

$$\bar{\alpha}_{m,l} = \max_{n \in \mathcal{N}_{m,l}^{\text{sc}}} \bar{\alpha}_{m,l}^n(\eta_{n,l}). \quad (4.22)$$

In practice it may not always be possible to obtain all design achievable data rate gains under the constraint that the transmit power scaling factor $\bar{\alpha}_{m,l}$, lies in the range of

$0 \leq \bar{\alpha}_{m,l} \leq 1$, $\forall m \in \mathcal{M}, \forall l \in \mathcal{L}$, as introduced in Section 4.2. Moreover, specific requirements on the transmit power of the macro BSs can be defined in the context of the LSA principle. Therefore, choosing $\bar{\alpha}_{\min}$ and $\bar{\alpha}_{\max}$, as the lower and upper bounds for the transmit power scaling factor, respectively, with $0 \leq \bar{\alpha}_{\min} \leq \bar{\alpha}_{\max} \leq 1$, a thresholded version of the transmit power scaling factor, denoted as $\tilde{\alpha}_{m,l}$, is applied in practice and computed as

$$\tilde{\alpha}_{m,l} = \begin{cases} \bar{\alpha}_{\min} & \text{if } \bar{\alpha}_{m,l} \leq \bar{\alpha}_{\min} \\ \bar{\alpha}_{m,l} & \text{if } \bar{\alpha}_{\min} \leq \bar{\alpha}_{m,l} \leq \bar{\alpha}_{\max} \\ \bar{\alpha}_{\max} & \text{if } \bar{\alpha}_{m,l} \geq \bar{\alpha}_{\max}, \end{cases} \quad (4.23)$$

with $\bar{\alpha}_{m,l}$ defined in (4.21). The thresholds $\bar{\alpha}_{\min}$ and $\bar{\alpha}_{\max}$ can be chosen to respect power budget limitations or to avoid that the cooperative macro BS $m \in \mathcal{M}$ is muted, respectively.

4.4 Simulation Results

In order to evaluate the performance of the proposed cooperative power control scheme, system-level simulations are carried out by following the 3GPP recommendations in [rGPP10, rGPP11, rGPP13c]. A total of $M = 57$ macro BSs and $S = 57$ pico cells, serve $N = 1710$ UEs in the downlink, with an inter-site distance of 500 m for the macro BSs. The selected transmission scheme is the Single-Input-Multiple-Output (SIMO) operation mode with users containing two receive antennas. The equivalent isotropically radiated power (EIRP) of the macro BSs and pico cells differ by 23.4 dBm, with maximum transmit powers of 63.4 dBm and 40 dBm, respectively. For the selection of the serving cell, the users apply a CRE off-set to prioritize the pico cells over the macro BSs. Thus, users connect to the pico cells even if the received power from the macro BSs is higher (up to 6 dB difference). Hence, off-loading the macro BSs. In this situation, users within the CRE area are affected by very high inter-cell interference. The UEs apply an MRC receiver which provides an effective SISO channel, as assumed in the formulation of Section 4.2. Moreover, ideal link adaptation and full-buffer transmissions are assumed, i.e., the decoding in the simulations is error-free and the users demand as much data as possible. For more information on 3GPP-compliant system-level simulations, including channel and path loss models, the interested reader is referred to [rGPP10] (see 3GPP Case 6.2 from Section A.2.1).

It is considered that the proposed cooperative power control scheme is performed between a macro BS and the pico cell located within its coverage area, as explained in Section 4.2. Moreover, it is assumed that the scheduling information from the pico cell is shared with the cooperative macro BS, in order to calculate the transmit power scaling factors $\tilde{\alpha}_{m,l}$, $\forall m \in \mathcal{M}$, $\forall l \in \mathcal{L}$, as defined in (4.23).

The results are presented in terms of the long-term average user throughput, which is calculated per UE as the total amount of received data over the simulated time. Therefore, the long-term average user throughput is expressed in bits per second (bps). Since

the performance of the cell-edge UEs is of particular interest, the *cell-edge throughput* is considered, where the average user throughput is calculated from the worst 5% of the UEs in the network. Moreover, the *mean* of the average user throughput is also presented, involving all the deployed UEs.

4.4.1 Impact of the transmit power reduction schemes

The simulation results presented in this section, illustrate the impact of applying transmit power control to the heterogeneous network under investigation. In order to assess the average influence of the proposed cooperative power control scheme on the user throughput of the UEs connected to the macro BSs and the small cells, the transmit power scaling factors of the macro BSs are set to constant values during the complete simulation time.

Potential gains for different network deployments

In order to analyze the performance of the proposed cooperative power control scheme, initial simulations are carried out to identify the deployment scenario of the small cells, in which the implementation of such a cooperative power control scheme can potentially improve the network performance in terms of user throughput. Four deployment scenarios are considered related to the distribution of the UEs in the network, and the separation distance of the small cells to the macro BSs. The UEs are either uniformly distributed in the studied area, denoted as “Un”, or in a hotspot fashion, labeled as “Hs”, where the probability of the UEs being located closer to a pico cell is higher. With respect to the separation distance between macro BSs and small cells, the small cells are located either at the cell-center or at the cell-edge, where in the former, a separation distance of 125 m from the cooperative macro BS is considered, labeled as “0.25”, and in the latter, a separation distance of 250 m from the cooperative macro BS is assumed, referred to as “0.5”, with the labels denoting the applied factor to the inter-site distance between the macro BSs.

The average user throughput of the cell-edge UEs, i.e., the cell-edge throughput, is presented in Figure 4.2 for the different network deployments, where a comparison with respect to a network without any cooperative power control scheme is illustrated. In the case of the cooperative power control scheme, the results are normalized with respect to the results obtained when no cooperation takes place. A constant value of the transmit power scaling factor is assumed for all M macro BSs, with $\tilde{\alpha}_{m,l} = 0.5$, $\forall m \in \mathcal{M}$, $\forall l \in \mathcal{L}$, that is, the macro BSs transmit with half of the maximum transmit power $\Phi_{m,l}$. Moreover, the results are presented with respect to the UEs served by the macro BSs, i.e., “Macro”, the UEs served by the pico cells, labeled as “Pico”, and all the UEs, referred to as “Total”. In Figure 4.2, it is observable that by applying the cooperative power control scheme with a constant transmit power scaling factor,

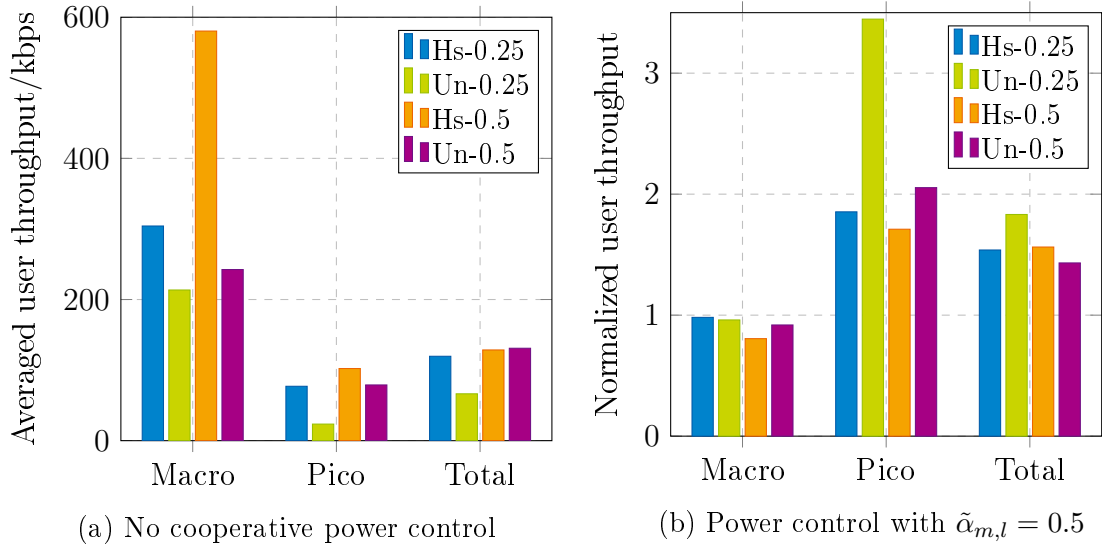


Figure 4.2. Cell-edge throughput for different heterogeneous network deployments. (a) Power control is not applied. (b) Constant power control with $\tilde{\alpha}_{m,l} = 0.5$, $\forall m \in \mathcal{M}$, $\forall l \in \mathcal{L}$, where the user throughput is normalized with respect to the scenario without any cooperation

the user throughput of the cell-edge UEs connected to the pico cells improves significantly, while the performance of the UEs served by the macro BSs is slightly reduced with respect to the scenario without any cooperation. Furthermore, the deployment scenario with uniformly distributed UEs and small cells located at the cell-center, i.e., “Un-0.25” presents the highest potential for the application of the cooperative power control scheme and it is, therefore, selected for the remaining simulations in this section. Similarly, the mean of the average user throughput is presented in Figure 4.3. However, as explained in Section 2.2.2, the cooperative schemes mainly target to improve the performance of the cell-edge UEs, and therefore minimal gains with respect to the scenario without cooperation are observable.

Performance with respect to the transmit power scaling factor

In the simulation results from figures 4.2 and 4.3, the transmit power scaling factors of the cooperative macro BSs were set constant to a value of $\tilde{\alpha}_{m,l} = 0.5$, $\forall m \in \mathcal{M}$, $\forall l \in \mathcal{L}$. In this section, a study of the performance gains in terms of user throughput, with respect to the constant value of the transmit power scaling factors $\tilde{\alpha}_{m,l}$, is presented for the selected deployment scenario Un-0.25.

The cell-edge and mean of the average user throughput are presented in Figure 4.4 for different values of the transmit power scaling factors $\tilde{\alpha}_{m,l}$, with $\tilde{\alpha}_{m,l} = \{0.1, \dots, 0.9\}$, $\forall m \in \mathcal{M}$, $\forall l \in \mathcal{L}$, where the results are normalized with respect

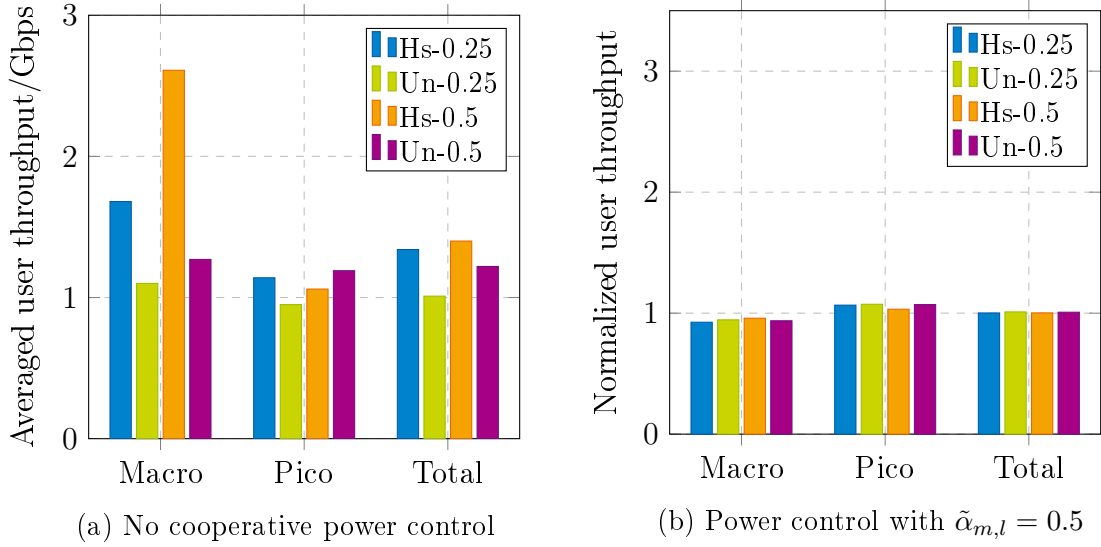


Figure 4.3. Mean of the average user throughput for different heterogeneous network deployments. (a) Power control is not applied. (b) Constant power control with $\tilde{\alpha}_{m,l} = 0.5, \forall m \in \mathcal{M}, \forall l \in \mathcal{L}$, where the user throughput is normalized with respect to the scenario without any cooperation

to a scenario without cooperation. Similar to the results from Figure 4.3, the mean of the average user throughput does not vary significantly with $\tilde{\alpha}_{m,l}$. On the other hand, the user throughput of the cell-edge UEs connected to the pico cells, significantly improves under larger reductions of the transmit powers of the cooperative macro BSs, i.e., larger transmit power scaling factors. However, such a larger reduction of the transmit powers, implies a negative effect on the cell-edge UEs served by the macro BSs as depicted in Figure 4.4. It is observable that for $\tilde{\alpha}_{m,l} = 0.8$, i.e., the macro BSs transmit with 20% of the maximum transmit power, the network achieves the best overall performance with maximum gain in the total cell-edge user throughput.

4.4.2 Performance of the proposed cooperative power control scheme

The performance of the proposed cooperative power control scheme as presented in Section 4.3 is evaluated for different configuration parameters as follows: *i*) with respect to the achievable data rate gain of the UEs $n \in \mathcal{N}$ served by the small cells $k \in \mathcal{S} \mid c_{n,k} = 1$ as defined in (4.16), three design values are selected with $\eta_{m,l} = \{1.5, 2, 3\}, \forall l \in \mathcal{L}$, and *ii*) regarding the maximum value of the transmit power scaling factor as introduced in (4.23), the threshold values are selected as $\bar{\alpha}_{\max} = \{0.2, 0.5, 0.8, 1\}, \forall m \in \mathcal{M}, \forall l \in \mathcal{L}$, where the minimum value is set to $\bar{\alpha}_{\min} = 0, \forall m \in \mathcal{M}, \forall l \in \mathcal{L}$. As previously mentioned, the studied deployment scenario corresponds to a uniform UE distribution with the pico cells located at the cell-center, i.e., Un-0.25.

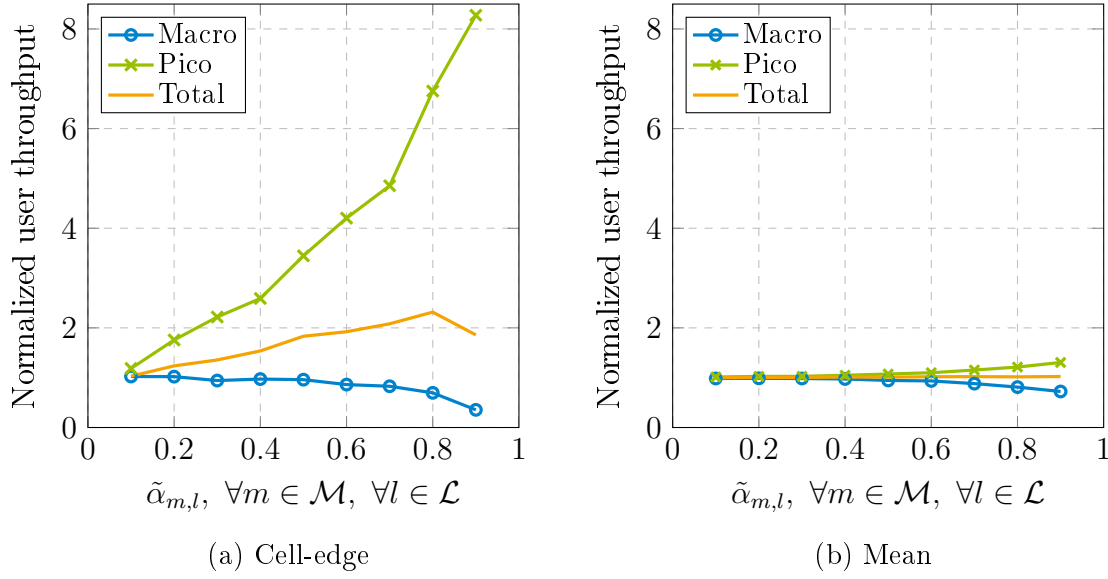


Figure 4.4. Cell-edge and mean of the average user throughput for different values of the transmit power scaling factors $\tilde{\alpha}_{m,l}$, $\forall m \in \mathcal{M}, \forall l \in \mathcal{L}$. Results are normalized with respect to a scenario without cooperation. The deployment scenario corresponds to Un-0.25

The cell-edge and the mean of the average user throughput, normalized with respect to a scenario without cooperation, are presented in Table 4.2 for all combinations of the design parameters $\eta_{n,l}$ and $\bar{\alpha}_{\max}$ as described above. The results in Table 4.2 agree with the observations from Section 4.4.1, where the performance of the UEs connected to the pico cells is improved by the reduction of transmit power of the cooperative macro BSs, i.e., larger transmit power scaling factors, while the UEs served by the macro BSs are negatively affected. In some scenarios, the performance of the UEs connected to the macro BSs is even worse than the scenario without cooperation, due to the impact of the cooperative power control on the spectral efficiency of the macro BSs. Nevertheless, such a loss is expected and it is minimal in comparison to the gains provided to the UEs served by the pico cells.

With respect to the maximum value that the transmit power scaling factor can take, i.e., $\bar{\alpha}_{\max}$, it is recognizable especially for the cell-edge user throughput, that a larger reduction of the transmit power of the cooperative macro BSs, provides a higher user throughput gain for the UEs served by the pico cells. As an example, the cell-edge user throughput of the UEs served by the pico cells is 98% higher than the scenario without any cooperation when the cooperative macro BSs can mute some PRBs, i.e., for $\bar{\alpha}_{\max} = 1$ and $\eta_{n,l} = 1.5$. The cell-edge user throughput gains reduce when α_{\max} decreases.

The target achievable data rate gains decrease when increasing the parameter $\eta_{n,l}$, which is contradictory to the purpose of such a parameter. To explain this contradictory behavior, it is worth noting that the cooperative power control scheme only takes

Table 4.2. Average user throughput normalized with respect to a scenario without any cooperation

Throughput type	UE type	Data rate gain	$\bar{\alpha}_{\max}$			
			0.2	0.5	0.8	1
Cell-edge	Macro	$\eta_{n,l} = 1.5$	1	1.03	0.98	1.03
	Pico		1.05	1.49	1.53	1.98
	Total		0.95	1.18	1.25	1.32
	Macro	$\eta_{n,l} = 2$	1.04	1.05	1.01	1.06
	Pico		0.96	1.07	1.39	1.4
	Total		0.99	0.99	1.19	1.16
	Macro	$\eta_{n,l} = 3$	1.02	1.01	1.06	1.06
	Pico		0.99	1.05	1.05	1.18
	Total		0.98	1.02	1.03	1.02
Mean	Macro	$\eta_{n,l} = 1.5$	1.01	0.99	0.96	0.96
	Pico		1.02	1.04	1.07	1.03
	Total		1.01	1.01	1.02	1
	Macro	$\eta_{n,l} = 2$	1	0.99	0.99	0.97
	Pico		1.02	1.04	1.06	1.06
	Total		1.01	1.02	1.03	1.01
	Macro	$\eta_{n,l} = 3$	1.01	0.99	1	0.99
	Pico		1.02	1.03	1.02	1.03
	Total		1.02	1.01	1.01	1.01

place for the UEs, connected to the pico cells, for which the expected throughput gain is achievable under the constraint on the minimum transmit power scaling factor of the cooperative macro BS. If the achievable throughput gain is lower than the target parameter $\eta_{n,l}$, then the cooperative macro BS transmits with maximum transmit power. For the case that $\bar{\alpha}_{\max} = 1$, the amount of times that the cooperative power control scheme selects a transmit power scaling factor $\tilde{\alpha}_{m,l}$, such that $0 < \tilde{\alpha}_{m,l} \leq \bar{\alpha}_{\max}$, is presented in Table 4.3, together with the average applied value. If the required achievable data rate gain is higher, the reduction in the transmit power of the cooperative macro BSs is larger and the transmit power scaling factor approximates $\bar{\alpha}_{\max}$. Moreover, the number of UEs connected to the pico cells, that can achieve the target data rate gains reduces with a higher target. The proposed power control scheme is only effectively used 14 % of the time when $\eta_{n,l} = 3$, with respect to the case when $\eta_{n,l} = 1.5$.

As a final remark, the macro BSs also interfere each other as described in (4.10). Therefore, an indirect result of the cooperative power control scheme is a reduction of

Table 4.3. Summary of cooperative power control scheme for $\bar{\alpha}_{\max} = 1$

Description	$\eta_{n,l} = 1.5$	$\eta_{n,l} = 2$	$\eta_{n,l} = 3$
Count of applied scheme	317.706 (1)	(0.46)	(0.14)
Average applied $\tilde{\alpha}_{m,l}$	0.72	0.83	0.91

the inter-cell interference experienced by the UEs served by the macro BSs, which is observable in Table 4.2, with the gains of the cell-edge user throughput for the UEs connected to the macro BSs.

4.5 Summary

In this chapter, a dynamic power control scheme was proposed to improve the performance of UEs heavily affected by inter-cell interference, i.e., cell-edge UEs. This inter-cell interference is produced by neighboring BSs operating in the same frequency bands. Therefore, the studied cooperative power control scheme reduces the transmit power of the interfering BSs in order to increase the SINR and the achievable data rates of the cell-edge UEs served by the neighboring BSs. The power reduction can even mute the cooperative BSs, which resembles the behavior of a CoMP DPB scheme.

In heterogeneous networks operating under the LSA principle, where the available time/frequency resources are shared by the incumbent system with the licensee BSs, the proposed cooperative power control scheme represents an attractive solution to limit the interference caused to the UEs connected to the incumbent BSs.

Simulation results demonstrate the capacity of the proposed scheme to reduce the interference caused to the cell-edge UEs in a dynamic manner and on a per PRB basis. Furthermore, the cooperative power control scheme is entirely based on measurements available in LTE-Advanced wireless networks, which makes its application possible in current and upcoming systems.

Despite the potential gains of the proposed cooperative power control scheme, the cooperation is limited to a reduction of the transmit power after the scheduling decisions have been made in an independent and uncoordinated fashion. Therefore, large transmit power reductions or even muting can be applied, which significantly affect the performance of the UEs connected to the BSs performing the power reduction. In the following chapters, cooperative schemes are presented that perform scheduling and power control decisions in a jointly manner.

Chapter 5

Centralized Coordinated Scheduling in Mobile Communication Networks

As mentioned in Section 4.5, the cooperative power control scheme investigated in Chapter 4 considers the cooperation of the BSs after the scheduling decisions have been independently made. Therefore, the cooperative scheme of Chapter 4 is limited to coordinating the transmit powers of the BSs in order to reduce the inter-cell interference. In this chapter, the cooperation between the BSs is extended to include the scheduling decisions. For that purpose, CoMP CS with muting in LTE-Advanced downlink networks is studied, as introduced in Section 2.2.2.

Throughout this dissertation, and unlike most existing approaches, the derived cooperative schemes do not rely on exact CSI but only make use of the specific CSI^{R-11} reports defined in the 3GPP standard, as introduced in Section 2.1.3. Therefore, in order to support the investigated CoMP CS schemes proposed in this chapter, the interference scenarios signaled by the CSI^{R-11} reports are limited to cooperation in the form of muting. This limitation with respect to the cooperative power control from Chapter 4, is introduced in order to restrict the signaling overhead.

In this chapter, the presence of a central controller with connectivity to the cooperative BSs is assumed, which coordinates the scheduling and muting decisions among multiple BSs in order to manage the inter-cell interference. In contrast to Chapter 4, the proposed cooperative schemes can be applied to different types of networks, such as macro-only and heterogeneous networks. The CS with muting problem is initially formulated as an integer non-linear program (INLP) and further reformulated to an equivalent ILP which can be efficiently solved by commercial solvers. Simulations of medium- to large-size networks are carried out to analyze the performance of the proposed CS with muting approaches. These simulations confirm available analytical results that report fundamental limitations in the cooperation, due to residual out-of-cluster interference [LJA13]. Nevertheless, the schemes proposed in this chapter show important gains in average user throughput of the cell-edge users, especially in the case of heterogeneous networks. Since the deployment of a central controller to coordinate the cooperation among the BSs may not be possible in some scenarios, a decentralized CS with muting scheme is derived in Chapter 6.

5.1 State-of-the-art and Contributions

Over the past years, important research has been carried out regarding CoMP schemes under different network architectures and CSI assumptions. In [MHV⁺12]

and [MVT⁺12], JT and DPS schemes based on the enhanced CSI reports supported by LTE-Advanced Release 11, i.e., CSI^{R-11} reports, have been investigated. The results therein show throughput gains, especially for the cell-edge users, and the possibility to improve mobility management by means of DPS. Even though the potential cell-edge user throughput gains of JT are high, the strict requirements on the reliability of the CSI^{R-11} reports represent a key drawback to its implementation. Barbieri et al. studied CS as a complement of enhanced-ICIC in heterogeneous networks in [BGG⁺12]. In their scheme, cooperation takes place in the form of CS supported by beamforming in order to mitigate the interference caused by the macro BSs, to the UEs connected to the small cells. Multiple CSI reports are generated, where all possible precoders the macro BS can select from a finite precoder codebook are considered for the cooperation. The results present negligible gain for the enhanced-ICIC with CS scheme, in comparison to the approach with only enhanced-ICIC. In [DMBP13], a Cloud-Radio Access Network (C-RAN) architecture is used for centralized CoMP JT in heterogeneous networks, which enables the cooperation of larger cluster sizes. In that case, gains over approaches with only enhanced-ICIC are observed, especially for large cluster sizes. Authors in [ABK⁺14] propose centralized and decentralized CoMP CS schemes that utilize CSI^{R-11} reports, in which muting is applied to one BS at a time. As mentioned in Chapter 1, a BS is called muted if it does not transmit data on a specific time/frequency resource to any of its connected UEs. It has been shown that under this muting condition, both centralized and decentralized schemes achieve similar performance, favoring the decentralized scheme due to the reduced information exchange. Moreover, in [GKN⁺15] the authors extend the cooperation scheme of [ABK⁺14], to introduce muting of more than one BS per scheduling decision in a larger network. A greedy CS algorithm is presented to solve the centralized problem, which yields limited additional gain with respect to the decentralized scheme with overlapping cooperation clusters. It is important to note that the coordination scheme of [GKN⁺15] consists of a greedy optimization procedure. It is therefore suboptimal and further investigation regarding the optimally achievable performance of coordination, in the case of CSI^{R-11} reports, has not been carried out. Additionally, the results are focused on macro-only networks, where the gains of cooperation are restricted due to similar interfering power levels experienced from multiple BSs.

Although the above mentioned works show that CoMP schemes enhance the user throughput with respect to a network operating without any cooperation, no detailed studies are carried out in order to establish the maximum achievable gains that CoMP schemes can offer in realistic network scenarios and under LTE-Advanced specific CSI reports, i.e., CSI^{R-11} reports. In [LJA13], it has been demonstrated from an analytical perspective that cooperative schemes have fundamentally limited gains. That is, even under the assumption of centralized coordination and ideal CSI in form of instantaneous channel coefficients, the cooperation gains are limited due to the residual interference from BSs outside of the cooperation area, the signaling overheads and the finite nature of the time/frequency/space resources. In this chapter, such limits are investigated under practical conditions by means of system-level evaluations. For that purpose, a CoMP CS with muting scheme is proposed and solved optimally for an LTE-Advanced downlink network with centralized architecture. The problem formu-

lation is based on multiple $\text{CSI}^{\text{R-11}}$ reports generated by the UEs and gathered by the central controller, which uses this information to determine the coordinated scheduling and muting decisions for all connected BSs. The central controller then decides which BSs serve their connected UEs on a given time/frequency resource, and which BSs are muted in order to reduce the interference caused to the UEs served by the neighboring transmitting BSs.

The major contributions of this chapter are summarized as follows.

- The CoMP CS with muting problem, where BSs cooperate by abstaining from transmitting on particular time/frequency resources based on standardized $\text{CSI}^{\text{R-11}}$ reports, is formulated as an INLP.
- The non-linear CS with muting problem is reformulated into a mathematically *equivalent* ILP, which enjoys low computational complexity and can be efficiently solved by commercial solvers. This reformulation is based on the lifting technique and exploits specific separability and reducibility properties of the problem. Thus, making the optimization scheme applicable as a valuable benchmark scheme in medium- to large-scale networks.
- A configurable heuristic algorithm is proposed as an extension to the greedy algorithm in [GKN⁺15], which achieves an excellent trade-off between performance and computational complexity.
- In order to assess the maximum achievable gains of the proposed and state-of-the-art CoMP CS schemes, numerical simulations are carried out under practical scenarios for macro-only and heterogeneous networks. The obtained results provide insights into the scheduling mechanism and fundamental limitations of the coordination.

5.2 System Model

Based on the system model presented in Chapter 3, in the following a description of the scenario investigated in this chapter is presented. A cellular network is considered, as illustrated in Figure 5.1, where a cooperation cluster of M BSs operating in FDD mode serves N UEs in the downlink. The BSs can be all of the same type, e.g., a macro-only network, or they can have different capabilities as in the case of heterogeneous networks, as introduced in Section 2.1.1. At each transmission time, all BSs can make use of the same L PRBs for transmission. Thus, inter-cell interference affects the UEs, especially of those located at the cell-edge. Additionally, interference from BSs outside of the cooperation cluster is considered. The operation of the cooperation cluster is managed by a central controller with backhaul connectivity to all M BSs, where it is worth to mention that this central controller can be deployed as a separate unit or

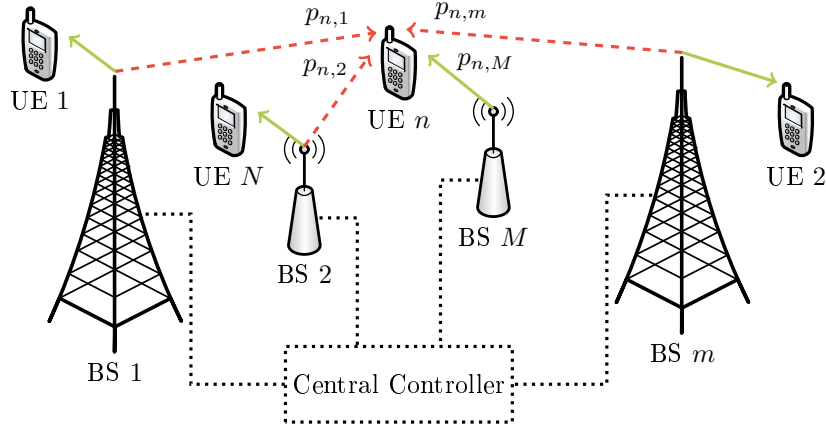


Figure 5.1. Cooperation cluster of M BSs and N UEs in the downlink. For UE n , the solid arrow represents the serving link while the dashed arrows correspond to the interfering links. The BSs are connected through the backhaul to a central controller (dotted lines)

as an extension of a BS. The sets of indices $\mathcal{M} = \{1, \dots, M\}$, $\mathcal{N} = \{1, \dots, N\}$ and $\mathcal{L} = \{1, \dots, L\}$ are used to address the BSs, UEs and PRBs, respectively, as introduced in Chapter 3.

The received power at UE $n \in \mathcal{N}$ from BS $m \in \mathcal{M}$ on PRB $l \in \mathcal{L}$, is denoted as $p_{n,m,l}$ and calculated as in (3.1). Similarly, (3.2) defines the total received power at UE n from BS m , denoted as $p_{n,m}$, as the sum of the received powers from BS m over all PRBs. In order to select the serving BS for UE n , different strategies are available depending on the network deployment. Thus, in the case of homogeneous networks, a typical serving BS selection strategy corresponds to choosing the BS from which the highest total received power $p_{n,m}$, $\forall m \in \mathcal{M}$, is obtained. On the other hand, in the case of heterogeneous networks, the CRE strategy is considered in order to achieve load balancing, as explained in Section 4.2, with (4.2) and (4.3) defining the CRE selection strategy and off-set, respectively. In this chapter, both homogeneous macro-only and heterogeneous networks are studied, where for the latter case, CRE is applied as in Chapter 4. The $N \times M$ connection matrix \mathbf{C} is defined, with elements as in (3.3) characterizing the serving conditions between BSs and UEs, where it is assumed that only one BS serves UE n over all PRBs as described by (3.4). As mentioned in Chapter 3, it is further assumed for simplicity, that the connection matrix \mathbf{C} is constant during the considered operation time.

Given the connection matrix \mathbf{C} , and the corresponding index sets for the interfering and strongest interfering BSs of UE $n \in \mathcal{N}$, denoted by \mathcal{I}_n and \mathcal{I}'_n , respectively, as introduced in Chapter 3, the set of indices of cooperative interfering BSs of UE n is given by

$$\mathcal{I}_n^c = \mathcal{I}'_n. \quad (5.1)$$

In (5.1), it is considered that the M' strongest interfering BSs of UE n can cooperate to improve the performance, in terms of user throughput of UE n . Therefore, the

cardinality of the set of indices of cooperative interfering BSs of UE n is given by $|\mathcal{I}_n^c| = M'$. It is worth noting that a different selection of the cooperative interfering BSs of UE n is possible, and has no implication in the discussion presented in the remainder of this chapter.

Within the cooperation cluster, the BSs cooperate in the form of CoMP CS with muting, as previously mentioned in Section 5.1. The central controller is then, in charge of managing the downlink transmissions of the BSs, where at each transmission time and on a per PRB basis, each BS can be requested to abstain from transmitting data. Hence, the interference caused to UEs located in neighboring BSs is reduced on the PRBs with muted BSs. Based on the transmit power control parameter $\bar{\alpha}_{m,l}$, as introduced in Chapter 3, in the following the binary *muting decision matrix* denoted as $\bar{\alpha}$, of dimensions $M \times L$ and elements

$$\bar{\alpha}_{m,l} = \begin{cases} 1 & \text{if BS } m \in \mathcal{M} \text{ is muted on PRB } l \in \mathcal{L} \\ 0 & \text{otherwise,} \end{cases} \quad (5.2)$$

is used in order to control the transmit power of the BSs. If $\bar{\alpha}_{m,l} = 0$, then BS m transmits on PRB l , with maximum transmit power $\Phi_{m,l}$. Thus, by following the definition in (3.7), the SINR on PRB l of UE $n \in \mathcal{N}$, which is served by BS $k \in \mathcal{M}$, is defined as

$$\gamma_{n,l}(\bar{\alpha}_l) = \frac{(1 - \bar{\alpha}_{k,l}) p_{n,k,l}}{I_{n,l}^{\text{cc}}(\bar{\alpha}_l) + I_{n,l}^{\text{oc}} + \sigma^2}. \quad (5.3)$$

The $M \times 1$ vector $\bar{\alpha}_l$, is equivalent to the l -th column of $\bar{\alpha}$. The numerator corresponds to the average received power at UE n from the serving BS k on PRB l , as defined in (3.1). The first term in the denominator, i.e., $I_{n,l}^{\text{cc}}(\bar{\alpha}_l)$, corresponds to the average inter-cell interference from the BSs within the cooperation cluster, with

$$\begin{aligned} I_{n,l}^{\text{cc}}(\bar{\alpha}_l) &= \sum_{b \in \mathcal{I}_n} (1 - \bar{\alpha}_{b,l}) p_{n,b,l} \\ &= \sum_{m' \in \mathcal{I}_n^c} (1 - \bar{\alpha}_{m',l}) p_{n,m',l} + \sum_{m \in \mathcal{I}_n \setminus \mathcal{I}_n^c} (1 - \bar{\alpha}_{m,l}) p_{n,m,l}. \end{aligned} \quad (5.4)$$

In (5.4), the inter-cell interference is further decomposed into two terms corresponding to the inter-cell interference from the cooperative interfering BSs of UE n , as addressed by the index set \mathcal{I}_n^c , and the remaining BSs in the cooperation cluster. Furthermore, the dependency of $I_{n,l}^{\text{cc}}$ on the muting decision matrix is highlighted. The second term in the denominator, i.e., $I_{n,l}^{\text{oc}}$, is the average out-of-cluster interference, which is assumed to be independent of the muting decision matrix $\bar{\alpha}$ since the central controller is not aware of the muting decisions made by the BSs outside of the cooperation cluster. Moreover, UE n experiences AWGN with power σ^2 , which is further assumed without loss of generality, to be constant for all UEs over all PRBs. Based on the SINR definition in (5.3), the achievable data rate on PRB l of UE n is modeled as in (3.9).

5.2.1 CSI reporting for centralized CS with muting

It is considered that the cooperation among the BSs takes place in the form of CoMP CS with muting. Therefore, in contrast to the cooperative power control scheme studied in Chapter 4, no distinction between the CSI reports for scheduling and cooperation is made in this section. In the following, a description of the $\text{CSI}^{\text{R-11}}$ reports available at the central controller, which are used to support the proposed CS with muting schemes, is presented. For that purpose, the $M \times L$ muting matrix α is used, as introduced in Section 3.1, in order to describe the assumed transmit/muting states of the BSs associated to a specific $\text{CSI}^{\text{R-11}}$ report.

For a cooperation cluster with M BSs, a total of $J = 2^M - 1$ muting decisions can be made per PRB $l \in \mathcal{L}$, where the decision corresponding to all BSs being muted is not considered, i.e., on each PRB l at least one BS transmits. In Section 5.2, it has been mentioned that each UE considers the cooperation from a subset of BSs within the cooperation cluster. Moreover, the set of cooperative interfering BSs of UE $n \in \mathcal{N}$, denoted by \mathcal{I}_n^c , has been defined as in (5.1), where only the M' strongest interfering BSs are considered for cooperation. The reason for such a definition relies on the fact that the SINR and the achievable data rates of UE n , are dominated by its strongest interfering BSs [ABK⁺14]. Therefore, UE n generates a total of $J' = 2^{M'}$ $\text{CSI}^{\text{R-11}}$ reports per PRB, with $J' < J$.

Each of the J' $\text{CSI}^{\text{R-11}}$ reports generated by UE $n \in \mathcal{N}$ on PRB $l \in \mathcal{L}$, reflects a unique interference scenario for its cooperative interfering BSs. More specifically, the interference scenario $j \in \mathcal{J}'$, with $\mathcal{J}' = \{1, \dots, J'\}$, is characterized by the *muting indicator* set $\mathcal{J}_{n,j}$, which contains the indices of the cooperative interfering BSs considered to be muted in the j -th $\text{CSI}^{\text{R-11}}$ report of UE n . Hence, the set $\mathcal{J}_n = \mathbb{P}(\mathcal{I}_n^c)$ contains all J' muting indicator sets for UE n , with $\mathbb{P}(\cdot)$ denoting the power set of its argument, i.e., the set of all subsets of \mathcal{I}_n^c . The set \mathcal{J}_n is common to all PRBs, due to the definition of the strongest interfering BSs of UE n as in (3.5). From the muting indicator set $\mathcal{J}_{n,j}$, the *muting pattern* of the j -th $\text{CSI}^{\text{R-11}}$ report of UE n on PRB l is defined as

$$\alpha_{n,m',l,j} = \begin{cases} 1 & \text{if } m' \in \mathcal{J}_{n,j} \text{ on PRB } l \\ 0 & \text{otherwise} \end{cases} \quad \forall m' \in \mathcal{I}_n^c, \quad (5.5)$$

i.e., $\alpha_{n,m',l,j} = 1$, if the cooperative interfering BS m' is muted on PRB l under interference scenario $j \in \mathcal{J}'$. The definition in (5.5) considers only the set of cooperative interfering BSs of UE n indexed by \mathcal{I}_n^c . Therefore, a constant muting state of the remaining BSs in the cooperation cluster is required for all interference scenarios indexed by \mathcal{J}' . In the following, it is assumed without loss of generality, that $\alpha_{n,m,l,j} = 0$, $\forall m \notin \mathcal{I}_n^c$, $\forall j \in \mathcal{J}'$. In other words, the $\text{CSI}^{\text{R-11}}$ reports of UE n are conservative with respect to the interference from the non-cooperative interfering BSs, by assuming them to transmit with maximum transmit power $\Phi_{m,l}$, $\forall m \notin \mathcal{I}_n^c$, $\forall l \in \mathcal{L}$, $\forall j \in \mathcal{J}'$. As explained in Section 3.1, although the definition of the muting pattern in (5.5) is similar to the definition of the muting decision

in (5.2), the two concepts are different. The muting pattern α describes the *assumed* muting conditions during the generation of the $\text{CSI}^{\text{R-11}}$ reports for the different interference scenarios, while the muting decision $\bar{\alpha}$ represents the *real* muting conditions of the BSs within the cooperation cluster, imposed by the central controller as the result of the implementation of the CS with muting scheme.

For the generation of the $\text{CSI}^{\text{R-11}}$ reports, UE $n \in \mathcal{N}$ calculates the SINR and the achievable data rates on PRB $l \in \mathcal{L}$ under interference scenario $j \in \mathcal{J}'$. Therefore, similar to (5.3), the SINR on PRB l of UE n , served by BS $k \in \mathcal{M}$, under interference scenario j , is defined as

$$\gamma_{n,l,j}(\alpha_{n,m',l,j}) = \frac{p_{n,k,l}}{I_{n,l,j}^c(\alpha_{n,m',l,j}) + I_{n,l}^{\text{nc}} + I_{n,l}^{\text{oc}} + \sigma^2}, \quad (5.6)$$

where the first term in the denominator of (3.7) has been decomposed into two terms corresponding to the interference from the cooperative interfering BSs of UE n , i.e., $I_{n,l,j}^c(\alpha_{n,m',l,j})$, and the interference from the remaining non-cooperative interfering BSs of UE n , denoted by $I_{n,l}^{\text{nc}}$. From the previous discussion on the muting patterns of UE n , the interference from the cooperative interfering BSs that can be muted to improve the SINR of UE n , depends on interference scenario j and thus, the muting pattern as

$$I_{n,l,j}^c(\alpha_{n,m',l,j}) = \sum_{m' \in \mathcal{I}_n^c} (1 - \alpha_{n,m',l,j}) p_{n,m',l}. \quad (5.7)$$

On the other hand, the interference from the non-cooperative interfering BSs of UE n is assumed to be constant and independent of the possible muting decisions, with

$$I_{n,l}^{\text{nc}} = \sum_{m \in \mathcal{I}_n \setminus \mathcal{I}_n^c} p_{n,m,l}. \quad (5.8)$$

Furthermore, the out-of-cluster interference, denoted by $I_{n,l}^{\text{oc}}$, and the noise variance σ^2 are also assumed to be constant terms among all the \mathcal{J}' interfering scenarios considered in the $\text{CSI}^{\text{R-11}}$ reports. Hence, sub-index j is not used in the last three terms of the denominator in (5.6).

To complete the information for the $\text{CSI}^{\text{R-11}}$ reports, $r_{n,l,j}$ denotes the achievable data rate on PRB $l \in \mathcal{L}$ of UE $n \in \mathcal{N}$ considered under interference scenario $j \in \mathcal{J}'$. The calculation of $r_{n,l,j}$ follows the definition in (3.9), with

$$r_{n,l,j} = f(\gamma_{n,l,j}). \quad (5.9)$$

Proposition 5.1. *For UE $n \in \mathcal{N}$ on PRB $l \in \mathcal{L}$, if $\mathcal{J}_{n,i} \subsetneq \mathcal{J}_{n,j}, \forall i, j \in \mathcal{J}', i \neq j$, then $\gamma_{n,l,i} < \gamma_{n,l,j}$.*

Proof. See Appendix A. □

The Proposition 5.1 implies that the SINR on PRB $l \in \mathcal{L}$ of UE $n \in \mathcal{N}$ increases when muting additional cooperative interfering BSs.

Table 5.1. $\text{CSI}^{\text{R-11}}$ reports for UE n on PRB l with $M' = 2$

Interference scenario ($j \in \mathcal{J}'$)	Muting indicator ($\mathcal{J}_{n,j}$)	Muting pattern ($\alpha_{n,l,j}$)	Achievable data rate
1	\emptyset	$[0, 0, 0, 0]$	$r_{n,l,1}$
2	$\{1, 2\}$	$[1, 1, 0, 0]$	$r_{n,l,2}$
3	$\{1\}$	$[1, 0, 0, 0]$	$r_{n,l,3}$
4	$\{2\}$	$[0, 1, 0, 0]$	$r_{n,l,4}$

Corollary 5.1. *For UE $n \in \mathcal{N}$ on PRB $l \in \mathcal{L}$, if $\mathcal{J}_{n,i} \subsetneq \mathcal{J}_{n,j}, \forall i, j \in \mathcal{J}', i \neq j$ and $f(\gamma_{n,l})$ introduced in (3.9) is a non-decreasing function, then $r_{n,l,i} \leq r_{n,l,j}$.*

Corollary 5.2. *The minimum achievable data rate on PRB $l \in \mathcal{L}$ of UE $n \in \mathcal{N}$ among all J' $\text{CSI}^{\text{R-11}}$ reports, corresponds to the interference scenario j^0 , with all M' cooperative interfering BSs transmitting with maximum transmit power $\Phi_{m,l}, \forall m \in \mathcal{I}_n^c$, i.e., with muting indicator set $\mathcal{J}_{n,j^0} = \emptyset$, where \emptyset denotes the empty set.*

Hence, based on the Corollary 5.1, the achievable data rate on PRB $l \in \mathcal{L}$ of UE $n \in \mathcal{N}$ increases or remains constant when muting additional cooperative interfering BSs. The observations in the Proposition 5.1, Corollary 5.1 and Corollary 5.2 dictate the solution of the CS with muting problem formulated in Section 5.3.

Example 5.1. *In an exemplary network with a cooperation cluster of $M = 4$ BSs, and a total of $M' = 2$ strongest interfering BSs per UE, UE $n \in \mathcal{N}$ selects BS 1 and BS 2 for cooperation such that $\mathcal{I}_n^c = \{1, 2\}$. Thus, UE n generates $J' = 4$ $\text{CSI}^{\text{R-11}}$ reports on PRB $l \in \mathcal{L}$ as summarized in Table 5.1. According to the Proposition 5.1, Corollary 5.1 and Corollary 5.2, the highest achievable data rate is reported by UE n on PRB l , when all the cooperative interfering BSs are muted, which corresponds to interference scenario $j = 2$. Furthermore, the lowest achievable data rate reported by UE n on PRB l occurs when the two cooperative interfering BSs are transmitting, i.e., interference scenario $j = j^0 = 1$. Thus, $r_{n,l,2} \geq r_{n,l,3}, r_{n,l,4} \geq r_{n,l,1}$.*

5.3 Centralized CS with Muting

In this section, the proposed CoMP CS with muting schemes are presented. The studied CS with muting schemes are implemented in the central controller, which relies on the $\text{CSI}^{\text{R-11}}$ reports as introduced in Section 5.2.1.

5.3.1 Proposed INLP - Problem formulation

At the central controller, the CSI^{R-11} reports generated by the UEs and forwarded by the BSs, are used in order to compute the CS with muting decision. The CS decision consists of two main components, namely, a scheduling decision that assigns PRBs to UEs, and a muting decision that mutes BSs on particular PRBs to reduce the interference experienced by the UEs connected to neighboring BSs. The matrix variable $\bar{\mathbf{S}}$ of dimensions $N \times L$ and elements

$$\bar{s}_{n,l} = \begin{cases} 1 & \text{if PRB } l \in \mathcal{L} \text{ is scheduled to UE } n \in \mathcal{N} \\ 0 & \text{otherwise,} \end{cases} \quad (5.10)$$

is used to denote the scheduling decision for all UEs on each PRB l , while the $M \times L$ matrix variable $\bar{\boldsymbol{\alpha}}$, with elements as introduced in (5.2), refers to the muting decision for all BSs on each PRB l . Both decisions depend on each other. On the one hand, the selection of the UEs to be served on a given PRB l , depends on the data rates these UEs can achieve under a particular muting decision. On the other hand, the muting decision depends on the margin by which the achievable data rates of the UEs to be served increases with respect to the loss on the achievable data rates of the UEs connected to the muted BSs, for that particular muting decision. In the following, an INLP is proposed, to carry out joint BS muting and UE scheduling in a coordinated network.

Typically, the schedulers in mobile communications pursue a trade-off between user throughput and fairness as explained in Section 3.2. In this chapter, the same objective is defined by maximizing the PF metric as given in (3.11), with the total instantaneous achievable data rate of UE n calculated similarly to (3.12) by

$$r_n = g(r_{n,l,j}, \bar{s}_n, \bar{\boldsymbol{\alpha}}) \quad \forall l \in \mathcal{L}, \forall j \in \mathcal{J}', \quad (5.11)$$

where $g(\cdot)$ denotes a function of the achievable data rates of UE n , as defined in (5.9), over the PRBs scheduled to UE n , as described by the n -th row of $\bar{\mathbf{S}}$, denoted by \bar{s}_n , and the muting decision matrix $\bar{\boldsymbol{\alpha}}$.

The LTE-Advanced CS with muting problem can be formulated as the following INLP

$$\begin{aligned} \max_{\{\bar{\mathbf{S}}, \bar{\boldsymbol{\alpha}}\}} \quad & \sum_{n \in \mathcal{N}} \Omega_n \\ \text{s.t.} \quad & \end{aligned} \quad (5.12a)$$

$$\bar{\alpha}_{m,l} + \sum_{n \in \mathcal{N}} c_{n,m} \bar{s}_{n,l} \leq 1 \quad \forall m \in \mathcal{M}, \forall l \in \mathcal{L}, \quad (5.12b)$$

$$r_n = \sum_{l \in \mathcal{L}} \rho(r_{n,l}, \bar{\boldsymbol{\alpha}}_l, \mathcal{I}_n^c) \bar{s}_{n,l} \quad \forall n \in \mathcal{N}, \quad (5.12c)$$

$$\bar{s}_{n,l} \in \{0, 1\} \quad \forall n \in \mathcal{N}, \forall l \in \mathcal{L}, \quad (5.12d)$$

$$\bar{\alpha}_{m,l} \in \{0, 1\} \quad \forall m \in \mathcal{M}, \forall l \in \mathcal{L}, \quad (5.12e)$$

where the objective in (5.12a) is to maximize the sum of the PF metrics over all UEs, with the PF metric of UE $n \in \mathcal{N}$ calculated as in (3.11). The constraints in (5.12b) link the scheduling decision $\bar{\mathbf{S}}$ with the muting decision $\bar{\boldsymbol{\alpha}}$. If BS $m \in \mathcal{M}$ is muted on PRB $l \in \mathcal{L}$, then PRB l cannot be scheduled to any UE n connected to BS m . Thus, if $\bar{\alpha}_{m,l} = 1$ in (5.12b) for BS m , the second term on the left-hand-side must be equal to zero, which is true in either of the following cases with the connection indicator $c_{n,m}$ given by (3.3):

- No UEs are connected to BS m , i.e., $c_{n,m} = 0$, $\forall n \in \mathcal{N}$.
- PRB l is not scheduled to any UE served by BS m , i.e., $\bar{s}_{n,l} = 0$, $\forall n \in \mathcal{N}$ such that $c_{n,m} = 1$.

Furthermore, in the case that BS m is not muted on PRB l , i.e., $\bar{\alpha}_{m,l} = 0$, the constraints in (5.12b) ensure that single-user transmissions are carried out, where each BS is allowed to serve a maximum of one UE per PRB. Additionally, the total instantaneous achievable data rate of UE n , denoted by r_n as introduced in (5.11), is calculated in (5.12c), with

$$g(r_{n,l,j}, \bar{\mathbf{s}}_n, \bar{\boldsymbol{\alpha}}) = \sum_{l \in \mathcal{L}} \rho(\mathbf{r}_{n,l}, \bar{\boldsymbol{\alpha}}_l, \mathcal{I}_n^c) \bar{s}_{n,l} \quad \forall n \in \mathcal{N}. \quad (5.13)$$

In (5.13), $\rho(\mathbf{r}_{n,l}, \bar{\boldsymbol{\alpha}}_l, \mathcal{I}_n^c)$ is a lookup table function that selects the achievable data rate on PRB l of UE n , based on the muting decision $\bar{\boldsymbol{\alpha}}_l$ of the cooperative interfering BSs of UE n , as indexed by \mathcal{I}_n^c . The lookup table function $\rho(\cdot)$, selects the achievable data rate from the $J' \times 1$ vector, $\mathbf{r}_{n,l}$, with elements $r_{n,l,j}$, $\forall j \in \mathcal{J}'$, obtained from the CSI^{R-11} reports of UE n on PRB l , as defined in (5.9).

Example 5.2. Based on the Table 5.1 from Example 5.1, with $J' = 4$ CSI^{R-11} reports, the lookup table function for UE $n \in \mathcal{N}$ on PRB $l \in \mathcal{L}$ provides the results as in Table 5.2. Note that the value of $\rho(\cdot)$ does not depend on the muting decision of the remaining non-cooperative BSs.

Due to the utilization of the J' CSI^{R-11} reports, the achievable data rate on PRB $l \in \mathcal{L}$ of UE $n \in \mathcal{N}$ under interference scenario $j \in \mathcal{J}'$, is constant in the problem formulation and limited to the set of reported muting patterns. Additionally, when assuming that the achievable data rate function $f(\gamma_{n,l})$, as defined in (5.9), is piece-wise non-decreasing, the following Proposition 5.2 applies.

Proposition 5.2. For UE $n \in \mathcal{N}$ on PRB $l \in \mathcal{L}$, if $\mathcal{J}_{n,i} \subsetneq \mathcal{J}_{n,j}$, $\forall i, j \in \mathcal{J}', i \neq j$ and $r_{n,l,i} = r_{n,l,j}$, then the interference scenario $i \in \mathcal{J}'$ provides the highest sum of PF metrics over all UEs in the cooperation cluster among both scenarios $i, j \in \mathcal{J}'$.

Proof. See Appendix B. □

Table 5.2. Lookup table function $\rho(\mathbf{r}_{n,l}, \bar{\boldsymbol{\alpha}}_l, \mathcal{I}_n^c)$ for UE n on PRB l with $M' = 2$

$\alpha_{m,l}, \forall m \in \mathcal{I}_n^c$	$\rho(\mathbf{r}_{n,l}, \bar{\boldsymbol{\alpha}}_l, \mathcal{I}_n^c)$
$[0, 0]$	$r_{n,l,1}$
$[0, 1]$	$r_{n,l,4}$
$[1, 0]$	$r_{n,l,3}$
$[1, 1]$	$r_{n,l,2}$

Hence, from Proposition 5.2, it follows that additional cooperative interfering BSs are only muted if the achievable data rate of UE $n \in \mathcal{N}$ is increased.

Moreover, as previously explained, the scheduling and muting matrix variables $\bar{\mathbf{S}}$ and $\bar{\boldsymbol{\alpha}}$ are binary as described by the constraints in (5.12d) and (5.12e), respectively.

The following remarks summarize the characteristics of the LTE-Advanced CS with muting problem formulation in (5.12).

- As mentioned in Section 5.2.1, given M' cooperative interfering BSs per each UE $n \in \mathcal{N}$, a total of $J' = 2^{M'}$ interfering scenarios per UE n are available. Hence, two special cases of the problem formulation are observed:
 - If $M' = 0$, each UE n generates one CSI^{R-11} report under the assumption of no BS muting. At the central controller, the CS with muting problem formulation becomes a PF scheduler without any cooperation. That is, the CSI^{R-11} report is equivalent to the CSI^{R-8} report introduced in Section 2.1.3.
 - If $M' = M - 1$, all the interfering BSs within the cooperation cluster can be muted to improve the performance of any UE on each PRB $l \in \mathcal{L}$. The formulated CS with muting problem has, at the central controller, a solution space of size $\prod_{m \in \mathcal{M}} (1 + \sum_{n \in \mathcal{N}} c_{n,m})^L$, i.e., each BS m can schedule PRB l to either one of the connected UEs, or BS m can be muted. If the network size is large, finding the solution while assuming cooperation of all interfering BSs for all UEs approximates an exhaustive search.
- The problem is purely integer, and furthermore binary because of the constraints in (5.12d) and (5.12e). Thus, only a discrete number of PRBs can be scheduled to any UE, and the BSs either transmit or are muted on PRB l .
- Due to the combinatorial nature of the problem formulation, it is classified as NP-hard [BHM77].
- The problem is non-linear because of the relation between the muting and the scheduling decision variables, $\bar{\boldsymbol{\alpha}}_l$ and $\bar{s}_{n,l}$, $\forall l \in \mathcal{L}$, $\forall n \in \mathcal{N}$, respectively, in the constraints in (5.12c).

Although the number of reported interference scenarios $J' = 2^{M'}$ can be limited by selecting a small value M' of cooperative interfering BSs per UE $n \in \mathcal{N}$, the CS with muting INLP formulation in (5.12) also depends on the number of UEs N , and the number of PRBs L . For certain network scenarios, N and L can be large. Therefore, given the non-linear nature of the problem in (5.12), finding a solution with commercial solvers may either not be possible or inefficient in terms of computation time. In the following, *separability*, *reducibility* and *lifting* concepts are used, in order to formulate parallel ILP sub-problems that scale better with the network size.

5.3.2 Proposed ILP - Parallelized sub-problem formulation

Separability. When analyzing the objective function described by (5.12a), the total PF metric corresponds to the sum of the individual PF metrics for all UEs. Furthermore, at each UE $n \in \mathcal{N}$, it is assumed that the total instantaneous achievable data rate is equivalent to the linear combination of the decoupled achievable data rates per scheduled PRBs, as given by (5.12c). Therefore, it is possible to separate the CS with muting problem in (5.12), into L independent sub-problems corresponding to the scheduling decision of one PRB each¹. By performing this parallelization, and by exploiting the advances in massively parallel processors [KmWH17], the computation time of the CS with muting problem is reduced without affecting the quality of the solution. In other words, the solution of the parallelized CS with muting problem remains optimal.

Reducibility. It is expected that some of the UEs connected to a common BS $m \in \mathcal{M}$, share one or more cooperative interfering BSs. From a BS perspective, the set

$$\mathcal{J}_m = \bigcup_{\substack{n \in \mathcal{N} \\ c_{n,m}=1}} \mathcal{J}_n \quad \forall m \in \mathcal{M}, \quad (5.14)$$

contains all the unique muting indicator sets associated to its connected UEs. Similar to the set \mathcal{J}_n of muting indicator sets for UE n , \mathcal{J}_m is common to all PRBs in the reporting period. The number of unique muting indicator sets for BS m , given by $J'_m = |\mathcal{J}_m|$, depends on the number of UEs connected to BS m and the maximum number J' of reported interference scenarios per UE, as introduced in Section 5.2.1. Thus, $J' \leq J'_m \leq \sum_{n \in \mathcal{N}} c_{n,m} J'$, where the lower bound corresponds to the case when all connected UEs are interfered by the same set of cooperative interfering BSs, and the upper bound represents the case with all UEs having different cooperative interfering BSs. For the unique muting indicator set $\mathcal{J}_{m,j'}$, where $j' \in \mathcal{J}'_m$ and $\mathcal{J}'_m = \{1, \dots, J'_m\}$, the set of indices of UEs, connected to BS m , with equal muting indicator set is defined as

$$\mathcal{N}_{m,j'} = \{n \in \mathcal{N} \mid c_{n,m} = 1, \mathcal{J}_{m,j'} \subsetneq \mathcal{J}_n, \forall m \in \mathcal{M}, \forall j' \in \mathcal{J}'_m\}. \quad (5.15)$$

Based on the definitions in (5.14) and (5.15), the following Proposition 5.3 is given.

¹It is worth mentioning that also non-linear combinations of the achievable data rates can be applied. One example is the Mutual Information based Exponential SNR Mapping (MIESM) [LKK12, WIN05]. However, in the case of non-linear combination, the formulation is no longer an ILP.

Proposition 5.3. Assume BS $m \in \mathcal{M}$, with unique muting indicator set index given by $j' \in \mathcal{J}'_m$ and the set $\mathcal{N}_{m,j'}$ as introduced in (5.15). If $|\mathcal{N}_{m,j'}| > 1$, then the optimal contribution of BS m on PRB $l \in \mathcal{L}$ to the total PF metric in (5.12a), corresponds to the PF metric of UE \hat{n} , with

$$\hat{n} = \arg \max_{n \in \mathcal{N}_{m,j'}} \Omega_{n,l,j} = \arg \max_{n \in \mathcal{N}_{m,j'}} \frac{r_{n,l,j}}{R_n} \quad \forall j \in \mathcal{J}' \mid \mathcal{J}_{n,j} = \mathcal{J}_{m,j'}, \quad (5.16)$$

where $\Omega_{n,l,j}$ is defined as in (3.11).

Proof. See Appendix C. □

Based on Proposition 5.3, it is sufficient that each BS $m \in \mathcal{M}$ forwards to the central controller on PRB $l \in \mathcal{L}$, the $\text{CSI}^{\text{R-11}}$ reports related to one UE per unique muting indicator set $\mathcal{J}_{m,j'}$, $\forall j' \in \mathcal{J}'_m$, instead of the $\text{CSI}^{\text{R-11}}$ reports from all connected UEs. The set of indices of UEs connected to BS m that maximize the PF metric on PRB l , in at least one of the unique muting indicator sets indexed by $j' \in \mathcal{J}'_m$, is defined as

$$\mathcal{N}'_{m,l} = \left\{ \hat{n} \mid \exists j : \hat{n} = \arg \max_{n \in \mathcal{N}_{m,j'}} \Omega_{n,l,j}, \quad \forall j' \in \mathcal{J}'_m, \quad \forall j \in \mathcal{J}' \mid \mathcal{J}_{n,j} = \mathcal{J}_{m,j'} \right\}. \quad (5.17)$$

The cardinality of the set $\mathcal{N}'_{m,l}$, is bounded as $1 \leq |\mathcal{N}'_{m,l}| \leq \sum_{n \in \mathcal{N}} c_{n,m}$, where the lower bound implies that only one UE provides the maximum PF metric on PRB l , among all unique muting indicator sets, and the upper bound corresponds to the case when each UE reports different muting indicator sets with respect to the other UEs connected to BS m .

Example 5.3. Assume a network with M BSs, where BS m serves a total of \tilde{N} UEs. It is further assumed that all \tilde{N} UEs served by BS m , have the same set of cooperative interfering BSs, such that $\mathcal{I}_n^c = \mathcal{I}'$, $\forall n \in \mathcal{N} \mid c_{n,m} = 1$, with $|\mathcal{I}'| = M'$. Thus, the number of unique muting indicator sets for BS m is $J'_m = 2^{M'}$. If the reducibility concept is not applied, BS m needs to forward to the central controller a total of $\tilde{N} \cdot J'_m$ $\text{CSI}^{\text{R-11}}$ reports on PRB $l \in \mathcal{L}$, corresponding to the interference scenarios of all connected UEs. However, if BS m applies the reducibility concept, the number of forwarded $\text{CSI}^{\text{R-11}}$ reports to the central controller decreases to J'_m , with $|\mathcal{N}'_{m,l}| \leq J'_m$. Hence, the total number of connected UEs impacts marginally the size of the solution space.

At the central controller, all the achievable data rates $r_{n,l,j}$, $\forall n \in \mathcal{N}'_{m,l}$, $\forall m \in \mathcal{M}$, $\forall l \in \mathcal{L}$, $\forall j \in \mathcal{J}'$, are per definition set to zero for the interference scenarios where UE n does not provide the maximum PF metric among the UEs connected to the same BS m . The set $\mathcal{N}'_l = \cup_{m \in \mathcal{M}} \mathcal{N}'_{m,l}$ is used to denote the indices of UEs to be considered in the reformulated ILP on PRB l . The cardinality of the set \mathcal{N}'_l is described as $M \leq |\mathcal{N}'_l| \leq N$. In the special case of $M' = 0$, all UEs report only one interference scenario where no cooperative interfering BS is muted, and thus, $|\mathcal{N}'_l| = M$.

Lifting. In order to linearize the constraints in (5.12c), a variable transformation is introduced based on the lifting technique [Bal05]. A new coordinated decision variable is defined, denoted by the tensor \mathbf{S} of dimensions $N \times L \times J'$. The new coordinated decision variable contains both, the scheduling and the muting decisions, and has elements

$$s_{n,l,j} = \begin{cases} 1 & \text{if PRB } l \in \mathcal{L} \text{ is scheduled to UE } n \in \mathcal{N} \\ & \text{under interference scenario } j \in \mathcal{J}' \\ 0 & \text{otherwise.} \end{cases} \quad (5.18)$$

The new decision variable, $s_{n,l,j}$, is related to the muting and scheduling decisions in (5.2) and (5.10), respectively, as

$$s_{n,l,j} = 1 \Leftrightarrow \bar{s}_{n,l} = 1 \wedge \bar{\alpha}_{m,l} = 1, \quad \forall n \in \mathcal{N}, \quad \forall l \in \mathcal{L}, \quad \forall j \in \mathcal{J}', \quad \forall m \in \mathcal{J}_{n,j}, \quad (5.19)$$

with \wedge denoting the logical *and* operator. Hence, the non-linear constraints in (5.12c) reduce to a linear combination of the achievable data rates, $r_{n,l,j}$, and the new decision variable, $s_{n,l,j}$.

Problem Reformulation. Using the above described concepts of separability, reducibility and lifting, the CS with muting INLP formulation in (5.12) can be reformulated as an ILP, which can be efficiently solved by commercial solvers as mentioned in Section 2.3. Hence, with the set \mathcal{N}'_l as introduced above, and defining the binary decision variable \mathbf{S}_l to have dimensions $|\mathcal{N}'_l| \times J'$, the sub-problem formulation for PRB $l \in \mathcal{L}$ is

$$\max_{\{\mathbf{S}_l\}} \sum_{n \in \mathcal{N}'_l} \Omega_{n,l} \quad (5.20a)$$

s.t.

$$s_{n,l,j} + \sum_{u \in \mathcal{N}'_l} \sum_{i \in \mathcal{J}'} c_{u,m} s_{u,l,i} \leq 1 \quad \forall n \in \mathcal{N}'_l, \quad \forall j \in \mathcal{J}', \quad \forall m \in \mathcal{J}_{n,j}, \quad (5.20b)$$

$$\sum_{n \in \mathcal{N}'_l} \sum_{j \in \mathcal{J}'} c_{n,m} s_{n,l,j} \leq 1 \quad \forall m \in \mathcal{M} \setminus \bigcup_{n \in \mathcal{N}'_l} \mathcal{I}_n^c, \quad (5.20c)$$

$$r_{n,l} = \sum_{j \in \mathcal{J}'} r_{n,l,j} s_{n,l,j} \quad \forall n \in \mathcal{N}'_l, \quad (5.20d)$$

$$s_{n,l,j} = 0 \quad \forall n \in \mathcal{N}'_l, \quad \forall j \in \mathcal{J}' \mid r_{n,l,j} = 0, \quad (5.20e)$$

$$s_{n,l,j} \in \{0, 1\} \quad \forall n \in \mathcal{N}'_l, \quad \forall j \in \mathcal{J}', \quad (5.20f)$$

where the objective in (5.20a) is to maximize the sum of the PF metric over all UEs on PRB l . The constraints in (5.20b) restrict the scheduling decisions of the cooperative interfering BSs of UE $n \in \mathcal{N}'_l$, i.e., $\forall m \in \mathcal{J}_{n,j}$, in order to agree with the muting state considered in the interference scenario $j \in \mathcal{J}'$. If PRB l is scheduled to UE n under the condition of muting the cooperative interfering BSs indexed by the set $\mathcal{J}_{n,j} \in \mathcal{J}_n$, then, no other UE connected to the muted BSs can be simultaneously assigned to the same PRB l . Thus, if $s_{n,l,j} = 1$ in (5.20b), the second term on the left-hand-side must be equal to zero. Furthermore, in the case that $s_{n,l,j} = 0$, the constraints in (5.20b) ensure that single-user transmissions are carried out, where each BS $m \in \mathcal{J}_{n,j}$ is allowed to

serve a maximum of one UE per PRB, over all possible interference scenarios $j \in \mathcal{J}'$. Since it is possible that specific BSs within the cooperation cluster do not belong to the set of cooperative interfering BSs of any UE, the constraints in (5.20c) complement the restriction on the single-user transmissions from (5.20b). Additionally, the total instantaneous achievable data rate on PRB l of UE n , denoted by $r_{n,l}$, is calculated in (5.20d) as the achievable data rate for the selected interference scenario j , as defined by the coordinated decision variable $s_{n,l,j}$. It is worth noting that from the CSI^{R-11} reports, $r_{n,l,j}$ is uniquely related to $s_{n,l,j}$, thus, no lookup table function as used in (5.13) is required. Furthermore, the constraints in (5.20e) are incorporated as a pre-processing step to ensure that no PRB is scheduled to UEs for which a maximum PF metric for the corresponding interference scenario j is not available. Finally, the elements of the coordinated decision matrix \mathbf{S}_l are binary as described by the constraints in (5.20f).

Theorem 5.1. *The LTE-Advanced CS with muting problem formulations in (5.12) and (5.20) are equivalent.*

Proof. See Appendix D. □

The proposed parallelized formulation in (5.20) reduces significantly the CS with muting problem complexity, enabling its application even for large-size networks as illustrated in Section 5.4.

5.3.3 State-of-the-art greedy heuristic algorithm

In this section, a brief description of the greedy heuristic deflation algorithm proposed in [GKN⁺15] (see algorithm in Section II) for the deployment scenario with centralized controller, is provided.

The greedy heuristic algorithm iteratively solves the CS with muting problem per PRB $l \in \mathcal{L}$. At each iteration, one BS is muted corresponding to the BS $m \in \mathcal{M}$ which, when muted, maximizes the sum of the PF metrics among all UEs on PRB l . The algorithm stops when muting any additional BS does not improve the sum of the PF metrics with respect to the previous iteration. The greedy heuristic algorithm for PRB $l \in \mathcal{L}$ is summarized as follows.

1. Initialize the reference PF metric

$$\Omega_l^{\text{ref}} = \sum_{m \in \mathcal{M}} \max_{n \in \mathcal{N}} c_{n,m} \Omega_{n,l,j} \quad \forall j \in \mathcal{J}' \mid \mathcal{J}_{n,j} = \emptyset, \quad (5.21)$$

with the value corresponding to the interference scenario where no BS is muted, i.e., PF scheduler without any cooperation. The symbol \emptyset denotes the empty set.

2. Initialize the set of indices of possible muted BSs as $\mathcal{M}' = \mathcal{M}$, and the set of indices of already muted BSs as $\check{\mathcal{M}} = \emptyset$.
3. For the set of indices of possible muted BSs \mathcal{M}' , calculate the PF metrics under the assumption that the BSs $\check{\mathcal{M}} \cup k$ are muted, denoted as Ω_l^k and given by

$$\Omega_l^k = \sum_{m \in \mathcal{M} \setminus \check{\mathcal{M}} \cup k} \max_{\{n,j\}} c_{n,m} \Omega_{n,l,j} \quad \forall k \in \mathcal{M}', \forall n \in \mathcal{N}, \forall j \in \mathcal{J}'. \quad (5.22)$$

Note that the selection of the interference scenario j , should not violate the assumption of only BSs $\check{\mathcal{M}} \cup k$ to be muted.

4. Select the muted BS $\check{m} \in \mathcal{M}'$, that maximizes the PF metric Ω_l^k , i.e.,

$$\check{m} = \arg \max_{k \in \mathcal{M}'} \Omega_l^k, \quad (5.23)$$

and set the result as $\Omega_l^{\max} = \Omega_l^{\check{m}}$.

5. Compare Ω_l^{\max} with Ω_l^{ref}
 - If $\Omega_l^{\max} > \Omega_l^{\text{ref}}$, set the selected BS \check{m} as muted and update the reference PF metric, that is, $\check{\mathcal{M}} = \check{\mathcal{M}} \cup \check{m}$, $\mathcal{M}' = \mathcal{M}' \setminus \check{m}$, $\Omega_l^{\text{ref}} = \Omega_l^{\max}$. Return to step 3.
 - If $\Omega_l^{\max} \leq \Omega_l^{\text{ref}}$, muting BS \check{m} brings no additional gain. The reference metric Ω_l^{ref} determines the resulting scheduling decision. Stop the algorithm for PRB l .

It is not guaranteed that the heuristic algorithm yields a globally optimal point, because the quality of the scheduling decision depends directly on the gain achieved from muting one interfering BS at a time.

Example 5.4. A new exemplary scenario is considered where three UEs are served by three BSs over one PRB. The connection matrix \mathbf{C} , with elements as defined in (3.3), is given by $\mathbf{C} = \mathbf{I}_{3 \times 3}$, where $\mathbf{I}_{3 \times 3}$ corresponds to a 3×3 identity matrix, i.e., UE k is served by BS k , $\forall k \in \{1, 2, 3\}$. At the central controller, the PF metric information for all possible muting patterns is summarized in Table 5.3. If no muting is applied, i.e., PF scheduler without any cooperation, the interference scenario corresponds to the last row of Table 5.3, with a total sum of the PF metric of 4.5. In the case of the state-of-the-art greedy heuristic algorithm, a first iteration is performed where only one BS is muted at a time, which corresponds to the first three rows of Table 5.3. When comparing the maximum achievable sum of the PF metrics obtained when muting either BS 1 or BS 3, with the sum of the PF metric obtained when no BS is muted, the results are equal, i.e., 4.5. Therefore, the greedy heuristic algorithm stops the iterative process and serves all the UEs without muting. Contrary to the greedy heuristic algorithm, the proposed ILP formulation analyzes all the possible interference scenarios. Thus, the scheduling decision of the ILP is to serve UE 3 while muting BS 1 and BS 2, which achieves the maximum sum of the PF metrics, equivalent to 6.

Table 5.3. PF metrics for different muting patterns

Muting Pattern $[\alpha_1, \alpha_2, \alpha_3]$	UE Index			$\sum_n \Omega_n$ $n \in \{1, 2, 3\}$
	1	2	3	
$[1, 0, 0]$	–	3	1.5	4.5
$[0, 1, 0]$	2.5	–	1.5	4.0
$[0, 0, 1]$	3	1.5	–	4.5
$[1, 1, 0]$	–	–	6	6
$[1, 0, 1]$	–	3	–	3
$[0, 1, 1]$	5	–	–	5
$[1, 1, 1]$	–	–	–	0
$[0, 0, 0]$	2	1.5	1	4.5

5.3.4 Generalized greedy heuristic algorithm

Given the disadvantage of the CS with muting greedy heuristic algorithm from [GKN⁺15] as mentioned in Section 5.3.3, an extension is proposed in this work called *generalized greedy heuristic algorithm*, which trades off computational complexity with performance gains. The main difference with respect to the algorithm in [GKN⁺15], is the evaluation of additional muting patterns per iteration. The proposed generalized greedy heuristic algorithm for PRB $l \in \mathcal{L}$ is summarized as follows.

1. Initialize the reference PF metric Ω_l^{ref} as in (5.21).
2. Initialize the set of indices of possible muted BSs as $\mathcal{M}' = \mathcal{M}$, and the set of indices of already muted BSs as $\check{\mathcal{M}} = \emptyset$.
3. Define the set of muting indicator sets as the union of binomial coefficients, such as

$$\hat{\mathcal{M}} = \bigcup_{\hat{m} \in \{1, \dots, \tilde{m}\}} \binom{\mathcal{M}'}{\hat{m}}, \quad (5.24)$$

where $[\hat{\mathcal{M}}]_i$ contains the indices of BSs to be muted under interference scenario i , and \tilde{m} is a configuration parameter to control the amount of muting patterns to be considered per iteration, with $\tilde{m} \leq M - 1$.

4. For the set of muting indicator sets $\hat{\mathcal{M}}$, calculate the PF metrics under the assumption that the BSs $\check{\mathcal{M}} \cup [\hat{\mathcal{M}}]_i$ are muted, denoted as Ω_l^i and given by

$$\Omega_l^i = \sum_{m \in \mathcal{M} \setminus \check{\mathcal{M}} \cup [\hat{\mathcal{M}}]_i} \max_{\{n, j\}} c_{n, m} \Omega_{n, l, j} \quad \forall i \in \{1, \dots, |\hat{\mathcal{M}}|\}, \quad \forall n \in \mathcal{N}, \quad \forall j \in \mathcal{J}'. \quad (5.25)$$

Note that the selection of the interference scenario j , should not violate the assumption of only BSs $\check{\mathcal{M}} \cup \left[\hat{\mathcal{M}} \right]_i$ to be muted.

5. Select the index \check{w} of the muting indicator sets that maximizes the PF metric Ω_l^i , i.e.,

$$\check{w} = \arg \max_{i \in \{1, \dots, |\hat{\mathcal{M}}|\}} \Omega_l^i, \quad (5.26)$$

and set the result as $\Omega_l^{\max} = \Omega_l^{\check{w}}$.

6. Compare Ω_l^{\max} with Ω_l^{ref}

- If $\Omega_l^{\max} > \Omega_l^{\text{ref}}$, set the selected BSs indexed by $\left[\hat{\mathcal{M}} \right]_{\check{w}}$ as muted and update the reference PF metric, that is, $\check{\mathcal{M}} = \check{\mathcal{M}} \cup \left[\hat{\mathcal{M}} \right]_{\check{w}}$, $\mathcal{M}' = \mathcal{M}' \setminus \left[\hat{\mathcal{M}} \right]_{\check{w}}$, $\Omega_l^{\text{ref}} = \Omega_l^{\max}$. Return to step 3.
- If $\Omega_l^{\max} \leq \Omega_l^{\text{ref}}$, muting the BSs indexed by $\left[\hat{\mathcal{M}} \right]_{\check{w}}$ brings no additional gain. The reference metric Ω_l^{ref} determines the resulting scheduling decision. Stop the algorithm for PRB l .

It is worth to mention that the configuration parameter \tilde{m} , with $1 \leq \tilde{m} \leq M - 1$, as introduced in (5.24), determines how many BSs are muted at a time. The configuration parameter \tilde{m} controls the complexity of the proposed generalized greedy heuristic algorithm by determining the muting patterns to be evaluated. If $\tilde{m} = 1$, the generalized greedy heuristic algorithm reduces to the heuristic algorithm from [GKN⁺15]. In the case that $\tilde{m} = M - 1$, the generalized greedy heuristic algorithm performs an exhaustive search.

Example 5.5. *Further elaborating on the Example 5.4, the generalized greedy heuristic algorithm with configuration parameter $\tilde{m} = 2$ evaluates all muting patterns involving one or two muted BSs. Thus, the generalized greedy heuristic algorithm serves UE 3 while muting BS 1 and BS 2, which achieves the maximum sum of the PF metrics, equivalent to 6. Therefore, the proposed generalized heuristic algorithm makes the same scheduling decision as the ILP formulated in Section 5.3.2, in contrast to the heuristic algorithm from [GKN⁺15] which does not mute any BS.*

5.4 Simulation Results

In this section, simulation results are presented to evaluate the performance of the CoMP CS schemes with respect to a PF scheduler without any cooperation, referred to as “non-coop. PFS”. The proposed parallelized sub-problem formulation as presented in Section 5.3.2, labeled as “ILP”, is examined together with the state-of-the-art greedy algorithm described in Section 5.3.3, denoted as “GA”, and the proposed generalized

greedy algorithm of Section 5.3.4, labeled as “GG”. In the simulations, $M' = 2$ strongest interfering BSs per UE are considered, which according to (5.1) are also assumed to be the cooperative interfering BSs per UE.

Similar to Chapter 4, the results are presented in terms of the long-term average user throughput, with particular interest on the cell-edge throughput corresponding to the average user throughput of the worst 5% of the UEs in the network. Additionally, the geometric mean of the average user throughput from all UEs is evaluated as proposed by the authors in [GKN⁺15] as a direct measure of the PF scheduler’s objective function.

5.4.1 Performance analysis

In order to study the performance of the CS with muting schemes, Monte Carlo standalone simulations have been carried out, where the CSI^{R-11} reports are generated based on channels obtained from a 3GPP compliant system-level simulator as specified in [rGPP10, rGPP12, rGPP13a, rGPP13b]. At each transmission time t , the average user throughput over time of UE $n \in \mathcal{N}$ is updated as defined in (3.13), where the total instantaneous achievable data rate of UE n at the previous transmission time, denoted by $r_n(t-1)$, is calculated as given by e.g., (5.20d). This average user throughput over time is further used to calculate the PF metric of UE n as in (3.11).

The performance of the CS with muting algorithms in terms of average user throughput, is studied with respect to the data rates the users can achieve per symbol and to the noise power level considered in the calculation of these achievable data rates. In practical LTE-Advanced systems, finite MCSs are used which restrict the achievable data rates per symbol. For the current analysis, two cases are considered with respect to the maximum achievable data rate: *i*) the MCS is unbounded, denoted as “Unb. MCS”, where the maximum achievable data rate can approach arbitrarily large values, and *ii*) a maximum achievable data rate of 5.4 bits/symbol is used, as imposed by a typical highest MCS bound in LTE-Advanced, referred to as “B. MCS”. Similarly, two noise power levels are considered, where in the first case, noise free decoding is assumed, denoted as “N.-less”, and in the second case, noise at the receivers is included, referred to as the “Noisy” case. The noise power level, in dBm, is calculated as

$$\sigma^2 = -174 + \varsigma + 10 \log_{10}(B), \quad (5.27)$$

where B corresponds to the transmission bandwidth in Hz, and ς represents the noise figure of the receiver in dB [SBT11], with

$$\varsigma = \begin{cases} -1000 \text{ dB} & \text{in the N.-less case} \\ 9 \text{ dB} & \text{in the Noisy case [rGPP10].} \end{cases} \quad (5.28)$$

The cell-edge and the geometric mean of the user throughput are shown in figures 5.2 and 5.3, respectively, for a scenario with $M = 3$ BSs, $N = 30$ UEs (ten UEs per BS)

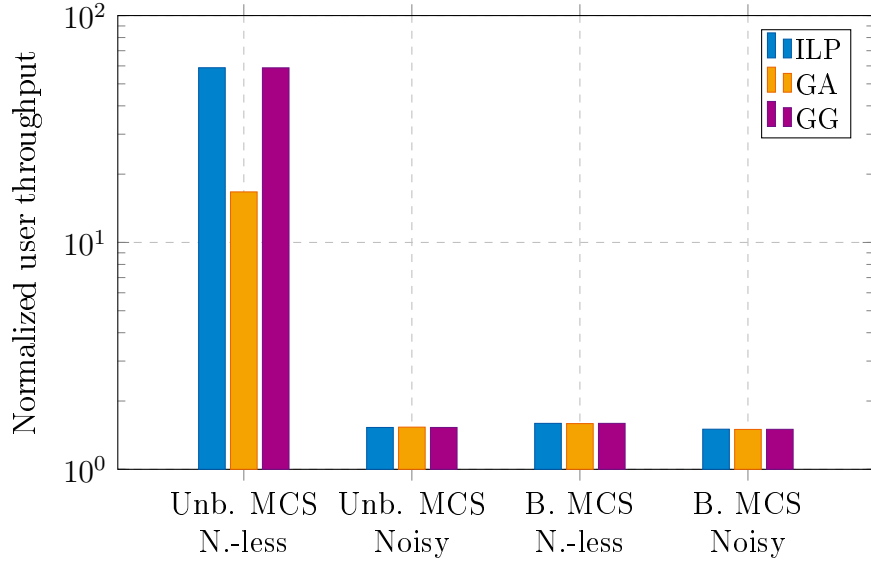


Figure 5.2. Cell-edge throughput for the CoMP CS schemes, normalized with respect to the non-coop. PFS. Scenario with $M = 3$ BSs, $N = 30$ UEs, $L = 10$ PRBs and $M' = 2$ BSs. Four cases with limitations on the maximum achievable data rate and the noise power level are considered. Out-of-cluster interference is not considered

and $L = 10$ PRBs. The user throughputs achieved by the CS with muting schemes ILP, GA and GG, are normalized by the resulting user throughput when no cooperative scheduler is applied, i.e., non-coop. PFS. Four cases are considered for different combinations of maximum achievable data rate and noise power level, as specified in the horizontal axis. No additional BSs are considered in the network, hence, the out-of-cluster interference $I_{n,l}^{oc} = 0$. Under no limitations on the achievable data rate and noise free receivers, i.e., Unb. MCS and N.-less, significant user throughput gains for both, the cell-edge and the geometric mean, are achieved by the cooperative schemes with respect to the non-coop. PFS. Moreover, the optimality of the proposed ILP formulation is notable, with the GA being unable to obtain the optimal solution. Due to the unboundedness of the MCS and the noise free decoder assumptions in this case, simultaneously muting the two cooperative interfering BSs can significantly increase the UE's data rate. Nevertheless, only muting one cooperative interfering BS does not yield sufficient PF metric gain, causing the GA scheme to stop prematurely. Such a limitation of the GA is not present in the proposed GG, which achieves the same optimal performance as the ILP scheme. Once limitations are assumed in the maximum achievable data rate or the noise power level, the observed gains from the CS with muting schemes with respect to the non-coop. PFS approach, vanish. Due to the low number of BSs in the cooperation cluster and given the above mentioned limitations, few users benefit from the simultaneous muting of the two cooperative interfering BSs. Thus, a greedy algorithm performs near-optimal under such practical network assumptions.

In Table 5.4, the average percentage of muted PRBs per BS is presented considering the four different scheduling schemes and four combinations of maximum achievable data

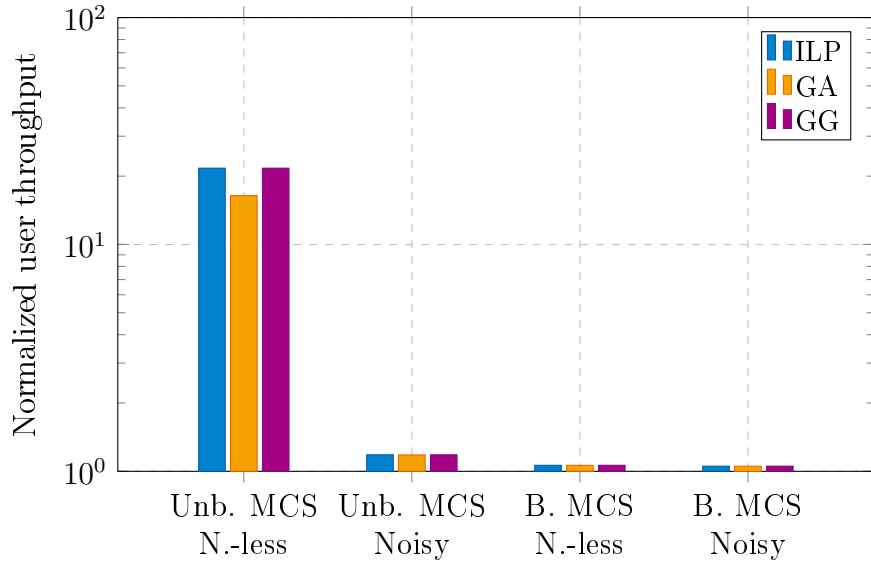


Figure 5.3. Geometric mean of the average user throughput for the CoMP CS schemes, normalized with respect to the non-coop. PFS. Scenario with $M = 3$ BSs, $N = 30$ UEs, $L = 10$ PRBs and $M' = 2$ BSs. Four cases with limitations on the maximum achievable data rate and the noise power level are considered. Out-of-cluster interference is not considered

Table 5.4. Average percentage of muted resources per BS

Scheduling scheme	non-coop. PFS	ILP	GA	GG
Unb. MCS & N.-less	0	0.67	0.53	0.67
Unb. MCS & Noisy	0	0.22	0.21	0.22
B. MCS & N.-less	0	0.08	0.08	0.08
B. MCS & Noisy	0	0.08	0.07	0.08

rate and noise power level. The non-coop. PFS does not apply muting, therefore the table contains zero entries for all cases. For the CS with muting schemes, according to figures 5.2 and 5.3, the average percentage of muted resources per BS reduces when the gain of muting is restricted. It is worth noting that even when the maximum achievable data rate is assumed to be unbounded above, i.e., Unb. MCS, and noiseless receivers are considered, i.e., N.-less, the ILP scheme mutes $2/3$ of the resources per BS, which means that each BS orthogonally serves its UEs over $1/M$ -th of the available resources. Further muting resources per BS, reduces the network performance because the user throughput distribution lacks fairness among the BSs. The value $1/M$, represents a fundamental limit of the cooperation and agrees with analytical studies presented by Lozano et al. in [LJA13]. Although the performance of the heuristic CS with muting schemes is near-optimal under current practical network conditions, it is envisioned that the evolution of mobile communications introduces, for future networks, receivers

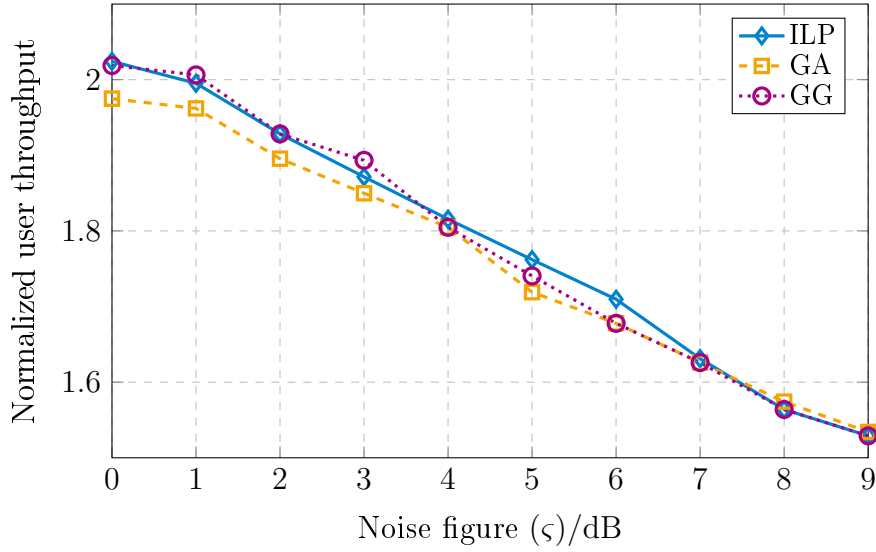


Figure 5.4. Cell-edge throughput, normalized with respect to the non-coop. PFS, for different noise figure values ζ . Scenario with $M = 3$ BSs, $N = 30$ UEs, $L = 10$ PRBs and $M' = 2$ BSs. Out-of-cluster interference is considered

with enhanced capabilities to suppress noise and to support the usage of higher MCSs. Hence, the results in figures 5.2 and 5.3, provide a reference to the potential gains of these heuristic schemes with respect to the optimal performance obtained with the proposed ILP.

In order to further illustrate the impact of the noise at the receiver on the performance of the studied CS with muting schemes, Figure 5.4 presents the average user throughput of the cell-edge users under different noise figure values, with $\zeta \in \{0, \dots, 9\}$ dB. This resulting noise power, calculated according to (5.27), can be also interpreted as residual interference from BSs outside of the cooperation cluster. From Figure 5.4, it is observable that the gain of the CS with muting schemes, with respect to the non-coop. PFS, reduces with a higher noise figure. Moreover, the gap between the proposed ILP and the state-of-the-art GA vanishes for typical noise figure values such as $\zeta = 9$ dB. Despite the cooperation between the BSs located within the cooperation cluster, the studied CS with muting schemes have no mechanisms to cope with the additional noise and possibly uncoordinated interference at the receivers, which further limits the performance gains of these cooperative schemes.

In order to study the performance of the CS with muting schemes with respect to the cooperation cluster size, the more practical scenario with a maximum achievable data rate of 5.4 bits/symbol and a noise figure $\zeta = 9$ dB is considered in the following. A network of seven BSs is simulated, where a single cooperation cluster of variable size, with $M \in \{3, \dots, 7\}$ is assumed. The BSs outside of the cooperation cluster are assumed to transmit data with maximum transmit power over the complete simulation time, i.e., $I_{n,l}^{\text{oc}} \geq 0$. Additionally, two alternatives for the number of cooperative interfering BSs per UE, denoted by M' , are considered with $M' = M - 1$ and $M' = 2$.

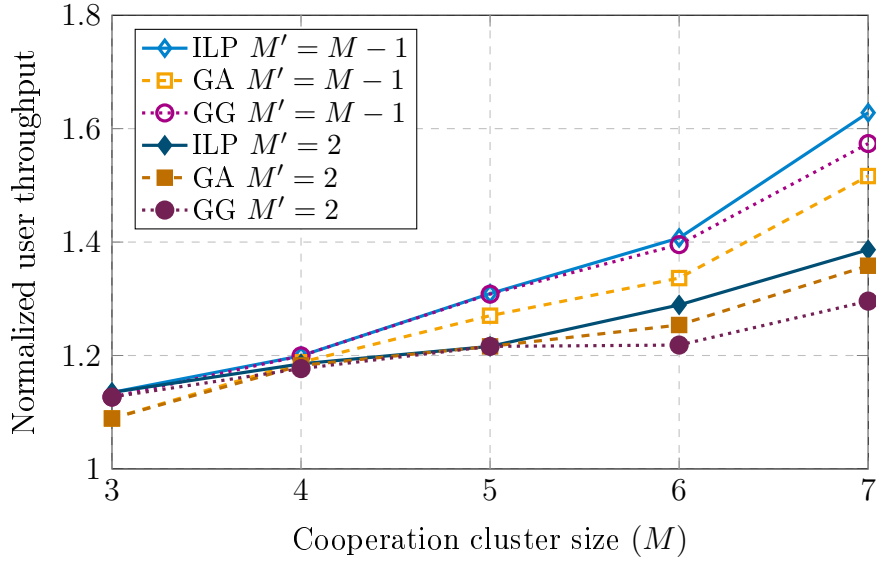


Figure 5.5. Cell-edge throughput, normalized with respect to the non-coop. PFS, for different values of the cooperation cluster size M . Scenario with $N = 10M$ UEs, $L = 10$ PRBs and $M' = \{2, M - 1\}$ BSs. Out-of-cluster interference is considered

In the latter case, in order to have a conservative estimation of the achievable data rate, the UEs generate CSI^{R-11} reports assuming maximum interference from the non-cooperative interfering BSs as defined in (5.8). Each BS serves ten UEs over $L = 10$ PRBs. The cell-edge throughput, as a function of the cooperation cluster size M , is shown in Figure 5.5 for the UEs served by the BSs within the cooperation cluster. The presented results are normalized with respect to the user throughput achieved by the same UEs if the non-coop. PFS is used. In accordance to the previous results, the CS with muting schemes provide gains with respect to a non-cooperative PF scheduler, with an increase in the gains for a larger cooperation cluster size. The reason for such an improvement is the opportunity of further reducing the interference, and thus enhancing the SINR by increasing the amount of BSs involved in the coordinated scheduling procedures. It is also observable that a larger number of M' cooperative interfering BSs per UE improves the gains of the CS with muting schemes, at the cost of additional computational complexity and signaling overhead. In agreement with the results presented in figures 5.2 and 5.3, the greedy algorithm of [GKN⁺15] shows a near-optimal performance under practical conditions, with the proposed GG algorithm performing better than the GA scheme when all possible cooperative interfering BSs are considered. Similar results were observed for the geometric mean of the user throughput as illustrated in Figure 5.6.

5.4.2 Potential gains

System-level simulation results are presented in order to demonstrate the achievable gains of the CS with muting schemes for LTE-Advanced macro-only and heterogeneous

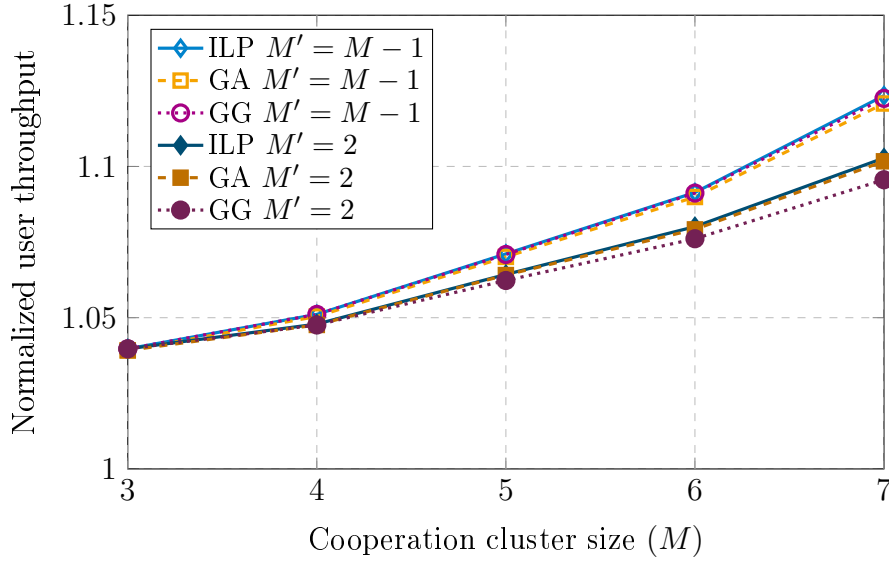


Figure 5.6. Geometric mean of the average user throughput, normalized with respect to the non-coop. PFS, for different values of the cooperation cluster size M . Scenario with $N = 10M$ UEs, $L = 10$ PRBs and $M' = \{2, M - 1\}$ BSs. Out-of-cluster interference is considered

networks in an urban deployment. In both cases, $N = 630$ UEs are served over $L = 10$ PRBs by $M = 21$ BSs in the macro-only network and $M = 42$ BSs in the heterogeneous case, where one pico cell is located within the coverage area of a macro BS with a separation distance of 125 m from the macro BS. The UEs are uniformly distributed in the macro-only case, while in the heterogeneous network the UEs are located in a hotspot fashion, where $2/3$ of the UEs are deployed in the vicinity of the pico BSs. In order to *move* UEs from the macro BSs to the small cells in the heterogeneous networks, CRE is used with a SINR off-set of 6 dB for the small cells. The out-of-cluster interference is modeled using the wrap-around technique [YDKS02], where additional BSs are deployed surrounding the M BSs of interest. Additionally, CSI^{R-11} reporting with periodicity of 5 ms is applied, where similar to the simulations in Section 5.4.1, a conservative estimation of the achievable data rates is calculated by assuming maximum interference from the remaining non-cooperative BSs. Full buffer conditions, ideal link adaptation and rank one transmissions are assumed, i.e., all users are always active and demand as much data as possible, the decoding is error-free and only transmit beamforming is applied, respectively. For more information on 3GPP-compliant system-level simulations, including channel and path loss models, the interested reader is referred to [rGPP10] (See 3GPP Case 1 and Case 6.2 from Section A.2.1).

The cell-edge and the geometric mean of the user throughput, normalized with respect to the non-coop. PFS, are presented in Figure 5.7 for a macro-only and in Figure 5.8 for a heterogeneous network. In order to follow the standard CSI^{R-11} reporting procedure, only $M' = 2$ cooperative interfering BSs within the cooperation cluster are reported by each UE. In terms of the geometric mean, gains are limited to values

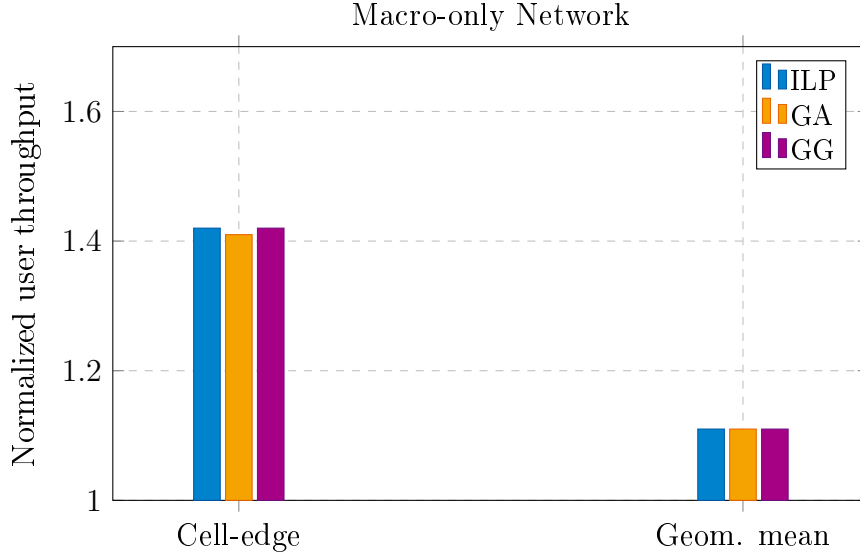


Figure 5.7. Cell-edge and geometric mean of the average user throughput, normalized with respect to the non-coop. PFS, for a scenario with $M = 21$ BSs, $N = 630$ UEs, $L = 10$ PRBs and $M' = 2$ BSs, with wrap-around technique. Results from system-level simulations of a macro-only network

around 11% for both cases, macro-only and heterogeneous networks. Additionally, the difference between the proposed schemes ILP and GG, and the state-of-the-art GA is negligible. As observed in Section 5.4.1, the out-of-cluster interference and the number of cooperative interfering BSs represent a limitation for the gains of the CS with muting schemes. For the UEs with the worst average user throughput, i.e., the cell-edge users, even with the limitation in the number of cooperative interfering BSs, the CS with muting schemes achieve a considerable gain in performance, with gains above 40% being observable. In the case of heterogeneous networks, the cell-edge gain is even higher due to the presence of a clear strongest interfering BS for the pico UEs corresponding to the macro BS, which is considered to cooperate within the restriction of $M' = 2$. The proposed generalized greedy algorithm GG performs better than the scheme in [GKN⁺15], i.e., GA, which follows from the flexibility to muting additional BSs. The average percentages of muted PRBs for the CS with muting schemes in the macro-only and heterogeneous networks are presented in Table 5.5. One implication of the muted PRBs is the opportunity to save transmit power at the BSs, with the proposed ILP and GG schemes muting more PRBs than the GA scheme.

Focusing on the proposed parallelized ILP, it is recognizable that the simplifications proposed in Section 5.3.2 enable the implementation of such a CS with muting approach even for medium- to large-size networks. Hence, instead of solving the CS with muting problem by considering the total of $N = 630$ UEs per PRB $l \in \mathcal{L}$, only $|\mathcal{N}'_l| = 136$ and $|\mathcal{N}'_l| = 213$ UEs were included in average for the macro-only and the heterogeneous network, respectively. That implies a reduction of 78% and 66% in the problem size, for each of the cases, respectively.

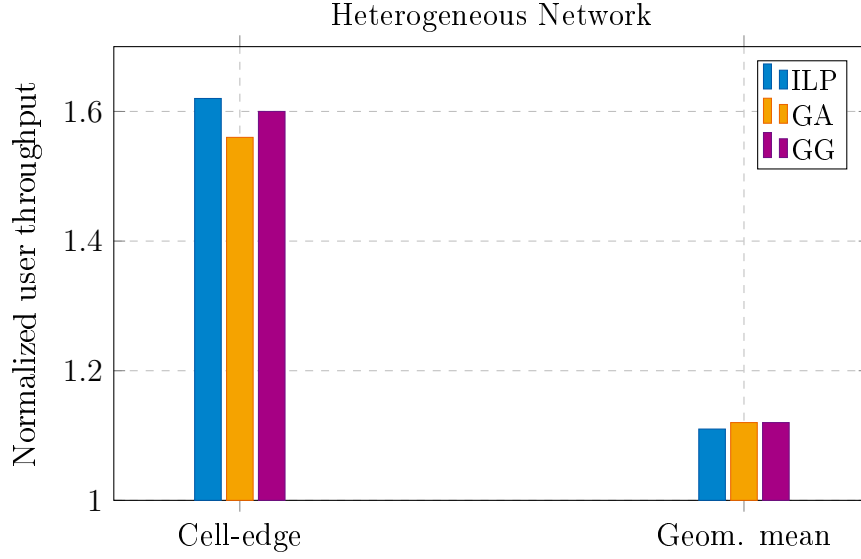


Figure 5.8. Cell-edge and geometric mean of the average user throughput, normalized with respect to the non-coop. PFS, for a scenario with $M = 42$ BSs, $N = 630$ UEs, $L = 10$ PRBs and $M' = 2$ BSs, with wrap-around technique. Results from system-level simulations of a heterogeneous network

Table 5.5. Average percentage of muted resources

Network	ILP	GA	GG
Macro-only	0.11	0.10	0.10
Heterogeneous	0.13	0.08	0.09

Finally, in contrast to the authors in [GKN⁺15], the analysis of the coordinated scheduling schemes in terms of the geometric mean of the user throughput, although meaningful, is not sufficient to evaluate the benefits of such schemes especially when the aim is to improve the performance of the cell-edge users.

5.5 Summary

In this chapter, the CoMP CS with muting problem in the framework of LTE-Advanced networks with a centralized controller has been studied, where the BSs connected to the central controller cooperate by jointly making scheduling and muting decisions. An INLP formulation has been proposed to solve the problem optimally, where a computationally efficient equivalent ILP reformulation has been presented to extend the applicability of the proposed scheme even to large-size networks. Moreover, a heuristic approach has been derived where the computational complexity can be adjusted according to configurable parameters.

System-level simulation results show that CS with muting can potentially improve the cell-edge user performance, with higher gains in heterogeneous networks. Nevertheless, these gains are limited by the remaining uncoordinated interference and the finite time/frequency/space resources to be shared in the network.

Given the still high computational complexity of the proposed ILP centralized scheme, heuristic algorithms such as the state-of-the-art greedy algorithm or the proposed generalized greedy algorithm are more appealing for practical implementations. However, the usage of the proposed ILP formulation is recommended as a benchmark to evaluate future schemes.

With respect to maximum achievable data rates and noise level at the receivers, although the simulation results have shown that the gap between the optimal ILP formulation and the suboptimal greedy algorithms reduces under current network parameters, it is worth to remark the difference in the performance of these schemes under relaxed network conditions. It is expected that the future technologies enable an evolution of the mobile communication systems towards such relaxed scenarios, where the proposed ILP proves to provide significant higher performance. Nevertheless, the low gap motivates the investigation of new schemes with lower computational complexity, such as the decentralized algorithms studied in Chapter 6.

Chapter 6

Decentralized Coordinated Scheduling in Mobile Communication Networks

In Chapter 5, CoMP CS has been investigated from a centralized architecture perspective, where a central controller manages the cooperation between the connected BSs. The CS with muting schemes proposed in that chapter enhance the user throughput performance, especially for the cell-edge users. Moreover, the performance improvement gap considering the solutions of the computational complex ILP formulation and the fast heuristic algorithms, is negligible under practical considerations of current LTE-Advanced networks. The implementation of a central controller represents some challenges in terms of costs and the need to ensure robustness to failures of the central processing unit. Therefore, alternative cooperative schemes that achieve similar performance gains and that do not require a central controller are desirable.

In this chapter, CoMP CS with muting is further investigated, where in contrast to Chapter 5 no central controller is available to coordinate the cooperation between the BSs. Therefore, the BSs cooperate in a decentralized manner by muting particular time/frequency resources in order to reduce the inter-cell interference experienced by the UEs connected to adjacent BSs. The proposed decentralized CS with muting scheme is derived to reduce the information exchange between the BSs, thus trading off user throughput performance and backhaul connectivity requirements.

6.1 State-of-the-art and Contributions

In [ABK⁺14], centralized and decentralized CS with muting schemes have been proposed where only one BS can be muted on a time/frequency resource. The results therein show that under such a muting condition, the performance of both, centralized and decentralized CS with muting schemes, is similar in terms of cell-edge and average user throughput, favoring the decentralized architecture due to the applicability in large-size networks and the reduced information exchange. Furthermore, in [GKN⁺15] the authors extend the CS with muting schemes from [ABK⁺14] to enable the simultaneous muting of multiple BSs on the same time/frequency resource. The proposed schemes in [ABK⁺14] and [GKN⁺15] are based on heuristics. In Chapter 5, it has been demonstrated with numerical simulations that the performance gap, in terms of user throughput, between the above mentioned CS with muting heuristics and the optimally solved ILP formulation vanishes under currently practical LTE-Advanced network conditions. Despite the near-optimal behavior of the state-of-the-art decentralized schemes proposed in [ABK⁺14] and [GKN⁺15], these state-of-the-art schemes still require to exchange a significant amount of messages between the neighboring BSs,

which can represent a limiting performance factor, especially under non-ideal backhaul links [GKN⁺15]. Therefore, in this chapter a novel decentralized CS with muting heuristic algorithm is proposed that requires low information exchange between the neighboring BSs by appealing to an *altruistic* behavior of the BSs.

The major contributions of this chapter are summarized as follows.

- A novel decentralized CS with muting heuristic algorithm is proposed based on LTE-Advanced standardized CSI^{R-11} reports, as presented in Section 2.1.3. Each BS independently decides to mute time/frequency resources to reduce the interference caused to UEs connected to neighboring BSs, without knowing the benefit that this muting decision can bring to the overall network.
- A limited amount of feedback is used in order to assess the benefit/loss of the muting decisions made in previous transmission times and react accordingly.
- The proposed CS with muting algorithm requires a considerably low information exchange between the BSs in comparison to the state-of-the-art decentralized heuristics in [ABK⁺14].

6.2 System Model

The decentralized CS with muting schemes are studied based on the system model as presented in Chapter 5 (see Section 5.2). However, as mentioned above, the absence of a central controller is considered in the following. Therefore, new definitions of the cooperation cluster and the cooperative interfering BSs per UE are required as explained below.

A cellular network is considered as in Figure 6.1, where M BSs serve N UEs in the downlink over the same L PRBs. Thus, inter-cell interference affects the UEs, especially of those located at the cell-edge. The BSs can be all of the same type, i.e., homogeneous networks, or they can have different capabilities as in the case of the heterogeneous networks introduced in Section 2.1.1. Moreover, limited backhaul connectivity between only adjacent BSs is considered, as depicted in Figure 6.1 by the dotted lines. The sets $\mathcal{M} = \{1, \dots, M\}$, $\mathcal{N} = \{1, \dots, N\}$ and $\mathcal{L} = \{1, \dots, L\}$ are used to address the indices of the BSs, UEs and PRBs, respectively, as introduced in Chapter 3.

The received power at UE $n \in \mathcal{N}$ from BS $m \in \mathcal{M}$ on PRB $l \in \mathcal{L}$, denoted as $p_{n,m,l}$, is defined as in (3.1). Moreover, the sum over all PRBs of the received power per BS m , constitutes the total received power at UE n from BS m , denoted by $p_{n,m}$, as defined in (3.2). The performance of the decentralized CS with muting schemes for macro-only and heterogeneous networks is studied where, for the latter, CRE strategy is considered as described in Section 4.2, with (4.2) and (4.3) defining the CRE selection strategy

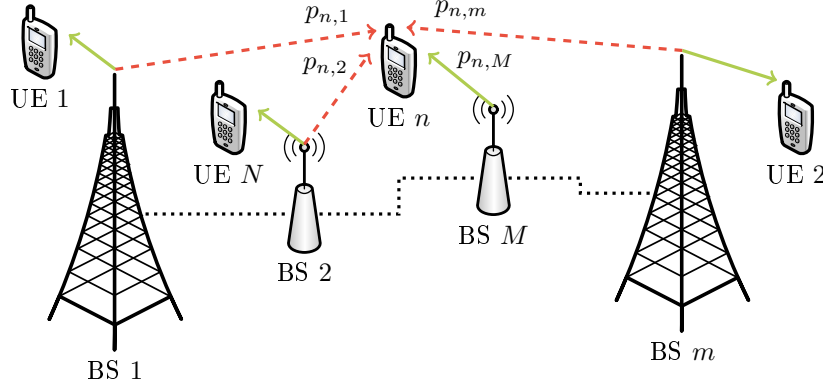


Figure 6.1. System model with M BSs and N UEs in the downlink. For UE n , the solid arrow represents the serving link while the dashed arrows correspond to the interfering links. The BSs are connected to their neighbors through backhaul links (dotted lines)

and off-set, respectively. Therefore, the $N \times M$ connection matrix \mathbf{C} is defined, with elements as in (3.3) characterizing the serving conditions between BSs and UEs.

In agreement to its centralized counterpart from Chapter 5, the decentralized CS with muting scheme studied in this chapter considers cooperation between the BSs in the form of muting time/frequency resources. Therefore, the binary muting decision matrix, denoted as $\bar{\alpha}$ and defined in (5.2), is used to describe the transmit powers of the BSs. If $\bar{\alpha}_{m,l} = 1$, BS $m \in \mathcal{M}$ is muted on PRB $l \in \mathcal{L}$. On the other hand, BS m transmits on PRB l with maximum transmit power $\Phi_{m,l}$, when the muting decision variable $\bar{\alpha}_{m,l} = 0$.

6.2.1 Decentralized cooperation clusters

From a BS perspective, cooperation can take place with the adjacent BSs from which connectivity is ensured via backhaul links. For BS $m \in \mathcal{M}$, the set $\hat{\mathcal{M}}_m \subsetneq \mathcal{M}$ contains the indices of BSs that can cooperate to improve the performance of the UEs connected to BS m according to the connection matrix \mathbf{C} . Multiple methods are available to define the index set $\hat{\mathcal{M}}_m$, such as static predefined cooperation clusters [MF11] or dynamic overlapping clusters [ABK⁺14]. In this work, each BS m selects its cooperation cluster based on the dynamic method from [ABK⁺14], where the \hat{M} BSs that produce the highest total interference power levels to the UEs connected to BS m are included in $\hat{\mathcal{M}}_m$, with $0 \leq \hat{M} < M$, such that $|\hat{\mathcal{M}}_m| = \hat{M}$. The total interference power level experienced at UE $n \in \mathcal{N}$ connected to BS m from BS $k \in \mathcal{M}$, such that $k \neq m$, is calculated as

$$I_{n,k} = p_{n,k}, \quad \forall n \in \mathcal{N}, \quad c_{n,m} = 1, \quad (6.1)$$

with $p_{n,k}$ defined in (3.2). Moreover, it is assumed that connectivity through backhaul links is available between BS m and the BSs indexed by $\hat{\mathcal{M}}_m$. Additionally, it is possible

that the cooperation sets of two BSs are not reciprocal. That is, although BS m considers BS k as part of its cooperation cluster, i.e., $k \in \hat{\mathcal{M}}_m$, the UEs connected to BS k may not experience significant interference from BS m , and therefore, $m \notin \hat{\mathcal{M}}_k$. Hence, the index set $\hat{\mathcal{K}}_m = \{k \mid m \in \hat{\mathcal{M}}_k, \forall k \in \mathcal{M}\}$, is used to address the indices of BSs that consider BS m as part of their cooperation clusters.

From a UE perspective, the UEs connected to BS $m \in \mathcal{M}$ as indicated by the connection matrix \mathbf{C} with elements given in (3.3), can only expect cooperation from the BSs belonging to the cooperation cluster of BS m , as indexed by the set $\hat{\mathcal{M}}_m$. Furthermore, the interference power levels experienced by the UEs from the BSs indexed by $\hat{\mathcal{M}}_m$ can vary significantly, depending on the channel coefficients between UEs and BSs as introduced in (3.1). In order to reduce the signaling overhead, the UEs connected to BS m generate CSI^{R-11} reports considering cooperation of only $M' \leq \hat{M}$ BSs, corresponding to the BSs from which the M' highest interference power levels are experienced. The set $\mathcal{I}_n^c \subseteq \hat{\mathcal{M}}_m$ addresses the indices of the cooperative interfering BSs considered in the CSI^{R-11} reports generated by UE $n \in \mathcal{N}$, with $|\mathcal{I}_n^c| = M'$.

6.2.2 CSI reporting for decentralized CS with muting

In the decentralized network architecture studied in this chapter, the CSI knowledge of the BSs is considered to be in form of the CSI^{R-11} reports as introduced in Section 3.1. These CSI^{R-11} reports contain information of a subset of possible muting decisions based on the cooperation cluster of the serving BS, as previously introduced in Section 6.2.1. Similar to Chapter 5, the muting matrix α is used as defined in Section 3.1, in order to describe the assumed transmit/muting states of the BSs associated with a specific CSI^{R-11} report.

In order to support the decentralized CS with muting scheme, UE $n \in \mathcal{N}$ served by BS $k \in \mathcal{M}$, generates CSI^{R-11} reports for all L PRBs containing information on the downlink data rates achievable under particular interference scenarios. As explained in Section 6.2.1, UE n considers only M' BSs indexed by \mathcal{I}_n^c , in the generation of the CSI^{R-11} reports. Therefore, UE n generates a total of $J' = 2^{M'}$ CSI^{R-11} reports per PRB $l \in \mathcal{L}$, corresponding to all possible combinations of transmit and muting states of the M' cooperative interfering BSs. To address the assumed interference scenarios in the J' CSI^{R-11} reports generated by UE n , the index set $\mathcal{J}' = \{1, \dots, J'\}$ is used. Moreover, the muting indicator set $\mathcal{J}_{n,j}$ is defined similarly to Section 5.2.1, containing the indices of the cooperative interfering BSs considered to be muted in the j -th CSI^{R-11} report of UE n . Hence, the muting pattern of the j -th CSI^{R-11} report of UE n on PRB l , is defined as

$$\alpha_{n,m',l,j} = \begin{cases} 1 & \text{if BS } m' \in \mathcal{J}_{n,j} \text{ on PRB } l \\ 0 & \text{otherwise} \end{cases} \quad \forall m' \in \mathcal{I}_n^c. \quad (6.2)$$

In the generation of the $\text{CSI}^{\text{R-11}}$ reports, the SINR on PRB $l \in \mathcal{L}$ of UE $n \in \mathcal{N}$ connected to BS $k \in \mathcal{M}$, under interference scenario $j \in \mathcal{J}'$, is given by

$$\gamma_{n,l,j}(\alpha_{n,m',l,j}) = \frac{p_{n,k,l}}{I_{n,l,j}^c(\alpha_{n,m',l,j}) + I_{n,l}^{\text{oc}} + \sigma^2}, \quad (6.3)$$

where the first term in the denominator corresponds to the interference from the cooperative interfering BSs of UE n , denoted as $I_{n,l,j}^c$ and defined as

$$I_{n,l,j}^c(\alpha_{n,m',l,j}) = \sum_{m' \in \mathcal{I}_n^c} (1 - \alpha_{n,m',l,j}) p_{n,m',l}, \quad (6.4)$$

the second term in the denominator, i.e., $I_{n,l}^{\text{oc}}$, refers to the interference from the remaining BSs in the network, given by

$$I_{n,l}^{\text{oc}} = \sum_{m \in \mathcal{M} \setminus \mathcal{I}_n^c} p_{n,m,l}, \quad (6.5)$$

where it is assumed that all remaining BSs in the network transmit on PRB l with maximum transmit power $\Phi_{m,l}$, in order to have conservative $\text{CSI}^{\text{R-11}}$ reports regarding the non-cooperative interfering BSs, and the last term in the denominator represents the AWGN power σ^2 , which is assumed without loss of generality, to be constant for all UEs over all PRBs as in Chapter 5. Moreover, the achievable data rate on PRB l of UE n under interference scenario j , denoted as $r_{n,l,j}$, is defined as in (5.9).

6.3 Decentralized CS with Muting

Based on the $\text{CSI}^{\text{R-11}}$ reports provided by the connected UEs, as described in Section 6.2.2, the BSs carry out the decentralized CS with muting scheme. This CS with muting scheme identifies which PRBs are used to serve the connected UEs, and on which PRBs the BSs are muted to reduce the interference experienced by UEs connected to neighboring BSs. The scheduling and muting decisions are made independently per PRB, which resembles the centralized schemes from Sections 5.3.2 to 5.3.4. In order to ease the comparison between the proposed decentralized CS with muting scheme and the state-of-the-art heuristic algorithms from [ABK⁺14], the notation used in the latter is adopted in the following.

Similar to the centralized CS with muting case, the decentralized scheme relies on the PF scheduling metric as given in (3.11) in order to obtain a trade-off between user throughput and fairness. Therefore, the PF metric on PRB $l \in \mathcal{L}$ of UE $n \in \mathcal{N}$ connected to BS $m \in \mathcal{M}$, under interference scenario $j \in \mathcal{J}'$, is defined as

$$\Omega_{n,l,j} = \frac{r_{n,l,j}}{R_n}, \quad (6.6)$$

where the numerator corresponds to the instantaneous achievable data rate on PRB l of UE n under interference scenario j , obtained from the $\text{CSI}^{\text{R-11}}$ reports as defined

in Section 6.2.2. The denominator refers to the average user throughput over time of UE n , considered to be constant among all L PRBs and updated according to (3.13).

Based on the CSI reports of UE $n \in \mathcal{N}$, the interference scenario $j_n^0 \in \mathcal{J}'$ is defined as the interference scenario where no BSs are muted, i.e., $\alpha_{n,k,l,j_n^0} = 0$, $\forall k \in \mathcal{I}_n^c$, $\forall l \in \mathcal{L}$. Hence, the interference scenario j_n^0 corresponds to the non-cooperative case, with all BSs transmitting with maximum transmit powers over all PRBs. The achievable PF metric on PRB l of BS $m \in \mathcal{M}$, when scheduling without muting takes place, denoted as $\Omega_{m,l}^0$, is given by

$$\Omega_{m,l}^0 = \max_{\substack{n \in \mathcal{N} \\ c_{n,m}=1}} \Omega_{n,l,j_n^0}, \quad (6.7)$$

with Ω_{n,l,j_n^0} calculated according to (6.6). On the other hand, in the case that BS $k \in \mathcal{M}$ is muted on PRB l , the *benefit metric* of BS m , which considers BS k as part of its cooperation cluster such that $k \in \hat{\mathcal{M}}_m$, is defined as

$$\beta_{m,l}^k = \max \{ \Omega_{m,l}^k - \Omega_{m,l}^0, 0 \}. \quad (6.8)$$

In (6.8), the PF metric on PRB l of BS m under the interference scenario where only BS k is muted, denoted as $\Omega_{m,l}^k$, is calculated similarly to (6.7), with $j_n^k \in \mathcal{J}'$ denoting the considered interference scenario with only BS k muted. It is worth noting that $\beta_{m,l}^k \geq 0$, since the scheduler is expected to select the best PF metric between either assuming that BS k is muted on PRB l , or that no cooperation is taking place. For BS k , which was assumed to be muted on PRB l according to (6.8), the *net benefit* metric is calculated as

$$B_{k,l} = \sum_{\substack{m \in \mathcal{M} \setminus k \\ k \in \hat{\mathcal{M}}_m}} \beta_{m,l}^k - \Omega_{k,l}^0. \quad (6.9)$$

The net benefit metric represents a measure of the impact on the network performance, of muting BS k on PRB l . If $B_{k,l} > 0$, the BSs that consider BS k as part of their cooperation clusters benefit more, in terms of PF metric, than the loss from muting BS k . On the other hand, if $B_{k,l} \leq 0$, muting BS k on PRB l , is not beneficial for the cooperative network.

6.3.1 State-of-the-art decentralized CS with muting scheme

The CS with muting scheme proposed in [ABK⁺14] (see Max-Net Benefit algorithm, Figure 6 in Section IV) is summarized as follows for PRB $l \in \mathcal{L}$ and transmission time t .

1. Calculate the benefit metrics as in (6.8):

$$\beta_{m,l}^k \quad \forall m \in \mathcal{M}, \quad \forall k \in \hat{\mathcal{M}}_m.$$

2. Report the calculated benefit metrics to the BSs belonging to the set of cooperative BSs:

$$\beta_{m,l}^k \rightarrow \text{BS } k \in \hat{\mathcal{M}}_m \quad \forall m \in \mathcal{M}.$$

3. Calculate the net benefit metrics as in (6.9):

$$B_{m,l} \quad \forall m \in \mathcal{M}.$$

4. Report the calculated net benefit metrics to the BSs belonging to the set of cooperative BSs:

$$B_{m,l} \rightarrow \text{BS } k \in \hat{\mathcal{M}}_m \quad \forall m \in \mathcal{M}.$$

5. Mute PRB l if BS m has the maximum net benefit metric among the known net benefit metrics, indexed by the set $\hat{\mathcal{K}}_m$ as defined in Section 6.2.1:

$$\bar{\alpha}_{m,l} = \begin{cases} 1 & \text{if } B_{m,l} \geq \max_{k \in \hat{\mathcal{K}}_m} B_{k,l} \\ 0 & \text{otherwise} \end{cases} \quad \forall m \in \mathcal{M}. \quad (6.10)$$

6. Report the muting decision to the BSs belonging to the set of cooperative BSs:

$$\bar{\alpha}_{m,l} \rightarrow \text{BS } k \in \hat{\mathcal{M}}_m \quad \forall m \in \mathcal{M}.$$

7. If not muted, perform PF scheduling as introduced in Section 3.2, based on the available information from the CSI^{R-11} reports and the known muting decisions from the BSs indexed by the set $\hat{\mathcal{K}}_m$. Transmit with maximum transmit power.

The above described Max-Net Benefit algorithm has two major disadvantages: *i)* three information exchange steps are required among the BSs in the cooperation clusters before the downlink transmissions take place, which can cause high latency depending on the quality of the backhaul links as investigated in [GKN⁺15], and *ii)* these three information exchange steps correspond to the reporting of all the benefit metrics, all the net benefit metrics and the resulting muting decisions for each PRB $l \in \mathcal{L}$, which represent a large amount of messaging between the BSs. It is worth to mention that, although an alternative method with only two information exchange steps is also derived in [ABK⁺14], referred to as *autonomous muting*, where the fourth step from the Max-Net Benefit algorithm is removed and muting applies if the net benefit metric is positive, the reduction in the amount of exchanged messages is negligible.

6.3.2 Proposed decentralized CS with muting scheme

To overcome the limitations of the state-of-the-art heuristic algorithms as mentioned in Section 6.3.1, in the following a decentralized CS with muting scheme that reduces

the amount of information exchanged between the BSs is proposed. In the proposed scheme, the BSs make muting decisions without current knowledge of the effect that these muting decisions have on the benefit metrics of the neighboring BSs. Hence, an altruistic behavior of the BSs is expected in the proposed scheme. To reduce the negative impact of the uninformed muting process on the BSs, a feedback method is considered which is carried out after the current transmit/muting procedures take place.

For BS $m \in \mathcal{M}$, the index set $\mathcal{L}_m(t) \subseteq \mathcal{L}$ is used to address the PRBs on which BS m is muted at transmission time t . Moreover, the variable $\mu_m(t) = |\mathcal{L}_m(t)|$ indicates the number of PRBs where BS m is muted. In the following, the proposed decentralized CS with muting scheme is presented for transmission time t , which is simultaneously carried out for all L PRBs.

Initialization ($t = 1$)

0. At transmission time $t = 1$, assign initial values to the index set of muted PRBs and the counting variable μ :

$$\mathcal{L}_m(t) = \emptyset, \mu_m(t) = 1 \quad \forall m \in \mathcal{M},$$

with \emptyset denoting the empty set.

Altruistic muting ($t \geq 1$)

1. Select PRBs with the lowest PF metrics, as defined in (6.7), to be muted:

$$\mathcal{L}'_m(t) = \left[\Omega_{m,l}^0 \right]_{\mu_m(t) - |\mathcal{L}_m(t)|} \quad \forall m \in \mathcal{M}, \forall l \in \mathcal{L} \setminus \mathcal{L}_m(t),$$

where the operator $\left[\Omega_{m,l}^0 \right]_y$ selects the y indices of PRBs corresponding to the lowest PF metrics.

2. Update the index set of muted PRBs and the counting variable μ :

$$\mathcal{L}_m(t) = \mathcal{L}_m(t) \cup \mathcal{L}'_m(t), \mu_m(t) = |\mathcal{L}_m(t)| \quad \forall m \in \mathcal{M}.$$

3. Set the muting decision according to the index set of muted PRBs:

$$\bar{\alpha}_{m,l} = \begin{cases} 1 & \text{if PRB } l \in \mathcal{L}_m(t) \\ 0 & \text{otherwise} \end{cases} \quad \forall m \in \mathcal{M}, \forall l \in \mathcal{L}. \quad (6.11)$$

4. Report the muting decision to the adjacent BSs that consider the reporting BS as part of their cooperation clusters:

$$\bar{\alpha}_{m,l} \rightarrow \text{BS } k \in \hat{\mathcal{K}}_m \quad \forall m \in \mathcal{M}, \forall l \in \mathcal{L}_m(t).$$

5. Perform PF scheduling as introduced in Section 3.2 on the PRBs where the BS is not muted, i.e., $\forall l \notin \mathcal{L}_m(t), \forall m \in \mathcal{M}$. The PF scheduling is based on the available information from the CSI^{R-11} reports and the known muting decisions from the BSs indexed by the set $\hat{\mathcal{M}}_m$. Transmit with maximum transmit power on the scheduled PRBs.

Feedback mechanism ($t \geq 1$)

6. After transmitting, calculate benefit metrics as defined in (6.8) on the PRBs, where the BSs belonging to the cooperation cluster were muted:

$$\beta_{m,l}^k \quad \forall m \in \mathcal{M}, \forall k \in \hat{\mathcal{M}}_m, \forall l \in \mathcal{L}_k(t).$$

7. Report the calculated benefit metrics to the BSs belonging to the set of cooperative BSs:

$$\beta_{m,l}^k \rightarrow \text{BS } k \in \hat{\mathcal{M}}_m \quad \forall m \in \mathcal{M}, \forall l \in \mathcal{L}_k(t).$$

8. Calculate net benefit metrics as in (6.9) for the muted PRBs:

$$B_{m,l} \quad \forall m \in \mathcal{M}, \forall l \in \mathcal{L}_m(t).$$

9. Evaluate impact of own muting decision. Configure the index set of muted PRBs and the counting variable μ for the next transmission time, accordingly:

$$\mathcal{L}_m(t+1) \rightarrow \begin{cases} l \in \mathcal{L}_m(t+1) & \text{if } B_{m,l} > 0 \\ l \notin \mathcal{L}_m(t+1) & \text{otherwise} \end{cases} \quad \forall l \in \mathcal{L}_m(t), \forall m \in \mathcal{M}. \quad (6.12)$$

$$\mu(t+1) = \begin{cases} \min \{\mu(t) + 1, L_{\max}\} & \text{if } |\mathcal{L}_m(t+1)| = \mu(t) \\ \max \{|\mathcal{L}_m(t+1)|, L_{\min}\} & \text{otherwise} \end{cases} \quad \forall m \in \mathcal{M}. \quad (6.13)$$

If the net benefit metric of BS m muted on PRB l is positive, the applied muting decision was beneficial for the network. Therefore, BS m remains muted on PRB l for the next transmission time $t+1$. Moreover, if all the net benefit metrics of BS m are positive, BS m increases the amount of PRBs on which it is muted for the next transmission time as described in (6.13), up to a maximum value $L_{\max} \leq L$. On the other hand, if the net benefit metric of BS m muted on PRB l is negative, then the muting decision negatively affected the network. Thus, BS m transmits data on PRB l for the next transmission time $t+1$. If all the net benefit metrics of BS m are negative, BS m sets the amount of PRBs on which it is muted to a minimum value for the next transmission time according to (6.13), with $L_{\min} \geq 1$ in order to avoid falling into a scenario without cooperation.

Since in the proposed CS with muting scheme the muting decisions are made by the BSs without current knowledge of the benefit metrics of the remaining BSs, the information exchange is reduced with respect to the state-of-the-art scheme in [ABK⁺14]. Moreover, the reporting of the muting decisions and the feedback of the benefit metrics are limited to only PRBs on which the BSs were muted, which further reduces the amount of messages exchanged between the BSs. Another mechanism from the proposed CS with muting scheme to reduce the information exchange, is to carry out muting decisions for multiple transmission times, where the feedback step is performed only once before the new muting decision is made.

6.4 Simulation Results

In this section, the system-level simulation results from Chapter 5 (see Section 5.4.2) are extended to include the results from the studied decentralized CS with muting schemes. Therefore, the same network scenarios as in Section 5.4.2 are considered, with $N = 630$ UEs served over $L = 10$ PRBs by $M = 21$ BSs in the case of a macro-only network and $M = 42$ BSs in a heterogeneous network, where one pico cell is located within the coverage area of a macro BS with a separation distance of 125 m from the macro BS. As explained in Section 6.2.1, each BS considers $\hat{M} = 6$ BSs as part of its cooperation cluster, while each UE generates CSI^{R-11} reports with $M' = 2$ cooperative interfering BSs.

Similar to Chapter 5, the performance of the decentralized CS with muting schemes is evaluated with respect to a PF scheduler without any cooperation, labeled as “non-coop. PFS”. The proposed decentralized CS with muting scheme as explained in Section 6.3.2, labeled as “dA”, is analyzed together with the Max-Net Benefit and the autonomous muting algorithms from [ABK⁺14], labeled as “dMB” and “dBA”, respectively. Additionally, for comparison purposes, results from two of the centralized CS with muting schemes presented in Section 5.4.2 are reproduced in the following, corresponding to the ILP scheme with optimal solution from Section 5.3.2, referred to as “cILP”, and the suboptimal heuristic algorithm from Section 5.3.3, denoted as “cGA”, where the prefix “c” is used to highlight the presence of the central controller.

The cell-edge and the geometric mean of the user throughput are shown in Figure 6.2 for the macro-only network, and in Figure 6.3 for the heterogeneous network, where the values are normalized with respect to the results obtained from a scenario without any cooperation, i.e., non-coop. PFS. In the case of the proposed decentralized scheme, the muting decisions are valid for a period of 1 ms, denoted by “dA1”, and a period of 5 ms, labeled as “dA5”. For all the additional schemes, 1 ms muting decisions are made. As expected, the decentralized CS with muting schemes behave worse than the centralized counterparts from Chapter 5. Nevertheless, the gains of the decentralized schemes with respect to the non-coop. PFS scheme are remarkable, especially for the cell-edge throughput. Although the proposed schemes, i.e., dA1 and dA5, are not aware

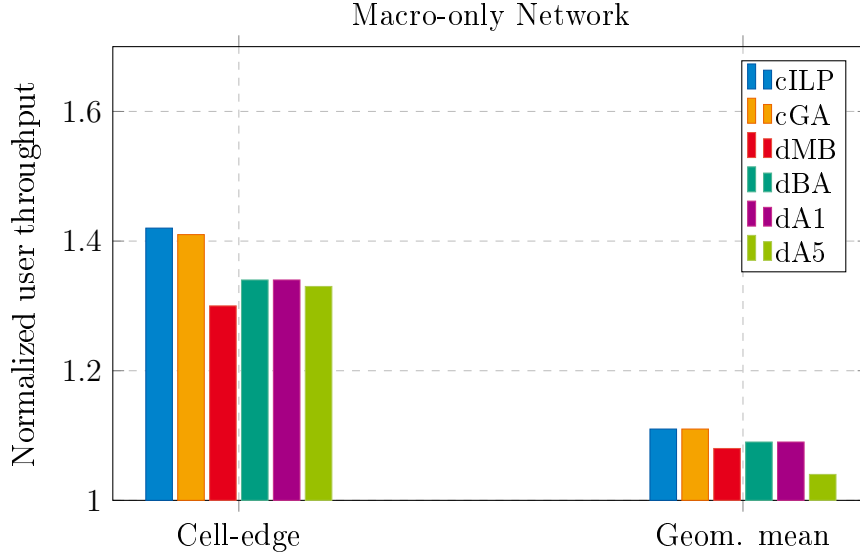


Figure 6.2. Cell-edge and geometric mean of the average user throughput, normalized with respect to the non-coop. PFS, for a scenario with $M = 21$ BSs, $N = 630$ UEs, $L = 10$ PRBs and $M' = 2$ BSs, with wrap-around technique. Results from system-level simulations of a macro-only network

of the current benefits the muting decisions can bring to the network, they perform close to the state-of-the-art approaches dMB and dBA. Furthermore, in the heterogeneous network case, the fact of providing muting decisions over a longer period of time, i.e., 5 ms in dA5, further improves the performance of the cell-edge UEs, achieving the highest gain between the decentralized schemes. In terms of the geometric mean, which measures the PF scheduler's objective function, since muting decisions without benefiting the network can occur, the proposed CS with muting schemes achieve the lowest performance, that is, they are less proportionally fair.

A comparison of the messages exchanged between the BSs for each decentralized CS with muting scheme is presented in Table 6.1, where the results are normalized with respect to the scheme with the largest information exchange, i.e., dMB. Each information exchange, e.g., the report of the muting decision or the benefit metric per PRB, is counted as a message, with the state-of-the-art dMB scheme transmitting a total of 3'979.801 and 5'908.347 messages in the macro-only and heterogeneous networks, respectively. The schemes proposed in this work require a minimum of 6 % and a maximum of 22 % of the messages exchanged in the state-of-the-art dMB method, which represents a significant reduction on the capacity and latency requirements of the backhaul links.

Furthermore, the dependency of the proposed dA scheme on the periodicity of the muting decisions, is presented in Figure 6.4 for the studied macro-only and heterogeneous networks, where the former is labeled as “M” and the latter is referred to as “H”. The cell-edge, i.e., “Edge”, and the geometric mean, labeled as “Gmean”, of the user

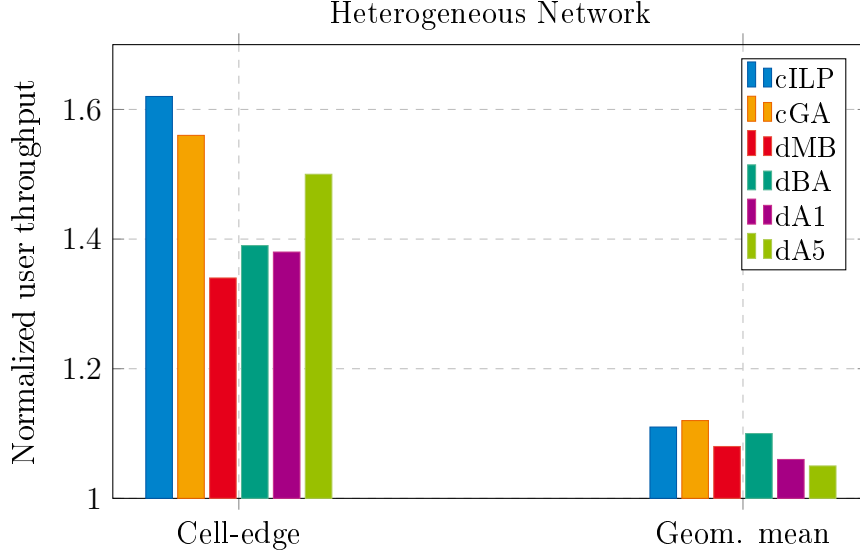


Figure 6.3. Cell-edge and geometric mean of the average user throughput, normalized with respect to the non-coop. PFS, for a scenario with $M = 42$ BSs, $N = 630$ UEs, $L = 10$ PRBs and $M' = 2$ BSs, with wrap-around technique. Results from system-level simulations of a heterogeneous network

Table 6.1. Relative amount of exchanged messages in the decentralized schemes

Network	CS scheme			
	dMB	dBA	dA1	dA5
Macro-only	1	0.83	0.16	0.06
Heterogeneous	1	0.82	0.22	0.07

throughput are illustrated, normalized with respect to the scenario without any cooperation, i.e., non-coop. PFS. In the macro-only case, higher periodicity values imply a reduction in performance for both, the cell-edge and the geometric mean of the average user throughput, which is explained by the risk of making *wrong* muting decisions for a longer period of time. In contrast, the cell-edge throughput of the heterogeneous networks benefits from higher periodicity values, as observed in the previous results. Nevertheless, muting time/frequency resources for longer time represents also a reduction in the geometric mean of the heterogeneous networks as a consequence of the lower spectral efficiency.

6.5 Summary

In this chapter, further investigations of the CoMP CS with muting schemes were carried out with focus on decentralized architectures. Similar to Chapter 5, the co-

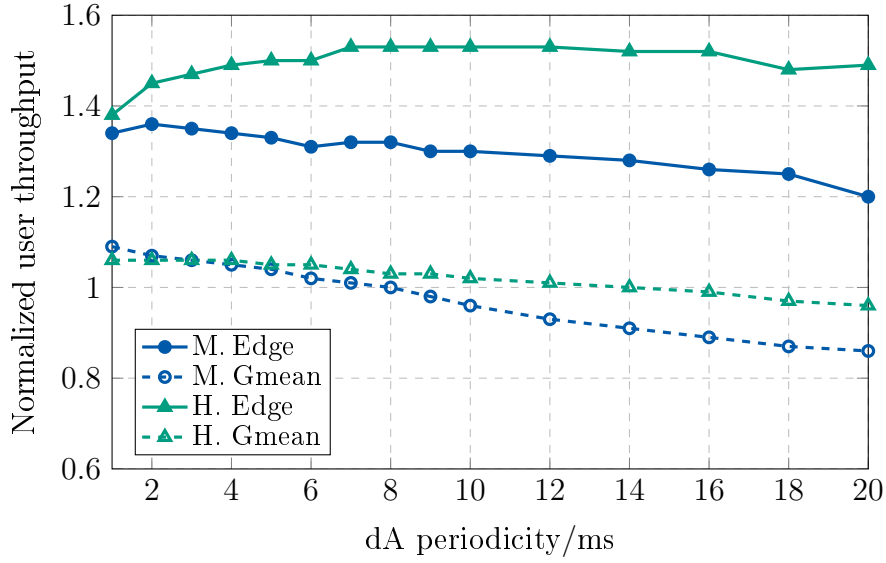


Figure 6.4. Cell-edge and geometric mean of the average user throughput of the proposed dA scheme, normalized with respect to the non-coop. PFS, for different periodicity values. Macro-only “M.” and heterogeneous “H.” networks are considered

operation takes place between the BSs by means of coordinating the scheduling and muting decisions in order to improve the performance, in terms of user throughput of the UEs, especially of those located at the cell-edge. However, in contrast to the schemes studied in Chapter 5, in this chapter the BSs cooperate in a decentralized fashion with only adjacent BSs, where low information exchange between the cooperative BSs is pursued.

System-level simulation results show that the proposed decentralized CS with muting scheme greatly reduces the amount of information exchange between the neighboring BSs, while achieving similar or even better results for the user throughput of the cell-edge UEs when compared to the state-of-the-art schemes in [ABK⁺14]. With respect to the results from the centralized CS with muting schemes as presented in Chapter 5, a reduction in performance is observable as expected for the decentralized case. Nevertheless, when considering that the cooperation is restricted to a limited number of adjacent BSs and that the computational complexity of the proposed scheme is negligible, the performance gap is remarkably small.

Chapter 7

Coordinated Scheduling under Bursty Traffic

The investigation of the cooperative resource allocation schemes from chapters 4 to 6, was carried out under the assumption of full-buffer systems for quasi-static scenarios, where the UEs demand as much data as possible while moving at very low speeds. For the link adaptation procedures, which establish the transmission parameters used per serving link, e.g., the transmit power, the modulation and the coding schemes, these relative stable conditions experienced by the UEs do not represent a significant challenge. Therefore, in full-buffer systems and even if no cooperation takes place, the link adaptation procedures at the BSs succeed to serve the UEs in the downlink with low error probabilities, because the CSI reports correctly reflect the channel conditions experienced by the UEs in terms of intended signal and interference. Although the full-buffer assumption is useful for the capacity analysis of the investigated schemes, this assumption does not typically hold true in practical communication networks. In mobile communication networks under bursty traffic conditions, the interference experienced by the UEs varies constantly. Therefore, the periodic reporting of CSI as explained in Section 2.1.3 becomes inaccurate and the performance of the link adaptation procedures deteriorates.

In this chapter, a centralized CoMP CS scheme is proposed to improve the performance of the link adaptation procedures for a non-full-buffer network in the downlink. For that purpose, an ILP problem is formulated, which at the time of serving a UE, attempts to reproduce the interference scenario as observed during the generation of the CSI report. Despite its combinatorial nature, the optimization framework proposed in this chapter is suitable for even medium- to large-scale networks. Additionally, CSI in form of $\text{CSI}^{\text{R-8}}$ reports is assumed in the scheme proposed in this chapter, which in contrast to the $\text{CSI}^{\text{R-11}}$ reports used in the schemes investigated in the previous chapters, does not cause any additional signaling overhead between the UEs and the BSs.

7.1 State-of-the-art and Contributions

The performance evaluation of interference mitigation techniques is generally carried out with a capacity enhancement perspective. Thus, the assumption of a full-buffer system where all UEs constantly demand as much data as possible is typically used. Hence, this kind of analysis considers a worst case scenario and provides lower bounds of the network performance [DGA13]. However, the full-buffer assumption might not hold true in many practical scenarios where the networks are over-dimensioned in order to ensure availability of time/frequency resources at any time, and where the UEs demand small data volumes. Several works take into account the network load in

their approaches to improve the user throughput. For instance, in [SPK⁺13] enhanced-ICIC is dynamically adapted according to the BS load. Thus, BSs with low load are muted more frequently in order to reduce the interference to UEs in neighboring BSs. In [CJXH13], a coordinated scheduling scheme is proposed where spectral resources and/or BSs are muted over time, in order to reduce energy consumption and interference when the network load is low.

In cellular networks, one way of performing the link adaptation procedures, i.e., the selection of the transmit powers and the MCS parameters for transmission [FYL⁺11], relies on the availability of CSI at the transmitter [3rd13]. As explained in Section 2.1.3 in the downlink case, such CSI is estimated and reported by the UEs in transmission times preceding the data transmission as depicted in Figure 2.5. In addition to the channel fluctuations, if the time/frequency resources are not fully occupied and the UEs demand short bursts of data, the interference scenario experienced by the UEs varies drastically due to changing transmission conditions of the BSs. As a consequence, the reported CSI may not correctly reflect the interference scenario to be experienced at the time of scheduling a new data transmission and therefore, the performance of the link adaptation procedures is affected, resulting in a significant increase of the BLER. Thus, more retransmissions are triggered that increase the delay and reduce the user throughput. Under such a non-full-buffer condition, instead of using traditional techniques designed for full-buffer networks to increase the achievable data rates, it is generally of higher importance to enhance the reliability of the CSI reports in order to reduce the BLER. Hence, retransmissions are avoided and the low demand caused by the bursty traffic of the UEs is satisfied within a short period of time.

In this chapter, a coordinated scheduling scheme is proposed in order to improve the performance of the link adaptation procedures for a non-full-buffer network with CSI^{R-8} feedback. The problem formulation aims to reduce the BLER by means of reproducing the interference scenario of the UEs to be served, at the time of generating the respective CSI^{R-8} reports.

The major contributions of this chapter are summarized as follows.

- The centralized CoMP CS problem under bursty traffic conditions is formulated as an ILP with the objective of reducing the BLER. The scheduling decisions pursue a trade-off between the user throughput and fairness, while considering the interference scenarios reflected in the CSI^{R-8} reports of the UEs to be served. Therefore, BSs can be muted in order to reproduce the interference scenario from the CSI^{R-8} report.
- The ILP is formulated under consideration of a low computational complexity, thus being also applicable in medium- to large-scale networks.
- System-level simulations are provided to evaluate the performance of the proposed scheme under different network loads.

7.2 System Model

In this chapter, the system model introduced in Chapter 3 is extended, where bursty traffic is incorporated as presented below. A cellular network is considered where M BSs serve N UEs in the downlink over L PRBs, as illustrated in Figure 7.1. Moreover, the BSs can be all of the same type, as in the case of homogeneous networks, or they can have different capabilities, such as in the case of heterogeneous networks as introduced in Section 2.1.1. The sets of indices $\mathcal{M} = \{1, \dots, M\}$, $\mathcal{N} = \{1, \dots, N\}$ and $\mathcal{L} = \{1, \dots, L\}$ are defined as in Chapter 3, to address the BSs, UEs and PRBs, respectively. Moreover, it is assumed that the BSs are connected via backhaul links to a central controller, which can be deployed as an independent entity or as part of a BS.

The received power at UE $n \in \mathcal{N}$ from BS $m \in \mathcal{M}$ on PRB $l \in \mathcal{L}$, denoted as $p_{n,m,l}$, is given by (3.1). Furthermore, the total received power at UE n from BS m over all L PRBs is denoted by $p_{n,m}$, as defined in (3.2). Similar to the previous chapters, different serving BS selection strategies can be carried out according to the network type. In the case of homogeneous networks, the serving BS corresponds to the BS which provides the largest total received power at the UE, while in the heterogeneous networks case, CRE strategy is applied as described by (4.2), with CRE off-set given by (4.3). Therefore, the $N \times M$ connection matrix \mathbf{C} is defined, with elements as in (3.3) characterizing the serving conditions between BSs and UEs. Moreover, the set of interfering BSs of UE n is defined as $\mathcal{I}_n = \{k \mid c_{n,k} = 0, \forall k \in \mathcal{M}\}$, as introduced in Chapter 3.

7.2.1 Traffic modeling

In order to simulate non-full buffer systems, time varying traffic at the UEs needs to be modeled. In the literature, especially when simulating LTE and LTE-Advanced networks, it is common to apply a File Transfer Protocol (FTP) traffic model to represent networks with underutilized time/frequency resources, as described in [rGPP10] (see Model 1 from Section A.2.1.3.1). The FTP traffic model considers UEs downloading single files of size V at a time, where the UEs are assumed to get active by following a Poisson process, with UE arrival rate of λ , $\lambda > 0$ [Ros10]. The arrival rate λ describes then, the activation time of the UEs. The Probability Density Function (PDF) of a Poisson process for variable values of the UE arrival rate λ is illustrated in Figure 7.2, where the horizontal axis corresponds to the number of active UEs, denoted by Λ , with $\Lambda \geq 0$, and the PDF is calculated as

$$\text{PDF} = \frac{\lambda^\Lambda}{\Lambda!} e^{-\lambda}. \quad (7.1)$$

Given that each UE downloads only one file at a time, the data demand of UE $n \in \mathcal{N}$ is defined as d_n , with $0 \leq d_n \leq V$.

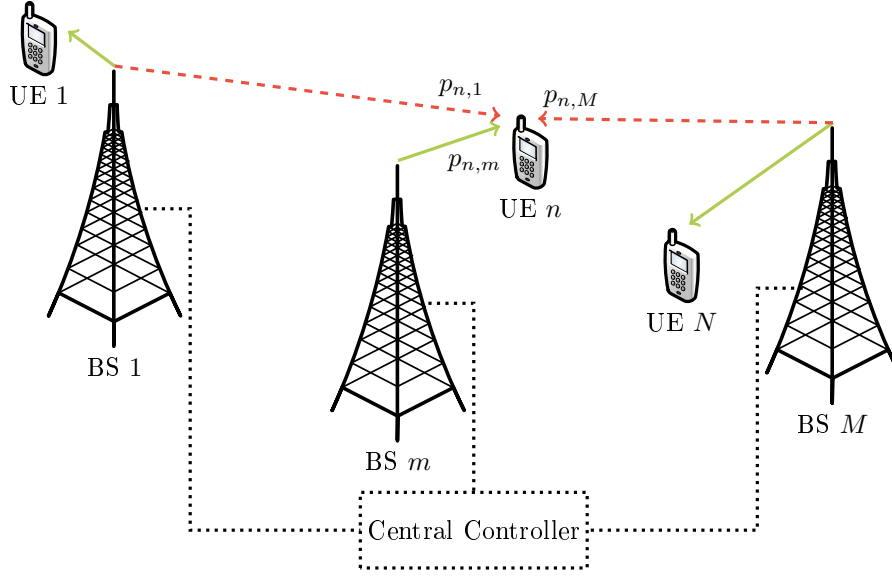


Figure 7.1. System model with M BSs and N UEs in the downlink. For UE n , the solid arrow represents the serving link while the dashed arrows correspond to the interfering links. The BSs are connected through the backhaul to a central controller (dotted lines)

Although the FTP traffic model enjoys high simplicity, the model lacks of flexibility to represent more complex interactions and service types available in wireless networks, such as streaming and voice services, among others. For that purpose, alternative traffic models based on Markov chains [Ros10, Sen06], have been proposed e.g., in [LAD⁺15, RCLD⁺14]. Since in this chapter the focus relies on networks with bursty traffic, the FTP traffic model is sufficient and it is therefore implemented in the system-level simulations of Section 7.4, with small file size V and low arrival rate λ .

Due to the non-full buffer assumption, the transmission state of the BSs varies according to the demand of their connected UEs. Therefore, at transmission time t , the state of BS $m \in \mathcal{M}$ on PRB $l \in \mathcal{L}$ is defined by the binary muting decision matrix $\bar{\alpha}$, of dimensions $M \times L$ and elements as introduced in (5.2). If $\bar{\alpha}_{m,l} = 0$, BS m transmits on PRB l with maximum transmit power $\Phi_{m,l}$. On the other hand, BS m is muted on PRB l , when the muting decision variable $\bar{\alpha}_{m,l} = 1$. In this chapter, three reasons can cause a muted BS under a non-full-buffer system, as follows.

- The demand of the connected UEs is served by the BS at the current transmission time t . In this case, the BS is muted on a subset of PRBs.
- The connected UEs are inactive, i.e., the UEs are not demanding data on the current transmission time t . Thus, the BS is muted on all L PRBs.
- The BS is muted as the result of the proposed CS scheme, in order to reflect the interference scenario as reported in the CSI^{R-8} report.

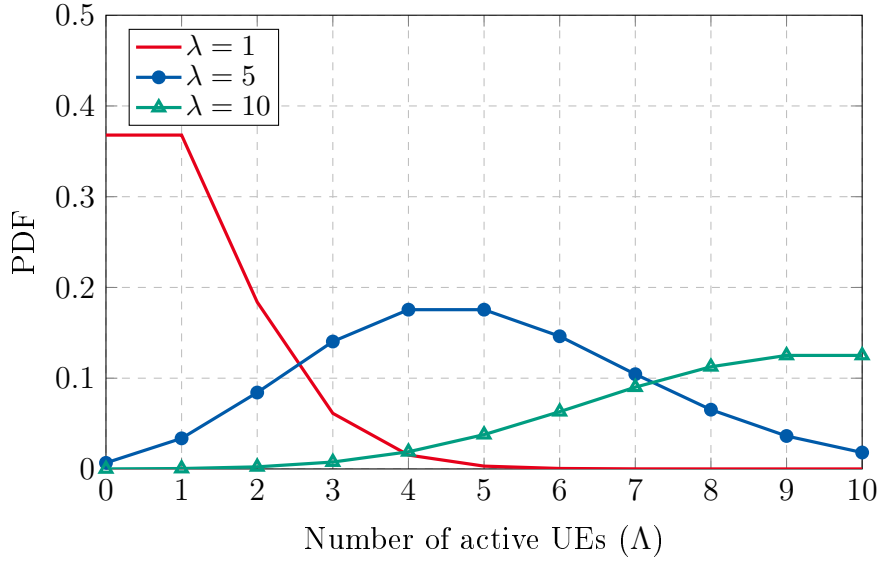


Figure 7.2. PDF of the Poisson distribution for different values of the UE arrival rates denoted by λ

7.2.2 CSI feedback and uncertainty

The transmitter requires CSI for the link adaptation procedures to determine a suitable MCS. In this chapter, it is assumed that the UEs use LTE standardized CSI^{R-8} reports as described in Section 2.1.3, where the UEs signal a CQI value per PRB. As previously explained in Section 7.2.1, the BSs can have different transmit/muting states depending on the demand of their connected UEs, as described by the muting decision matrix $\bar{\alpha}$. Thus, the CSI^{R-8} reports reflect the transmit/muting states of the BSs at the time of generating such reports, where the SINR on PRB $l \in \mathcal{L}$ of UE $n \in \mathcal{N}$ served by BS $m \in \mathcal{M}$, is defined as

$$\gamma_{n,l} = \frac{p_{n,m,l}}{\sum_{k \in \mathcal{I}_n} (1 - \alpha_{k,l}) p_{n,k,l} + \sigma^2}. \quad (7.2)$$

The numerator of (7.2) corresponds to the received power from the serving BS m , as defined in (3.1). For the purpose of generating the CSI^{R-8} report, it is assumed that the serving BS transmits with maximum transmit power $\Phi_{m,l}$, i.e., $\alpha_{m,l} = 0$. Moreover, the denominator of (7.2) is the sum of the received powers from the interfering BSs of UE n , indexed by the set \mathcal{I}_n and controlled by the muting state matrix α , and the AWGN power at the receiver, denoted by σ^2 and assumed without loss of generality, to be constant for all UEs over all PRBs. It is worth noting that, as explained in Section 3.1, the notation α is used in order to describe the assumed transmit/muting state of the BSs at the moment of generating the CSI^{R-8} report. Moreover, due to the utilization of CSI^{R-8} reports, both variables, $\bar{\alpha}$ and α , coincide at the transmission time t when the report is generated. Furthermore, the achievable data rate on PRB l of UE n , denoted as $r_{n,l}$, is modeled as a function of the UE's SINR, as defined in (3.9).

As explained in Section 2.1.3, the estimation and reporting process of CSI is typically performed in a periodic fashion, where UE $n \in \mathcal{N}$ feeds the generated $\text{CSI}^{\text{R-8}}$ reports back to its serving BS $m \in \mathcal{M}$ at time t . The $\text{CSI}^{\text{R-8}}$ report is then available for the scheduling and the link adaptation procedures at the serving BS m , after a delay of δ transmission times, and it is used for a period of T transmission times as depicted in Figure 2.5. It is commonly assumed that the BSs try to serve the UEs quickly using as few resources as possible, hence having available time/frequency resources to serve additional users. Thus, when considering bursty traffic, the BSs may serve the requested data demands using only a subset of the available PRBs, leaving the remaining PRBs unused, i.e., the BSs are inactive on the remaining PRBs. As a consequence of this common scheduling practice, the PRB utilization in the network is rapidly changing and the UEs experience drastically time-varying interference levels from the neighboring BSs. Based on Figure 2.5, the time of generating a $\text{CSI}^{\text{R-8}}$ report is defined as t_1 , and the time of using it at the BS is defined as t_2 , where t_2 is bounded by $t_1 + \delta \leq t_2 \leq t_1 + T + \delta$. Thus, by denoting $\gamma_n^{\text{R-8}}$ and $\gamma_n^{t_2}$, as the SINR of UE n at times t_1 and t_2 , respectively, three different interference scenarios are distinguished.

- If $\gamma_n^{\text{R-8}} < \gamma_n^{t_2}$, then the $\text{CSI}^{\text{R-8}}$ report was generated in a situation with higher interference than in the case when the $\text{CSI}^{\text{R-8}}$ report is actually used. Thus, the $\text{CSI}^{\text{R-8}}$ report pessimistically recommends the utilization of a lower MCS, resulting in lower user throughput.
- If $\gamma_n^{\text{R-8}} = \gamma_n^{t_2}$, then the interference scenarios at the generation and utilization times t_1 and t_2 , respectively, coincide, and the $\text{CSI}^{\text{R-8}}$ report correctly represents the current interference condition.
- If $\gamma_n^{\text{R-8}} > \gamma_n^{t_2}$, then the reported $\text{CSI}^{\text{R-8}}$ underestimated the interference at the time t_2 of using the $\text{CSI}^{\text{R-8}}$ report. This is the most critical situation because the utilization of a higher MCS increases the probability of a higher BLER. Once the transmissions are not successful, the time required to serve the UEs' demands increases due to retransmissions, thus reducing the experienced user throughput.

It is worth to mention that channel variations over time, due to time selective fading, also lead to $\text{CSI}^{\text{R-8}}$ report mismatch. However, these fading effects generally occur on a much slower time scale and are less drastic to the CSI mismatch than the variations in PRB utilization. Therefore, this chapter is focused on the impact of bursty traffic, while considering the channels to be time invariant.

7.3 Coordinated Scheduling for Link Adaptation

In this section two schedulers are presented corresponding to a common non-cooperative scheduler and the proposed coordinated scheduling approach. In both cases, due to the

burstiness of the UE traffic, the scheduling decisions are carried out by selecting one PRB at a time, together with the UE to be served by each BS on the selected PRB. Moreover, as mentioned in Section 7.2, in the case of the coordinated scheduling formulation, the BSs can be muted on specific PRBs in order to improve the performance of the link adaptation procedures of the UEs to be served by neighboring BSs. In the following, the index $\tau \in \{1, \dots, L\}$ is used to refer to the iterative scheduling process of selecting one PRB at a time.

7.3.1 Non-cooperative scheduling

A non-cooperative PF scheduler is considered, which is widely used to evaluate the performance of current cellular networks due to its simplicity, as introduced in Section 3.2. To obtain the scheduling decision, each BS independently maximizes the PF metric per PRB among its served UEs, as given by (3.11), which represents a trade-off between user throughput and fairness.

At each transmission time t , the PF scheduler at BS $m \in \mathcal{M}$ iteratively schedules the PRBs to the UEs served by BS m . In order to describe the iterative process of the PF scheduler, with iteration index $\tau \in \{1, \dots, L\}$ as introduced above, the following definitions are required. At iteration τ , the sets $\mathcal{D}_m^{(\tau)}$ and $\tilde{\mathcal{L}}_m^{(\tau)}$ contain the indices of the UEs to be served by BS m , and the indices of PRBs of BS m available for scheduling, respectively. Thus, $\mathcal{D}_m^{(\tau)}$ is defined as

$$\mathcal{D}_m^{(\tau)} = \{n \mid c_{n,m} = 1, d_n > 0, v_n^{(\tau)} < d_n, \forall n \in \mathcal{N}\} \quad \forall m \in \mathcal{M}, \quad (7.3)$$

where UE $n \in \mathcal{N}$ still requires scheduling of PRBs at iteration τ , if its data demand d_n is not covered by its total scheduled data volume at transmission time t , denoted as $v_n^{(\tau)}$ and given by

$$v_n^{(\tau)} = \begin{cases} 0 & \text{if } \tau = 1 \\ g(r_{n,l}, \tilde{\mathcal{L}}_n) & \text{if } \tau > 1 \end{cases} \quad \forall n \in \mathcal{N}. \quad (7.4)$$

At iteration $\tau = 1$, no PRB has been scheduled and therefore $v_n^{(1)} = 0, \forall n \in \mathcal{N}$. In the next iterations, the total scheduled data volume for UE n is calculated as a function $g(\cdot)$ of the instantaneous data rates $r_{n,l}$, over the scheduled PRBs as indexed by the set $\tilde{\mathcal{L}}_n$. The instantaneous data rates of UE n , denoted as $r_{n,l}$ and defined in (3.9), are available from the CSI^{R-8} reports. Moreover, the set of indices of PRBs scheduled to UE n , denoted as $\tilde{\mathcal{L}}_n$, is given by

$$\tilde{\mathcal{L}}_n = \{l^{(\zeta)} \mid n^{(\zeta)} = n, \zeta = 1, \dots, \tau - 1\} \quad \forall n \in \mathcal{N}. \quad (7.5)$$

Example 7.1. The function $g(\cdot)$ to calculate the scheduled data volume $v_n^{(\tau)}$ of UE $n \in \mathcal{N}$ at iteration τ , with $\tau > 1$, can be given by

$$g(r_{n,l}, \tilde{\mathcal{L}}_n) = \sum_{\tilde{l} \in \tilde{\mathcal{L}}_n} r_{n,\tilde{l}}, \quad (7.6)$$

with the achievable data rates $r_{n,l}$ as defined in (3.9), and the set of indices of scheduled PRBs of UE n , denoted as $\tilde{\mathcal{L}}_n$, defined in (7.5).

Furthermore, the index set of available PRBs of BS $m \in \mathcal{M}$ at iteration τ , denoted as $\tilde{\mathcal{L}}_m^{(\tau)}$, is given by

$$\tilde{\mathcal{L}}_m^{(\tau)} = \begin{cases} \mathcal{L} & \text{if } \tau = 1 \\ \tilde{\mathcal{L}}_m^{(\tau-1)} \setminus l^{(\tau-1)} & \text{if } \tau > 1 \end{cases} \quad \forall m \in \mathcal{M}, \quad (7.7)$$

where the already scheduled PRBs, denoted as $l^{(\zeta)}$, $\zeta = 1, \dots, \tau - 1$, are removed for the next iterations. At iteration $\tau \in \{1, \dots, L\}$, the non-cooperative scheduler of BS m selects the tuple of PRB $l^{(\tau)}$ to be scheduled to the UE $n^{(\tau)}$, which maximizes the PF metric $\Omega_{n,l}$, as defined in (3.11), $\forall n \in \mathcal{D}_m^{(\tau)}$, $\forall l \in \tilde{\mathcal{L}}_m^{(\tau)}$. Mathematically, the iterative non-cooperative PF scheduler decision is given by

$$\{n^{(\tau)}, l^{(\tau)}\} = \arg \max_{n \in \mathcal{D}_m^{(\tau)}, l \in \tilde{\mathcal{L}}_m^{(\tau)}} \Omega_{n,l} \quad \forall \tau \in \{1, \dots, L\}, \quad (7.8)$$

where the scheduling procedure finalizes when all the L PRBs have been scheduled, i.e., $\tilde{\mathcal{L}}_m^{(\tau)} = \emptyset$, or when the demand of all UEs has been covered, i.e., $\mathcal{D}_m^{(\tau)} = \emptyset$, with \emptyset denoting the empty set.

In Section 7.2.2, it has been explained in which sense the bursty traffic generates uncertainties in the CSI^{R-8} reports. If at the time t_1 of generating the CSI^{R-8} report, one or multiple BSs were inactive on a particular PRB, then it is expected that the CSI^{R-8} report describes this PRB as suitable for high achievable data rates, simply because the interference experienced on that PRB was low. Moreover, multiple UEs connected to different BSs generate CSI^{R-8} reports simultaneously, reflecting the same beneficial condition on the PRB with low interference. In this case, when the non-cooperative PF scheduler is used at the BSs according to (7.8), it is then expected that several BSs select the same reported high data rate PRBs for transmission at time t_2 , with $t_1 + \delta \leq t_2 \leq t_1 + T + \delta$. Thus, the interference is increased with respect to the scenario from the CSI^{R-8} report. Therefore, the non-cooperative PF scheduler strengthens the negative effect of underestimating the interference.

Example 7.2. *An example of the consequences of CSI uncertainty when applying the non-cooperative PF scheduler is shown in Figure 7.3, where at transmission time $t = t_1$, the CSI^{R-8} report \mathcal{R}_0 is generated by the UEs, with the BSs utilizing the frequency resources as depicted. At transmission time $t = t_2$, with $t_1 + \delta \leq t_2 \leq t_1 + T + \delta$, the BSs use CSI^{R-8} report \mathcal{R}_0 for scheduling, where the previously unloaded PRBs are selected by each BS independently because they provide, with high probability, the largest PF metrics. However, that scheduling decision is going to increase significantly the interference along with the probability of a higher BLER.*

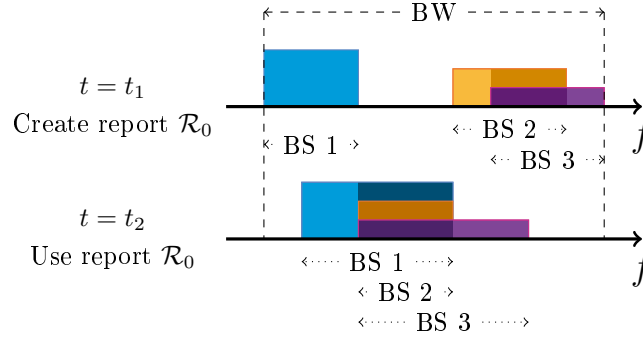


Figure 7.3. Example of CSI uncertainty with non-cooperative PF scheduler. At transmission time $t = t_1$ the CSI^{R-8} report \mathcal{R}_0 is generated with no interference in a portion of the frequency band. By independently using \mathcal{R}_0 at time $t = t_2$, each BS decides to schedule transmissions in the reported low interference region, causing collisions and possible increase of the BLER

7.3.2 Cooperative scheduling

In this section, a cooperative scheduling scheme is proposed, where an ILP is formulated to improve the performance of the link adaptation procedures. When serving a UE, the proposed scheme targets to reproduce the same or even a more favorable interference scenario than experienced during the time of generating the CSI^{R-8} report. This cooperative approach assumes the presence of a central entity that performs the scheduling decision for all BSs. By making the decisions, the central entity keeps track of the interference scenarios in which the CSI^{R-8} reports were generated. Thus, the proposed scheme introduces only additional signaling between the BSs and the central controller, without increasing the complexity or signaling overhead at the UE side, i.e., support of CSI^{R-11} reports is not needed. In order to reduce the computational complexity, the scheduling decision is performed per PRB for all connected BSs, in contrast to the non-cooperative PF scheduler of (7.8), which is performed independently per BS over all PRBs.

Before formulating the ILP, the set of indices of cooperative interfering BSs of UE $n \in \mathcal{N}$ served by BS $m \in \mathcal{M}$, denoted as \mathcal{I}_n^c as introduced in Section 3.1, is given by

$$\mathcal{I}_n^c = \{k \mid c_{n,k} = 0, p_{n,k} \geq \nu_n p_{n,m}, \forall k \in \mathcal{M}\} \quad \forall n \in \mathcal{N}. \quad (7.9)$$

In (7.9), BS k belongs to the set \mathcal{I}_n^c , if it does not serve UE n and its total received power $p_{n,k}$ is above a threshold determined by a fraction of the total received power from the serving BS m , as defined in (3.2). The factor ν_n , with $0 \leq \nu_n \leq 1$, is used to determine the threshold level for the selection of the strongest interfering BSs of UE n . It is worth noting that $\mathcal{I}_n^c \subseteq \mathcal{I}_n$ and, thus, the maximum cardinality of the set \mathcal{I}_n^c is equivalent to $M - 1$, if the received power from all interfering BSs is above the threshold determined by ν_n , e.g., by setting $\nu_n = 0$. Additionally, the set of indices of muted cooperative interfering BSs of UE n on PRB $l \in \mathcal{L}$, denoted as $\mathcal{M}_{n,l}$,

represents the cooperative interfering BSs of UE n , that did not schedule transmissions on PRB l , while UE n generated the currently used CSI^{R-8} report. Therefore, $\mathcal{M}_{n,l} = \{k \mid \alpha_{k,l} = 1, \forall k \in \mathcal{I}_n^c\}$, with $\alpha_{k,l}, \forall k \in \mathcal{I}_n^c$, representing the transmit/muting state of the cooperative interfering BSs of UE n , at the time of generating the CSI^{R-8} report, as introduced in Section 7.2.2. Since the set $\mathcal{M}_{n,l}$ considers only the indices of the cooperative interfering BSs of UE n , then $\mathcal{M}_{n,l} \subseteq \mathcal{I}_n^c$. A cooperative interfering BS may not schedule PRBs for transmitting data either because the connected UEs are not demanding data, or because the proposed coordinated scheduling scheme mutes the BS in order to reproduce a former interference scenario. Since the set \mathcal{I}_n^c depends on the total received power at UE n , and the set $\mathcal{M}_{n,l}$ depends on the currently used CSI^{R-8} reports, these sets remain constant in the current transmission time and can be determined upfront the CS scheme.

Similar to the non-cooperative PF scheduler of Section 7.3.1, the CoMP CS scheme at the central controller iteratively schedules the PRBs to the UEs. In contrast, however, to (7.3) and (7.7), where the sets were defined per BS $m \in \mathcal{M}$, in the proposed cooperative scheduling scheme, new sets $\mathcal{D}^{(\tau)}$ and $\tilde{\mathcal{L}}^{(\tau)}$ are considered which are defined for all M BSs. Thus,

$$\mathcal{D}^{(\tau)} = \{n \mid d_n > 0, v_n^{(\tau)} < d_n, \forall n \in \mathcal{N}\}, \quad (7.10)$$

with $v_n^{(\tau)}$ given in (7.4), and $\tilde{\mathcal{L}}^{(\tau)}$ is calculated as in (7.7) for the complete network. With the sets defined as above, the proposed CS scheme for iteration $\tau \in \{1, \dots, L\}$ is formulated as the following ILP

$$\max_{\{\mathbf{s}_{l^{(\tau)}}\}} \sum_{n \in \mathcal{D}^{(\tau)}} \Omega_{n,l^{(\tau)}} s_n \quad (7.11a)$$

s.t.

$$s_n + \sum_{u \in \mathcal{D}^{(\tau)}} c_{u,m} s_u \leq 1 \quad \forall n \in \mathcal{D}^{(\tau)}, \forall m \in \mathcal{M}_{n,l^{(\tau)}}, \quad (7.11b)$$

$$\sum_{n \in \mathcal{D}^{(\tau)}} c_{n,m} s_n \leq 1 \quad \forall m \in \mathcal{A}_{l^{(\tau)}}, \quad (7.11c)$$

$$s_n \in \{0, 1\} \quad \forall n \in \mathcal{D}^{(\tau)}, \quad (7.11d)$$

where the parameter

$$l^{(\tau)} = \arg \max_{n \in \mathcal{D}^{(\tau)}, l \in \tilde{\mathcal{L}}^{(\tau)}} \Omega_{n,l}, \quad (7.12)$$

corresponds to the PRB with the maximum PF metric $\Omega_{n,l}$ as given in (3.11), among all UEs and all available PRBs at iteration τ . The objective in (7.11a) is to maximize the sum of the PF metric $\Omega_{n,l}$, over all UEs with demand as indexed by the set $\mathcal{D}^{(\tau)}$. The scheduling decision variable $\mathbf{s}_{l^{(\tau)}}$, corresponding to a vector of dimensions $|\mathcal{D}^{(\tau)}| \times 1$, with elements

$$s_n = \begin{cases} 1 & \text{if PRB } l^{(\tau)} \text{ is scheduled to UE } n \in \mathcal{D}^{(\tau)} \\ 0 & \text{otherwise,} \end{cases} \quad (7.13)$$

is used to express the result of the ILP formulation for PRB $l^{(\tau)}$. The constraints in (7.11b) ensure that the interference experienced by the served UEs is not higher than

the interference experienced at the time of generating the CSI^{R-8} report. In detail, the constraints in (7.11b) consider the case when PRB $l^{(\tau)}$ is scheduled to UE n and the cooperative interfering BSs in $\mathcal{M}_{n,l^{(\tau)}}$ were muted at the moment of generating the CSI^{R-8} report. For (7.11b) to be fulfilled, the second term on the left-hand-side must be equal to zero, which is true in either of the following cases, with $c_{u,m}$ given by (3.3) and \emptyset denoting the empty set.

- No cooperative interfering BS was muted during the generation of the CSI^{R-8} report, i.e., $\mathcal{M}_{n,l^{(\tau)}} = \emptyset$.
- The UEs served by the cooperative interfering BSs in $\mathcal{M}_{n,l^{(\tau)}}$ are not demanding data, i.e., $c_{u,m} = 0$, $\forall u \in \mathcal{D}^{(\tau)}$, $\forall m \in \mathcal{M}_{n,l^{(\tau)}}$, $\mathcal{M}_{n,l^{(\tau)}} \neq \emptyset$.
- PRB $l^{(\tau)}$ is not scheduled to any UE served by the cooperative interfering BSs in $\mathcal{M}_{n,l^{(\tau)}}$, i.e., $s_u = 0$, $\forall u \in \mathcal{D}^{(\tau)}$, such that $c_{u,m} = 1$, $\forall m \in \mathcal{M}_{n,l^{(\tau)}}$, $\mathcal{M}_{n,l^{(\tau)}} \neq \emptyset$.

In the case that PRB $l^{(\tau)}$ is not scheduled to serve UE n , i.e., $s_n = 0$, the constraints in (7.11b) restrict each BS indexed by the set $\mathcal{M}_{n,l^{(\tau)}}$, $\forall n \in \mathcal{D}^{(\tau)}$, to serve only one UE per PRB, i.e., single-user transmissions per BS are enforced. Since cooperative interfering BSs of UE n can be transmitting at the time of generating the CSI^{R-8} reports, and hence, these BSs are not indexed by the set $\mathcal{M}_{n,l^{(\tau)}}$, $\forall n \in \mathcal{D}^{(\tau)}$, the constraints in (7.11c) are used to complement the single-user transmission requirement on the remaining BSs, indexed by the set $\mathcal{A}_{l^{(\tau)}} = \mathcal{M} \setminus \bigcup_{n \in \mathcal{D}^{(\tau)}} \mathcal{M}_{n,l^{(\tau)}}$. Moreover, the constraints in (7.11d) ensure that the decision variable is integer and furthermore, binary. Similar to the non-cooperative case, the coordinated scheduling procedure is finalized if $\hat{\mathcal{L}}^{(\tau)} = \emptyset$, or $\mathcal{D}^{(\tau)} = \emptyset$.

7.4 Simulation Results

In this section, system-level simulations are carried out to show the performance of the proposed CS scheme based on an LTE network as described in [rGPP10] (see 3GPP Case 1 from Section A.2.1.1.1). For the simulations, a first scenario is considered with $M = 10$ BSs serving ten UEs each, i.e., $N = 100$, over a total of $L = 50$ PRBs. The channels between the BSs and the UEs are assumed to be time invariant, but frequency selective [rGPP12]. The FTP traffic model from Section 7.2.1 is used, where the UEs download files of size $V = 1$ KB with arrival rates of $\lambda \in \{0.25, 0.5, 1, 1.5, 2.5, 3.5\}$, in order to vary the network resource utilization in terms of scheduled PRBs. The average data rate over time of UE n , used to calculate the PF metric in (3.11) is updated for the next transmission time $t + 1$, according to (3.13). The total scheduled data volume to UE $n \in \mathcal{N}$, v_n , is calculated as described in (7.4), where an average achievable data rate of UE n over the scheduled PRBs is obtained by using the MIESM procedure as described in [LKK12, WIN05].

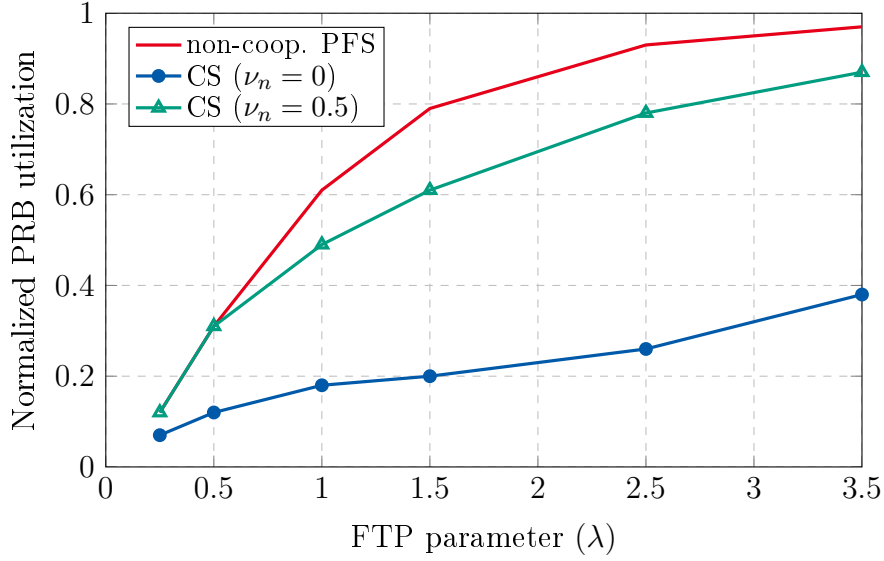


Figure 7.4. Average network PRB utilization as a function of the FTP arrival rate λ . The PRB utilization is normalized by the total number of PRBs, ML . Scenario with $N = 100$ UEs, $M = 10$ BSs, $L = 50$ PRBs

Table 7.1. Average BLER for different FTP parameter λ

FTP model (λ)	non-coop. PFS	CS ($\nu_n = 0$)	CS ($\nu_n = 0.5$)
0.25	0.33	1e-3	0.27
0.5	0.43	1e-3	0.34
1	0.36	1e-3	0.30
1.5	0.26	1e-3	0.25
2.5	0.12	1e-3	0.15
3.5	0.06	3e-3	0.08

The average PRB utilization normalized by the total number of PRBs in the network, i.e., ML , is given in Figure 7.4 as a function of the FTP parameter λ . These results illustrate the network load situation for the non-cooperative PF scheduler, labeled as “non-coop. PFS”, and the proposed coordinated scheduling scheme, referred to as “CS”. In the CS case, two different values of ν_n , $\forall n \in \mathcal{N}$, have been used to control the level of coordination between the BSs, as described in (7.9), with $\nu_n = 0$, $\forall n \in \mathcal{N}$, meaning that all interfering BSs are considered to cooperate. The results in Figure 7.4 show that the network load increases with the arrival rate λ . The proposed CS scheme has a lower average PRB utilization than the non-coop. PFS, because the former introduces orthogonal transmissions from the BSs in order to keep a more persistent interference scenario. Additionally, the average BLER is presented in Table 7.1, where it is observed that the average BLER is inversely proportional to the network load. This observation is an expected result due to the more persistent interference situation when all BSs

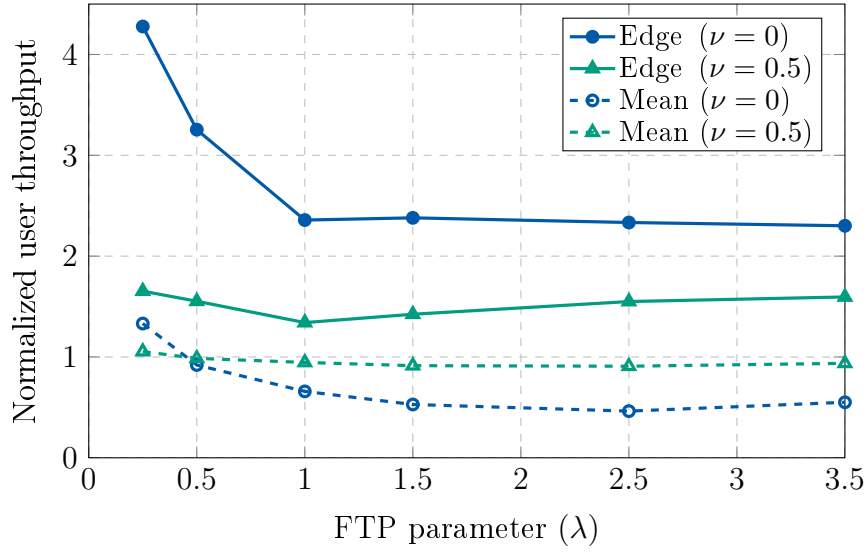


Figure 7.5. User throughput of the proposed CS scheme, normalized by the non-coop. PFS. Scenario with $N = 100$ UEs, $M = 10$ BSs, $L = 50$ PRBs

constantly transmit over all PRBs. Therefore, when all available PRBs are constantly utilized for transmissions and the channel is time-invariant, the BLER reduces to zero even in the case of non-coop. PFS. Under non-full-buffer conditions, the proposed CS scheme with $\nu_n = 0$ provides the lowest BLER by introducing cooperation among all BSs. Therefore, the CS scheme with $\nu_n = 0$ significantly improves the performance of the link adaptation procedures compared to the non-coop. PFS. In the case of CS with $\nu_n = 0.5$, the average BLER is not as improved as in the case of $\nu_n = 0$, because a lower number of interfering BSs are considered to cooperate per UE.

The average user throughput of the proposed CS scheme, normalized with respect to the non-coop. PFS, is presented in Figure 7.5 for the cell-edge users, labeled as “Edge”, and for all users, referred to as “Mean”. Based on the results from Figure 7.4, low values of the UE arrival rate λ correspond to scenarios with low PRB utilization. Furthermore, scenarios with intermediate and high PRB utilization occur for large values of λ . In a scenario with low PRB utilization and as a consequence of the persistent interference constraints described by (7.11b), the proposed CS scheme favors the scheduling of orthogonal transmissions where no interference affects the served UEs. Therefore, the proposed CS scheme enhances significantly the user throughput performance of the cell-edge users, especially in the case of $\nu_n = 0$. In scenarios with intermediate and high PRB utilization, such orthogonal transmissions represent a reduction in the average user throughput with respect to the non-coop. PFS scheme, since more PRBs are required for data transmission. Hence, any muting decision despite positive for the UE that triggers such a decision, impacts negatively the average performance of the remaining UEs which were not served due to the unavailability of PRBs. In the CS case with $\nu_n = 0.5$, since less BSs are considered to cooperate in serving UE $n \in \mathcal{N}$, the throughput performance is closer to the non-coop. PFS scheme for both, the cell-edge users and in average.

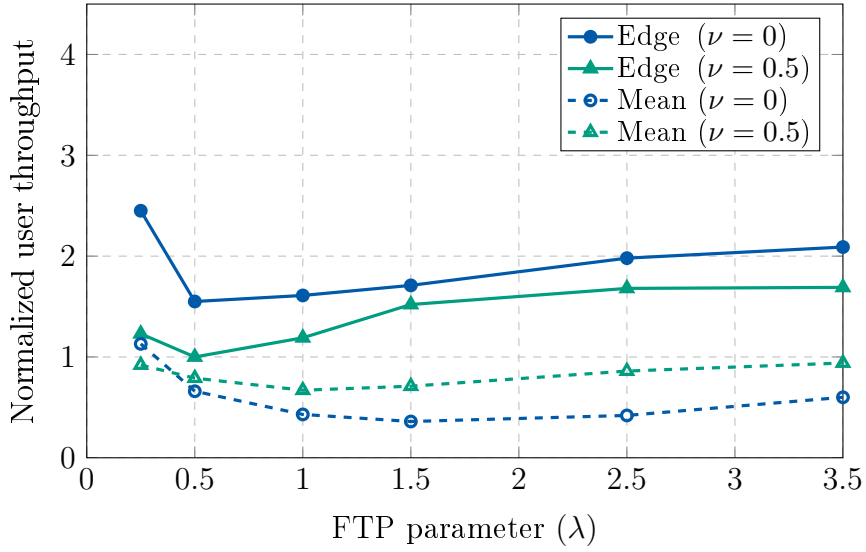


Figure 7.6. User throughput of the proposed CS scheme, normalized by the non-coop. PFS. Scenario with $N = 210$ UEs, $M = 21$ BSs, $L = 50$ PRBs

In a second scenario, the proposed CS scheme is applied in a larger-scale network of $M = 21$ BSs, $N = 210$ UEs and $L = 50$ PRBs, for the same FTP parameters V and λ , as mentioned above. On the one hand, the results for the average network PRB utilization and BLER show the same characteristics as in the case with $M = 10$ BSs, given in Figure 7.4 and Table 7.1, respectively. On the other hand, the user throughput of the proposed CS scheme, normalized with respect to the non-coop. PFS, presented in Figure 7.6, is lower than in the smaller-scale network with $M = 10$ BSs, especially for the cell-edge users. The reason for such a decrease is the scheduling of orthogonal transmissions among a larger number of BSs, while maintaining a constant number of PRBs. Thus, it is better to limit the set of cooperating BSs per UE, which is shown by a reduction in the performance gap between the CS schemes with $\nu_n = 0$ and $\nu_n = 0.5$.

The dependency of the proposed CS scheme on the parameter ν_n , $\forall n \in \mathcal{N}$, used to control the level of coordination between the BSs is presented in Figure 7.7 for the cell-edge and the average user throughput of the network corresponding to the second simulation scenario. The results are normalized with respect to the non-coop. PFS, where a constant value of the UE arrival rate for the FTP model has been used with $\lambda = 2.5$. The larger the parameter ν_n , the lower the number of interfering BSs that cooperate to improve the performance of the UEs connected to neighboring BSs. Therefore, the cell-edge gain decreases with respect to the non-coop. PFS. On the other hand, given the lower number of muted BSs per UE, the negative impact in the average user throughput is reduced with a larger value of ν_n . It is worth noting that even in the extreme case of setting up the selection threshold to $\nu_n = 0.9$, i.e., the cooperative interfering BSs correspond to the BSs with a total interfering power of 90% the total received power from the serving BS, the cell-edge gain is close to 50%.

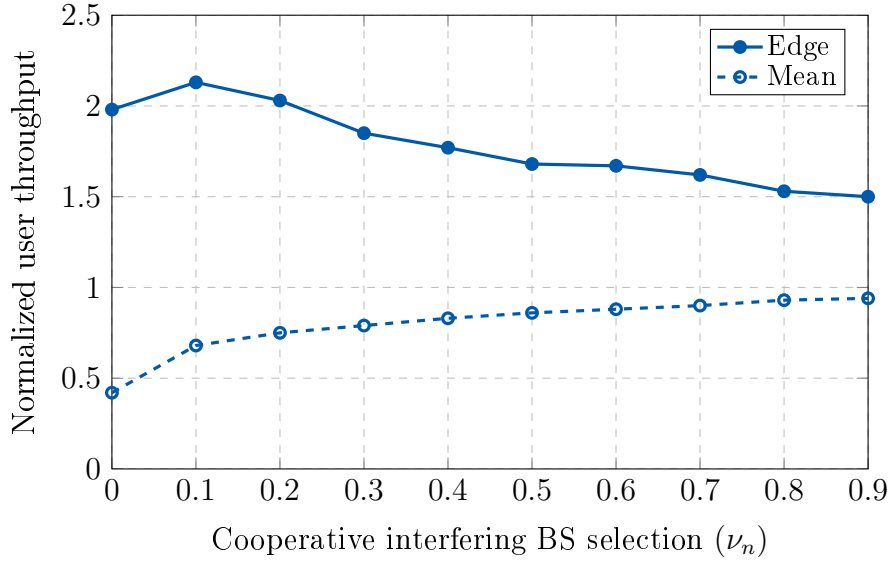


Figure 7.7. User throughput of the proposed CS scheme for different values of ν_n , normalized by the non-coop. PFS. Scenario with $N = 210$ UEs, $M = 21$ BSs, $L = 50$ PRBs and $\lambda = 2.5$

7.5 Summary

In this chapter, a CoMP CS scheme has been proposed to improve the performance of the link adaptation procedures of wireless networks with bursty traffic. The proposed CS scheme reproduces the same or even better interfering conditions, as experienced by the served UEs at the time of generating the CSI reports. Due to the presence of a central controller that manages and keeps track of the scheduling decisions, the proposed CS scheme represents no additional signaling or processing overhead at the UEs, which are requested to feedback standardized LTE CSI^{R-8} reports.

Simulation results show the effectiveness of the proposed ILP formulation to reduce the BLER. In the proposed scheme, the UE throughput, especially of the heavily interfered users, is significantly improved with respect to a standard non-cooperative PF scheduler. Moreover, since the proposed CS scheme is solved per PRB, it enjoys low computational complexity and it is, therefore, applicable in medium- to large-scale networks.

The proposed scheme is derived for a network under non-full-buffer conditions, where the users' demand is characterized by bursty traffic. In such a scenario, the average resource utilization is low and the link adaptation procedures benefit from the more stable interfering conditions enforced by the proposed cooperative scheme. In scenarios with a high average resource utilization, as in full-buffer systems, the cooperative scheme proposed in this chapter behaves as a non-cooperative scheme with all BSs constantly transmitting. For full-buffer conditions, the implementation of the approaches derived in chapters 4 to 6 is recommended.

Chapter 8

Conclusions and Outlook

In this dissertation, five cooperative resource allocation schemes are developed for mobile downlink communication networks. The proposed schemes pursue to enhance the network performance, in terms of user throughput, by means of mitigating the inter-cell interference experienced by the users. For that purpose, two main forms of cooperation are investigated, where in a first case, cooperative power control is dynamically applied in order to reduce the interference caused to users connected to neighboring base stations, and in a second case, joint scheduling and muting decisions are performed in order to trade off spectral efficiency and inter-cell interference.

One major contribution of this thesis is the consideration of practical channel state information in the derivation of the cooperative resource allocation approaches. Hence, channel state information in form of data rate measurement reports is considered, which follows standard compliant procedures of current mobile networks such as LTE and LTE-Advanced. These reports limit the knowledge of the network to a finite set of achievable data rates under specific assumptions on the interference scenarios experienced by the users. The inclusion of this type of channel state information, enables the assessment of the proposed cooperative schemes under a more practical perspective of modern and future mobile communication networks.

The cooperative resource allocation schemes are mainly formulated as optimization problems and heuristic algorithms. In the first case, integer linear programs are proposed that make use of the finite nature of the resources to be allocated, such as users, time/frequency resources and reported data rates. Despite its combinatorial nature, the proposed integer linear programs are applicable in medium- to large-size networks due to the simplifications introduced in this work. Nevertheless, the assumption of central entities with connectivity to the base stations is required in the formulation of the proposed optimization problems. On the other hand, heuristic algorithms applicable in centralized and decentralized architectures are also proposed in this thesis, where the performance gains are traded off by the reduction in computational complexity and signaling overheads.

The simulation results obtained from a standard-compliant system-level simulator, demonstrate the potential of the proposed cooperative schemes and their advantages over state-of-the-art approaches. In general, the results in this thesis show gains in the throughput of the cell-edge users, which experience high inter-cell interference. In detail, the following observations are made.

In hierarchical mobile communication networks, the application of the cooperative power control scheme proposed in this thesis provides an effective alternative to selectively manage the inter-cell interference caused by a particular group of base stations.

In this dissertation, the inter-cell interference caused by the macro base stations to the users connected to the small cells deployed in the coverage area of the former, is controlled by dynamically reducing the transmit power of the macro base stations. In especial cases, when the affected user is located at the cell-edge of the small cell, the macro base stations can be even muted in order to enhance the user throughput of the cell-edge users. Although the improvement of the user throughput by the proposed cooperative scheme is observable with respect to approaches that do not consider cooperation, the application is limited to scenarios where the users are clearly affected by one interfering base station. In other scenarios, where additional base stations have comparable interfering power levels, more advanced cooperative schemes are recommended, such as coordinated scheduling.

Coordinated scheduling with muting in centralized and decentralized architectures is also investigated in this dissertation. The proposed schemes have no restrictions with respect to the type of mobile communication networks in which they are deployed. Thus, the applicability of the previously mentioned cooperative power control scheme is extended. The cooperation takes place between neighboring base stations, where the scheduling and muting decisions are jointly made in order to enhance the overall network throughput. Although cooperative power control can be incorporated, the schemes derived in this thesis consider only on-off power control decisions where the base stations transmit either with maximum transmit power or they are muted. This restriction is imposed in order to follow the standardized reporting of channel state information and to reduce the signaling overhead. For both, centralized and decentralized schemes, significant gains in the user throughput are observed for the cell-edge users, with respect to scenarios without cooperation. In agreement with analytical results available in the literature, the achievable user throughput gains are limited by parameters which are not directly controlled by the proposed cooperative schemes. Such parameters correspond to the number of available time/frequency resources, which are predefined in the network, and the noise and residual inter-cell interference caused by non-cooperative base stations. Moreover, although the solution of the proposed centralized scheme is optimal, the difference in performance gains with respect to state-of-the-art heuristic algorithms is negligible under current practical network conditions. Therefore, the application of the proposed decentralized schemes is recommended in an initial stage, until new technologies emerge that enable the complete utilization of the benefits provided by the centralized architecture.

Coordinated scheduling with muting is additionally studied for bursty traffic, with the objective of improving the link adaptation procedures by enhancing the reliability of the reported channel state information. In this particular scenario, the users are not expected to demand high data rates, but to be served with low latency and in a reliable fashion. By applying the cooperative scheme derived in this work, the transmission error probability is significantly reduced and hence, the link adaptation procedures are improved. In scenarios with higher demands, where the serving and interference conditions experienced by the users are more stable, the benefits of the proposed cooperative scheme reduce and non-cooperative schemes can be preferred.

It is worth to mention that the benefits observed in this dissertation are mainly focused on the user throughput of the cell-edge users. In average, the network marginally benefits by the application of the proposed cooperative schemes, with respect to the non-cooperative counterparts. Therefore, no network capacity enhancements should be expected from the studied forms of cooperation. A trade-off between inter-cell interference and average user throughput is present, where the former is reduced at the expense of the latter. Hence, the cooperative schemes derived in this thesis sacrifice the network's capacity in order to improve the performance of the cell-edge users.

Several interesting directions are envisioned for extending the work presented in this dissertation, as listed below.

- The impact of residual interference and noise is a main limiting factor on the performance of the cooperative schemes. Although the noise at the receivers is being reduced with the advent of new and more capable devices, the residual interference from uncoordinated sources still represents a challenge to be addressed. Therefore, investigations on deriving robust algorithms to residual interference are left open for future work.
- In spite of the practical considerations, especially with respect to the channel state information, the implementation of the optimal proposed schemes in real-world scenarios might be limited by the computational capabilities of the devices on which the cooperative schemes are executed. For the proposed integer linear programs, a study of possible equivalent linear formulations is recommended. If possible, the reformulated linear programs could compete in terms of computational complexity with the heuristic algorithms proposed in this work.
- Inter-cell coordination is considered as one of the key features for the upcoming generations of mobile communications. Research on new scenarios such as co-operation on multi-cell massive MIMO systems or device-centric coordination is recommended.

Appendix

A Proof of Proposition 5.1

Given the condition that $\mathcal{J}_{n,i} \subsetneq \mathcal{J}_{n,j}, \forall i, j \in \mathcal{J}', i \neq j$, the common cooperative interfering BSs of UE $n \in \mathcal{N}$ are considered to be muted in the interference scenarios i and j . Thus, from the definition of the muting patterns in (5.5), $\alpha_{n,m,l,i} = \alpha_{n,m,l,j} = 1, \forall m \in \mathcal{J}_{n,i}$. Furthermore, interference scenario j mutes additional cooperative interfering BSs in comparison to interference scenario i , i.e., $\alpha_{n,m,l,i} = 0, \alpha_{n,m,l,j} = 1, \forall m \in \mathcal{J}_{n,j} \setminus \mathcal{J}_{n,i}$. Thus, from (5.7),

$$I_{n,l,i}^c(\alpha_{n,m,l,i}) > I_{n,l,j}^c(\alpha_{n,m,l,j}). \quad (\text{A.1})$$

In (5.6), the interference from the cooperative interfering BSs of UE n is the only term depending on interference scenarios i and j . Therefore, taking into account the inequality in (A.1), the SINR on PRB $l \in \mathcal{L}$ of UE n under interference scenario j , is higher.

B Proof of Proposition 5.2

The set $\mathcal{N}_{n,j} = \{u \mid c_{u,m} = 1, \forall u \in \mathcal{N}, \forall m \in \mathcal{J}_{n,j}\}$ is defined, denoting the indices of UEs connected to the cooperative interfering BSs of UE $n \in \mathcal{N}$ for interference scenario $j \in \mathcal{J}'$. Given that $\mathcal{J}_{n,i} \subsetneq \mathcal{J}_{n,j}$, then $\mathcal{N}_{n,i} \subsetneq \mathcal{N}_{n,j}, \forall i, j \in \mathcal{J}', i \neq j$. Based on (5.12a) and (5.12c), the sum of the PF metrics over all UEs on PRB $l \in \mathcal{L}$, under interference scenario $w \in \mathcal{J}'$ of UE n , can be written as

$$\sum_{n' \in \mathcal{N}} \Omega_{n',l}^w = \Omega_{n,l}^w + \sum_{u \in \mathcal{N}_{n,w}} \Omega_{u,l} + \sum_{v \in \mathcal{N} \setminus \{n, \mathcal{N}_{n,w}\}} \Omega_{v,l}, \quad (\text{B.1})$$

where the first right-hand-side term corresponds to the PF metric on PRB l of UE n under interference scenario w . The second term corresponds to the sum of the PF metrics of the UEs connected to the cooperative interfering BSs of UE n , considered to be muted in the interference scenario w , and the last term represents the sum of the PF metrics of the UEs connected to the remaining non-cooperative BSs. If it is assumed that the muting decision agrees with interference scenario w , then the second term on the right-hand-side is equal to zero, because the cooperative interfering BSs are muted. Thus, for interference scenarios i and j , agreeing with the muting decision $\bar{\alpha}_l$, (B.1) is rewritten as

$$\sum_{n' \in \mathcal{N}} \Omega_{n',l}^i = \Omega_{n,l}^i + \sum_{v \in \mathcal{N} \setminus \{n, \mathcal{N}_{n,i}\}} \Omega_{v,l}, \quad (\text{B.2a})$$

$$\sum_{n' \in \mathcal{N}} \Omega_{n',l}^j = \Omega_{n,l}^j + \sum_{v \in \mathcal{N} \setminus \{n, \mathcal{N}_{n,j}\}} \Omega_{v,l}. \quad (\text{B.2b})$$

If $r_{n,l,i} = r_{n,l,j}$, then $\Omega_{n,l}^i = \Omega_{n,l}^j$. Hence, the only difference between (B.2a) and (B.2b) lays on the second term on the right-hand-side. This term is determined by the sets $\mathcal{N} \setminus \{n, \mathcal{N}_{n,j}\} \subsetneq \mathcal{N} \setminus \{n, \mathcal{N}_{n,i}\}$ due to $\mathcal{N}_{n,i} \subsetneq \mathcal{N}_{n,j}$, $\forall i, j \in \mathcal{J}', i \neq j$. Therefore, it is possible to conclude that, $\sum_{v \in \mathcal{N} \setminus \{n, \mathcal{N}_{n,i}\}} \Omega_{v,l} > \sum_{v \in \mathcal{N} \setminus \{n, \mathcal{N}_{n,j}\}} \Omega_{v,l}$ and thus,

$$\sum_{n' \in \mathcal{N}} \Omega_{n',l}^i > \sum_{n' \in \mathcal{N}} \Omega_{n',l}^j, \quad (\text{B.3})$$

where it has been assumed that each non-muted BS serves one UE with a non-zero PF metric.

C Proof of Proposition 5.3

It is assumed, without loss of generality, that J' CSI^{R-11} reports are generated by UEs $\{u, v\} \in \mathcal{N}$ and received by BS $m \in \mathcal{M}$, with equal muting indicator sets indexed by $\{j, i\} \in \mathcal{J}'$, respectively, such that $\mathcal{J}_{u,j} = \mathcal{J}_{v,i}$. Hence, from a BS perspective, the unique muting indicator set $j' \in \mathcal{J}'_m \mid \mathcal{J}_{m,j'} = \mathcal{J}_{u,j} = \mathcal{J}_{v,i}$, implies that $\mathcal{N}_{m,j'} = \{u, v\}$. Based on (3.11), the PF metrics on PRB $l \in \mathcal{L}$ of UEs u and v under unique muting indicator set $\mathcal{J}_{m,j'}$, correspond to

$$\begin{aligned} \Omega_{u,l,j} &= \frac{r_{u,l,j}}{R_u}, \\ \Omega_{v,l,i} &= \frac{r_{v,l,i}}{R_v}. \end{aligned} \quad (\text{C.1})$$

Thus, the following relations are possible between the PF metrics from (C.1): $\Omega_{u,l,j} = \Omega_{v,l,i}$, $\Omega_{u,l,j} < \Omega_{v,l,i}$ or $\Omega_{u,l,j} > \Omega_{v,l,i}$. In the first case, no effect on the total sum of the PF metrics is observable if BS m schedules PRB l to any of the both UEs, since the PF metrics are equal. In the remaining cases, however, selecting the UE with the lowest PF metric corresponds to a lower total sum of the PF metrics. Hence, the optimal allocation of PRB l , under muting indicator set $\mathcal{J}_{m,j'}$, is given by (5.16).

D Proof of Theorem 5.1

Both problem formulations, (5.12) and (5.20), are related by the lifting procedure where

$$s_{n,l,j} = \bar{s}_{n,l} \prod_{m \in \mathcal{J}_{n,j}} \bar{\alpha}_{m,l} \quad \forall n \in \mathcal{N}, \forall l \in \mathcal{L}, \forall j \in \mathcal{J}'. \quad (\text{D.1})$$

Thus, as mentioned in (5.19) and repeated below for convenience,

$$s_{n,l,j} = 1 \Leftrightarrow \bar{s}_{n,l} = 1 \wedge \bar{\alpha}_{m,l} = 1, \quad \forall n \in \mathcal{N}, \forall l \in \mathcal{L}, \forall j \in \mathcal{J}', \forall m \in \mathcal{J}_{n,j}, \quad (\text{D.2})$$

with \wedge denoting the logical *and* operator. Based on the previous definition in (D.1) and the implication in (D.2), a one-to-one equivalence of both problems is shown as follows.

Equivalence between (5.12a) and (5.20a): the objective of both problem formulations corresponds to maximize the sum of the PF metrics. In the case of (5.12a), the sum is over all UEs, while in the case of (5.20a), the sum is restricted to the UEs that maximize the PF metric in at least one of the unique muting indicator sets on PRB $l \in \mathcal{L}$, as introduced in Section 5.3.2. According to Proposition 5.3, it is sufficient to evaluate the objective function on the index set $\mathcal{N}'_l \subseteq \mathcal{N}$. Moreover, since the objective in (5.12) is decoupled in the PRBs, then the objectives of both problem formulations are clearly equivalent.

Equivalence between (5.12b), (5.20b) and (5.20c): the constraints in (5.12b) and (5.20b) ensure that the muting and scheduling decisions agree. For that purpose, no PRB $l \in \mathcal{L}$ is scheduled to any UE served by any muted BS. It is worth noting that the perspective in both problems is different. Due to the separation of muting and scheduling decisions, the constraints in (5.12b) focus on the muted BS $m \in \mathcal{M}$, while the constraints in (5.20b) focus on UE $n \in \mathcal{N}'_l$, for which PRB l has been scheduled under interference scenario $j \in \mathcal{J}'$, where the cooperative interfering BSs indexed by $\mathcal{J}_{n,j} \in \mathcal{J}_n$ are muted. Hence, from (D.2), if $s_{n,l,j} = 1$, then $\bar{\alpha}_{m,l} = 1, \forall m \in \mathcal{J}_{n,j}$, for UE n on PRB l under interference scenario j . Thus, the constraints in (5.12b) and (5.20b), reduce to

$$\sum_{u \in \mathcal{N}} c_{u,m} \bar{s}_{u,l} = 0 \quad \forall u \in \mathcal{N}, \forall j \in \mathcal{J}', \forall m \in \mathcal{J}_{n,j}, \forall l \in \mathcal{L}, \quad (\text{D.3})$$

and

$$\sum_{u \in \mathcal{N}'_l} \sum_{i \in \mathcal{J}'} c_{u,m} s_{u,l,i} = 0 \quad \forall n \in \mathcal{N}'_l, \forall j \in \mathcal{J}', \forall m \in \mathcal{J}_{n,j}, \forall l \in \mathcal{L}, \quad (\text{D.4})$$

respectively. It can be observed, that (D.3) and (D.4) are equivalent. On the other hand, if $s_{n,l,j} = 0$, then no muting is imposed to the cooperative interfering BSs of UE n on PRB l under interference scenario j , i.e., $\bar{\alpha}_{m,l} = 0, \forall m \in \mathcal{J}_{n,j}$. Therefore, the constraints in (5.12b) and (5.20b) enforce single-user transmissions and are rewritten as

$$\sum_{u \in \mathcal{N}} c_{u,m} \bar{s}_{u,l} \leq 1 \quad \forall m \in \mathcal{M}, \forall l \in \mathcal{L}, \quad (\text{D.5})$$

and

$$\sum_{u \in \mathcal{N}'_l} \sum_{i \in \mathcal{J}'} c_{u,m} s_{u,l,i} \leq 1 \quad \forall n \in \mathcal{N}'_l, \forall j \in \mathcal{J}', \forall m \in \mathcal{J}_{n,j}, \forall l \in \mathcal{L}, \quad (\text{D.6})$$

respectively, which are equivalent for the BSs identified as cooperative interfering BSs of any UE. For the remaining non-cooperative BSs in problem (5.20), the constraints in (5.20c) are used. Similar to the objective function in (5.20a), Proposition 5.3 states that it is enough to consider the set $\mathcal{N}'_l \in \mathcal{N}$ of indices of UEs.

Equivalence between (5.12c) and (5.20d): both constraints, (5.12c) and (5.20d), define the calculation of the instantaneous achievable data rate on each PRB $l \in \mathcal{L}$ of UE $n \in \mathcal{N}$. In the case of the constraints in (5.12c), the lookup table function $\rho(\mathbf{r}_{n,l}, \bar{\alpha}_l, \mathcal{I}_n^c)$ maps the achievable data rate of UE n to the muting decision $\bar{\alpha}_l$ of the cooperative interfering BSs of UE n , as indexed by \mathcal{I}_n^c . The total instantaneous achievable data rate is calculated as the sum of the instantaneous achievable data rates per scheduled PRB, as defined by the scheduling decision $\bar{s}_{n,l}$. Similarly, the constraints in (5.20d) consider directly the achievable data rates of UE n under the interference scenarios $j \in \mathcal{J}'$, as given in the CSI^{R-11} reports. Although the constraints in (5.20d) consider only the scheduling decision for the current PRB l , given by $s_{n,l,j}$, the separability concept introduced in Section 5.3.2 indicates the equivalence of both constraints, given the linear calculation of the total instantaneous achievable data rate and the constant value of the average user throughput over time for all PRBs.

Binary decision variables: in (5.12d), (5.12e) and (5.20f), both problem formulations consider the decision variables to be integer, and furthermore, binary.

List of Abbreviations

1-9

3GPP 3rd Generation Partnership Project

A

ABS Almost Blank Subframe

AWGN Additive white Gaussian noise

B

BLER Block Error Rate

BS Base station

C

CoMP Coordinated Multi-Point

CQI Channel Quality Indicator

C-RAN Cloud-Radio Access Network

CRE Cell-range expansion

CRS Cell-Specific Reference Signal

CS Coordinated Scheduling

CSI Channel state information

CSI-RS CSI Reference Signal

D

DAS Distributed Antenna System

DC Direct Current

DPB Dynamic Point Blanking

DPS Dynamic Point Selection

E

EIRP Equivalent isotropically radiated power

F

FDD Frequency Division Duplexing

FTP File Transfer Protocol

I

ICIC Inter-Cell Interference Cancellation

ILP Integer linear program

IMT International Mobile Telecommunications

INLP Integer non-linear program

ITU International Telecommunications Union

J

JT Joint Transmission

L

LSA License Shared Access

LTE Long Term Evolution

M

MCS Modulation and coding scheme

MIESM Mutual Information based Exponential SNR Mapping

MIMO Multiple-Input-Multiple-Output

MRC Maximum Ratio Combining

N

NP Non-deterministic polynomial-time

O

OFDM Orthogonal Frequency Division Multiplexing

OFDMA Orthogonal Frequency Division Multiple Access

P

PDF Probability Density Function

PF Proportional Fair

PMI Precoding Matrix Index

PRB Physical Resource Block

R

RE Resource Element

RI Rank Indication

RR Round-Robin

RRH Remote Radio Head

RS Reference signal

S

SCM Spatial Channel Model

SIMO Single-Input-Multiple-Output

SINR Signal-to-interference-plus-noise ratio

SISO Single-Input-Single-Output

T

TDD Time Division Duplexing

U

UE User equipment

W

WCDMA Wideband Code Division Multiple Access

Z

ZF Zero-forcing

List of Symbols

Symbols

$\alpha_{m,l}$	Transmit power control parameter of BS m on PRB l (assumed by the CSI report)
$\bar{\alpha}_{m,l}$	Transmit power control parameter of BS m on PRB l (defined by the cooperative scheme)
$\alpha_{n,m,l,j}$	Muting pattern of BS m on PRB l under interference scenario j of UE n
B	Transmission bandwidth in Hz
$B_{k,l}$	Net benefit metric of BS k , when muted on PRB l
$\beta_{m,l}^k$	Benefit metric of BS m on PRB l , when BS k is muted
\mathbf{C}	Connection matrix with elements $c_{n,m} \in \{0, 1\}$
d_n	Data demand of UE n
δ	CSI report activation delay
$\gamma_{n,l}$	SINR on PRB l of UE n
$\gamma_{n,l,j}$	SINR on PRB l of UE n under interference scenario j
$h_{n,m,l}$	Instantaneous channel coefficient between BS m and UE n on PRB l
$I_{n,l}$	Average interference power at UE n on PRB l
$I_{n,l}^c$	Average interference power at UE n on PRB l from the cooperative interfering BSs
$I_{n,l}^{nc}$	Average interference power at UE n on PRB l from the non-cooperative interfering BSs
κ	Forgetting factor of the PF scheduler
λ	UE arrival rate for FTP traffic model
Λ	Number of active UEs in FTP traffic model
$\mu_m(t)$	Number of PRBs on which BS m is muted at time t
ν	Threshold level parameter for selection of cooperative interfering BSs
$\Omega_{n,l}$	PF metric on PRB l of UE n
$\Omega_{n,l,j}$	PF metric on PRB l of UE n under interference scenario j
Ω_l^m	Sum of PF metrics on PRB l with muted BS m
$\Omega_{m,l}^0$	PF metric on PRB l of BS m when not muted
$p_{n,m}$	Total received power at UE n from BS m
$p_{n,m,l}$	Received power at UE n from BS m on PRB l
$\phi_{m,l}$	Transmit power of BS m on PRB l
$\Phi_{m,l}$	Maximum transmit power of BS m on PRB l
φ_m	CRE off-set parameter for BS m
r_n	Total instantaneous achievable data rate of UE n
$r_{n,l}$	Instantaneous achievable data rate on PRB l of UE n
$r_{n,l,j}$	Instantaneous achievable data rate on PRB l of UE n under interference scenario j
R	Average user throughput over time
$\bar{\mathbf{S}}$	Scheduling decision matrix with elements $s_{n,l} \in \{0, 1\}$
\mathbf{S}	Scheduling and muting decision tensor with elements $s_{n,l,j} \in \{0, 1\}$
σ^2	AWGN power level at the receiver
ς	Noise figure at the receiver in dB

T	Periodicity of CSI reporting process
τ	Iteration number
$v_n^{(\tau)}$	Total scheduled data volume of UE n at iteration τ
V	Download FTP file size

Sets

\mathcal{A}	Set of indices of available BSs, which were transmitting at the time of generating the CSI report
$\mathcal{D}_m^{(\tau)}$	Set of indices of UEs to be served by BS m at iteration τ
\mathcal{I}_n	Set of indices of interfering BSs of UE n
\mathcal{I}'_n	Set of indices of strongest interfering BSs of UE n
\mathcal{I}_n^c	Set of indices of cooperative interfering BSs of UE n
\mathcal{J}	Set of indices of interference scenarios
$\mathcal{J}_{n,j}$	Muting indicator set of UE n under interference scenario j
$\tilde{\mathcal{K}}_m$	Set of indices of BSs that consider BS m as cooperative BS
\mathcal{L}	Set of indices of PRBs
$\mathcal{L}_m(t)$	Set of indices of PRBs in which BS m is muted at time t
$\tilde{\mathcal{L}}^{(\tau)}$	Set of indices of available PRBs at iteration τ
$\tilde{\mathcal{L}}_n$	Set of indices of PRBs scheduled to UE n
\mathcal{M}	Set of indices of BSs
$\hat{\mathcal{M}}_m$	Set of indices of cooperative BSs of BS m
$\mathcal{M}_{n,l}$	Set of indices of cooperative interfering BSs of UE n , muted on PRB l in the CSI report
\mathcal{N}	Set of indices of UEs
\mathcal{N}'_l	Set of indices of UEs considered for scheduling on PRB l
\mathcal{S}	Set of indices of small cells
\mathcal{S}_m	Set of indices of small cells located within the coverage area of macro BS m
\emptyset	Empty set

Notation

$f(\cdot)$	Mapping from SINR to achievable data rate
$g(\cdot)$	Function of instantaneous achievable data rates
$\mathbb{P}(\cdot)$	Power set (set of all sets)
$\rho(\cdot)$	Lookup table function selecting achievable data rates from muting patterns
$[\cdot]^T$	Transpose operation
$\binom{a}{b}$	Binomial coefficient operator (choose b from a)
$[\mathcal{M}]_i$	i -th set of $\tilde{\mathcal{M}}$
$[\Omega_{m,l}^0]_y$	Select the y indices with the lowest values in $\Omega_{m,l}^0$
$\mathbf{0}_{M \times L}$	$M \times L$ matrix with zero elements
$\mathbf{0}_{M \times L}^m$	$M \times L$ matrix with zero elements in all but the m -th row
$\mathbf{I}_{N \times N}$	$N \times N$ identity matrix

Bibliography

- [3rd13] *TS 36.213 v11.3.0 – Physical Layer Procedures (Release 11)*, 3rd Generation Partnership Project Std., June 2013.
- [ABB⁺07] P. Almers, E. Bonek, A. Burr, N. Czink, M. Debbah, V. Degli-Esposti, H. Hofstetter, P. Kyösti, D. Laurenson, G. Matz, A. F. Molisch, C. Oestges, and H. Özcelik, “Survey of Channel and Radio Propagation Models for Wireless MIMO Systems,” *EURASIP Journal on Wireless Communications and Networking*, vol. 2007:19070, February 2007.
- [ABK⁺14] R. Agrawal, A. Bedekar, S. Kalyanasundaram, N. Arulselvan, T. Kolding, and H. Kroener, “Centralized and Decentralized Coordinated Scheduling with Muting,” in *IEEE 79th Vehicular Technology Conference (VTC Spring)*, May 2014, pp. 1–5.
- [ABS07] A. Ancora, C. Bona, and D. T. Slock, “Down-Sampled Impulse Response Least-Squares Channel Estimation for LTE OFDMA,” in *IEEE International Conference on Acoustics, Speech and Signal Processing (ICASSP)*, April 2007, pp. 293–296.
- [And13] J. G. Andrews, “Seven Ways that HetNets Are a Cellular Paradigm Shift,” *IEEE Communications Magazine*, vol. 51, no. 3, pp. 136–144, March 2013.
- [Bal29] S. Ballantine, “Reciprocity in Electromagnetic, Mechanical, Acoustical, and Interconnected Systems,” in *Proceedings of the Institute of Radio Engineers*, vol. 17, no. 6, June 1929, pp. 927–951.
- [Bal05] E. Balas, “Projection, Lifting and Extended Formulation in Integer and Combinatorial Optimization,” *Springer Annals of Operations Research*, vol. 140, no. 1, pp. 125–161, November 2005.
- [BBB14] P. Baracca, F. Boccardi, and N. Benvenuto, “A dynamic clustering algorithm for downlink CoMP systems with multiple antenna UEs,” *EURASIP Journal on Wireless Communications and Networking*, vol. 2014:125, August 2014.
- [BGG⁺12] A. Barbieri, P. Gaal, S. Geirhofer, T. Ji, D. Malladi, Y. Wei, and F. Xue, “Coordinated Downlink Multi-Point Communications in Heterogeneous Cellular Networks,” in *Information Theory and Applications Workshop (ITA)*, February 2012, pp. 7–16.
- [BHM77] S. P. Bradley, A. C. Hax, and T. L. Magnanti, *Applied Mathematical Programming*. Addison Wesley, 1977.
- [BO16] A. Beylerian and T. Ohtsuki, “Multi-point fairness in resource allocation for C-RAN downlink CoMP transmission,” *EURASIP Journal on Wireless Communications and Networking*, vol. 2016:12, January 2016.

- [BPG⁺09] G. Boudreau, J. Panicker, N. Guo, R. Chang, N. Wang, and S. Vrzic, "Interference Coordination and Cancellation for 4G Networks," *IEEE Communications Magazine*, vol. 47, no. 4, pp. 74–81, April 2009.
- [Car29] J. R. Carson, "Reciprocal Theorems in Radio Communication," in *Proceedings of the Institute of Radio Engineers*, vol. 17, no. 6, June 1929, pp. 952–956.
- [CHS⁺14] P.-H. Chiang, P.-H. Huang, S.-S. Sun, W. Liao, and W.-T. Chen, "Joint Power Control and User Association for Traffic Offloading in Heterogeneous Networks," in *IEEE Global Communications Conference (GLOBECOM)*, December 2014, pp. 4424–4429.
- [Cis17] Cisco. (2017, February) Cisco Visual Networking Index: Global Mobile Data Traffic Forecast Update, 2016-2021. www.cisco.com.
- [CJ08] V. R. Cadambe and S. A. Jafar, "Interference Alignment and Degrees of Freedom of the K-User Interference Channel," *IEEE Transactions on Information Theory*, vol. 54, no. 8, pp. 3425–3441, August 2008.
- [CJXH13] H. Chen, Y. Jiang, J. Xu, and H. Hu, "Energy-Efficient Coordinated Scheduling Mechanism for Cellular Communication Systems with Multiple Component Carriers," *IEEE Journal on Selected Areas in Communications*, vol. 31, no. 5, pp. 959–968, May 2013.
- [CKL⁺11] B. Clerckx, Y. Kim, H. Lee, J. Cho, and J. Lee, "Coordinated Multi-Point Transmission in Heterogeneous Networks: A Distributed Antenna System Approach," in *IEEE 54th International Midwest Symposium on Circuits and Systems (MWSCAS)*, August 2011, pp. 1–4.
- [CPP12] Y. Cheng, A. Philipp, and M. Pesavento, "Dynamic rate adaptation and multiuser downlink beamforming using mixed integer conic programming," in *20th European Signal Processing Conference (EUSIPCO)*, August 2012, pp. 824–828.
- [CWW⁺13] M. Cierny, H. Wang, R. Wichman, Z. Ding, and C. Wijting, "On Number of Almost Blank Subframes in Heterogeneous Cellular Networks," *IEEE Transactions on Wireless Communications*, vol. 12, no. 10, pp. 5061–5073, October 2013.
- [DGA13] H. S. Dhillon, R. K. Ganti, and J. G. Andrews, "Load-Aware Modeling and Analysis of Heterogeneous Cellular Networks," *IEEE Transactions on Wireless Communications*, vol. 12, no. 4, pp. 1666–1677, April 2013.
- [DMBP13] A. Davydov, G. Morozov, I. Bolotin, and A. Papathanassiou, "Evaluation of Joint Transmission CoMP in C-RAN based LTE-A HetNets with Large Coordination Areas," in *IEEE Globecom Workshops (GC Wkshps)*, December 2013, pp. 801–806.

- [DMW⁺11] A. Damnjanovic, J. Montojo, Y. Wei, T. Ji, T. Luo, M. Vajapeyam, T. Yoo, O. Song, and D. Malladi, "A Survey on 3GPP Heterogeneous Networks," *IEEE Wireless Communications*, vol. 18, no. 3, pp. 10–21, June 2011.
- [Don79] V. H. M. Donald, "Advanced Mobile Phone Service: The Cellular Concept," *The Bell System Technical Journal*, vol. 58, no. 1, pp. 15–41, January 1979.
- [DPS14] E. Dahlman, S. Parkvall, and J. Sköld, *4G: LTE/LTE-Advanced for Mobile Broadband*, 2nd ed. Elsevier, 2014.
- [Flo95] C. A. Floudas, *Nonlinear and mixed-integer optimization: fundamentals and applications*. Oxford University Press, 1995.
- [FSCK10] M. Feng, X. She, L. Chen, and Y. Kishiyama, "Enhanced Dynamic Cell Selection with Muting Scheme for DL CoMP in LTE-A," in *IEEE 71st Vehicular Technology Conference (VTC Spring)*, May 2010, pp. 1–5.
- [FYL⁺11] J. Fan, Q. Yin, G. Y. Li, B. Peng, and X. Zhu, "MCS Selection for Throughput Improvement in Downlink LTE Systems," in *20th International Conference on Computer Communications and Networks (ICCCN)*, July 2011, pp. 1–5.
- [GKN⁺15] S. Gulati, S. Kalyanasundaram, P. Nashine, B. Natarajan, R. Agrawal, and A. Bedekar, "Performance Analysis of Distributed Multi-cell Coordinated Scheduler," in *IEEE 82nd Vehicular Technology Conference (VTC Fall)*, September 2015, pp. 1–5.
- [GL14] J.-C. Guey and L. D. Larsson, "Modeling and Evaluation of MIMO Systems Exploiting Channel Reciprocity in TDD Mode," in *IEEE 60th Vehicular Technology Conference (VTC Fall)*, September 2014, pp. 4265–4269.
- [GLBC17] G. Giambene, V. A. Le, T. Bourgeau, and H. Chaouchi, "Iterative Multi-Level Soft Frequency Reuse With Load Balancing for Heterogeneous LTE-A Systems," *IEEE Transactions on Wireless Communications*, vol. 16, no. 2, pp. 924–938, February 2017.
- [GMD13] C. Galiotto, N. Marchetti, and L. Doyle, "The Role of the Total Transmit Power on the Linear Area Spectral Efficiency Gain of Cell-Splitting," *IEEE Communications Letters*, vol. 17, no. 12, pp. 2256–2259, December 2013.
- [Gol05] A. Goldsmith, *Wireless Communications*. Cambridge University Press, 2005.
- [GRM⁺10] A. Ghosh, R. Ratasuk, B. Mondal, N. Mangalvedhe, and T. Thomas, "LTE-Advanced: Next Generation Wireless Broadband Technology," *IEEE Wireless Communications*, vol. 17, no. 3, pp. 10–22, June 2010.

- [GS05] A. B. Gershman and N. D. Sidiropoulos, Eds., *Space-Time Processing for MIMO Communications*. John Wiley & Sons, 2005.
- [HYW⁺13] S. Han, C. Yang, G. Wang, D. Zhu, and M. Lei, “Coordinated Multi-Point Transmission Strategies for TDD Systems with Non-Ideal Channel Reciprocity,” *IEEE Transactions on Communications*, vol. 61, no. 10, pp. 4256–4270, October 2013.
- [IDM⁺11] R. Irmer, H. Droste, P. Marsch, M. Grieger, G. Fettweis, S. Brueck, H.-P. Mayer, L. Thiele, and V. Jungnickel, “Coordinated Multipoint: Concepts, Performance, and Field Trial Results,” *IEEE Communications Magazine*, vol. 49, no. 2, pp. 102–111, February 2011.
- [Int15] *Detailed specifications of the terrestrial radio interface of International Mobile Telecommunications-Advanced (IMT-Advanced) (Recommendation ITU-R M.2012-2)*, International Telecommunication Union Std., September 2015.
- [Kö6] V. Kühn, *Wireless Communications over MIMO Channels. Applications to CDMA and Multiple Antenna Systems*. John Wiley & Sons, 2006.
- [KBL⁺14] Q. Kuang, J. Belschner, M. Lossow, P. Arnold, and O. D. Ramos-Cantor, “Mobility Performance of LTE-Advanced Heterogeneous Networks with Control Channel Protection,” in *World Telecommunications Congress (WTC)*, June 2014, pp. 1–6.
- [KG08] S. G. Kiani and D. Gesbert, “Optimal and Distributed Scheduling for Multicell Capacity Maximization,” *IEEE Transactions on Wireless Communications*, vol. 7, no. 1, pp. 288–297, January 2008.
- [KmWH17] D. B. Kirk and W. mei W. Hwu, *Programming Massively Parallel Processors*, 3rd ed. Elsevier, 2017.
- [KOG07] S. G. Kiani, G. E. Oien, and D. Gesbert, “Maximizing Multicell Capacity Using Distributed Power Allocation and Scheduling,” in *IEEE Wireless Communications and Networking Conference (WCNC)*, March 2007, pp. 1690–1694.
- [KPRA15] K. Koutlia, J. Perez-Romero, and R. Agusti, “On Enhancing Almost Blank Subframes Management for efficient eICIC in HetNets,” in *IEEE 81st Vehicular Technology Conference (VTC Spring)*, May 2015, pp. 1–5.
- [KW15] G. Ku and J. M. Walsh, “Resource Allocation and Link Adaptation in LTE and LTE Advanced: A Tutorial,” *IEEE Communication Surveys & Tutorials*, vol. 17, no. 3, pp. 1605–1633, Third Quarter 2015.
- [LAD⁺15] M. Lossow, P. Arnold, H. Droste, G. Kadel, and O. D. Ramos-Cantor, “Methodology to evaluate user experience in non-fully loaded wireless communication systems,” in *21th European Wireless Conference*, May 2015, pp. 1–6.

- [LCLV14] Y. L. Lee, T. C. Chuah, J. Loo, and A. Vinel, "Recent Advances in Radio Resource Management for Heterogeneous LTE/LTE-A Networks," *IEEE Communication Surveys & Tutorials*, vol. 16, no. 4, pp. 2142–2180, June 2014.
- [LHAL11] H. Li, J. Hajipour, A. Attar, and V. C. M. Leung, "Efficient HetNet Implementation Using Broadband Wireless Access with Fiber-Connected Massively Distributed Antennas Architecture," *IEEE Wireless Communications*, vol. 18, no. 3, pp. 72–78, June 2011.
- [LHXQ13] Q. C. Li, R. Q. Hu, Y. Xu, and Y. Qian, "Optimal Fractional Frequency Reuse and Power Control in the Heterogeneous Wireless Networks," *IEEE Transactions on Wireless Communications*, vol. 12, no. 6, pp. 2658–2668, June 2013.
- [LHZ09] J. Lee, J.-K. Han, and J. C. Zhang, "MIMO Technologies in 3GPP LTE and LTE-Advanced," *EURASIP Journal on Wireless Communications and Networking*, vol. 2009:302092, July 2009.
- [LJ08] E. G. Larsson and E. A. Jorswieck, "Competition Versus Cooperation on the MISO Interference Channel," *IEEE Journal on Selected Areas in Communications*, vol. 26, no. 7, pp. 1059–1069, September 2008.
- [LJ10] A. Lozano and N. Jindal, "Transmit Diversity vs. Spatial Multiplexing in Modern MIMO Systems," *IEEE Transactions on Wireless Communications*, vol. 9, no. 1, pp. 186–197, January 2010.
- [LJA13] A. Lozano, R. W. H. Jr., and J. G. Andrews, "Fundamental Limits of Cooperation," *IEEE Transactions on Information Theory*, vol. 59, no. 9, pp. 5213–5226, September 2013.
- [LKK12] I. Latif, F. Kaltenberger, and R. Knopp, "Link abstraction for multi-user MIMO in LTE using interference-aware receiver," in *IEEE Wireless Communications and Networking Conference (WCNC)*, April 2012, pp. 842–846.
- [LKL⁺12] J. Lee, Y. Kim, H. Lee, B. L. Ng, D. Mazzaresse, J. Liu, W. Xiao, and Y. Zhou, "Coordinated Multipoint Transmission and Reception in LTE-Advanced Systems," *IEEE Communications Magazine*, vol. 50, no. 11, pp. 44–50, November 2012.
- [LPGdlR⁺11] D. Lopez-Perez, I. Güvenc, G. de la Roche, M. Kounttouris, T. Q. Quek, and J. Zhang, "Enhanced Intercell Interference Coordination Challenges in Heterogeneous Networks," *IEEE Wireless Communications*, vol. 18, no. 3, pp. 22–30, June 2011.
- [LPVdlRZ09] D. Lopez-Perez, A. Valcarce, G. de la Roche, and J. Zhang, "OFDMA Femtocells: A Roadmap on Interference Avoidance," *IEEE Communications Magazine*, vol. 47, no. 9, pp. 41–48, September 2009.

- [LS06] Y. Li and G. L. Stüber, Eds., *Orthogonal Frequency Division Multiplexing for Wireless Communications*. Springer Signals and Communication Technology, 2006.
- [MBS⁺10] R. Madan, J. Borran, A. Sampath, N. Bhushan, A. Khandekar, and T. Ji, “Cell Association and Interference Coordination in Heterogeneous LTE-A Cellular Networks,” *IEEE Journal on Selected Areas in Communications*, vol. 28, no. 9, pp. 1479–1489, December 2010.
- [Mes15] A. Messac, *Optimization in Practice with MATLAB*. Cambridge University Press, 2015.
- [MF11] P. Marsch and G. Fettweis, “Static Clustering for Cooperative Multi-Point (CoMP) in Mobile Communications,” in *IEEE International Conference on Communications (ICC)*, June 2011, pp. 1–6.
- [MHV⁺12] H.-L. Määttänen, K. Hämäläinen, J. Venäläinen, K. Schober, M. Enescu, and M. Valkama, “System-level performance of LTE-Advanced with joint transmission and dynamic point selection schemes,” *EURASIP Journal on Advances in Signal Processing*, vol. 2012:247, November 2012.
- [MM01] M. Morelli and U. Mengali, “A Comparison of Pilot-Aided Channel Estimation Methods for OFDM Systems,” *IEEE Transactions on Signal Processing*, vol. 49, no. 12, pp. 3065–3073, December 2001.
- [Mot06] Motorola. (2006, March) R1-060877 - Frequency Domain Scheduling for E-UTRA. www.3gpp.org.
- [MVT⁺12] B. Mondal, E. Visotsky, T. A. Thomas, X. Wang, and A. Ghosh, “Performance of Downlink CoMP in LTE Under Practical Constraints,” in *IEEE 23rd International Symposium on Personal, Indoor and Mobile Radio Communications (PIMRC)*, September 2012, pp. 2049–2054.
- [NTP15] K. Ntougias, N. Taramas, and C. B. Papadias, “Low-feedback cooperative opportunistic transmission for dynamic licensed shared access,” in *23rd European Signal Processing Conference (EUSIPCO)*, August 2015, pp. 1222–1226.
- [OH12] J. Oh and Y. Han, “Cell Selection for Range Expansion with Almost Blank Subframe in Heterogeneous Networks,” in *IEEE 23rd International Symposium on Personal, Indoor and Mobile Radio Communications (PIMRC)*, September 2012, pp. 653–657.
- [PFR⁺11] K. I. Pedersen, F. Frederiksen, C. Rosa, H. Nguyen, L. G. U. Garcia, and Y. Wang, “Carrier Aggregation for LTE-Advanced: Functionality and Performance Aspects,” *IEEE Communications Magazine*, vol. 49, no. 6, pp. 89–95, June 2011.
- [PNG03] A. Paulraj, R. Nabar, and D. Gore, *Introduction to Space-Time Wireless Communications*. Cambridge University Press, 2003.

- [Pra04] R. Prasad, *OFDM for Wireless Communications Systems*. Artech House, 2004.
- [Rad11] Radio Spectrum Policy Group, “RSPG11-392 – Report on Collective Use of Spectrum (CUS) and other spectrum sharing approaches,” RSPG, Tech. Rep., November 2011.
- [RCBHP17] O. D. Ramos-Cantor, J. Belschner, G. Hegde, and M. Pesavento, “Centralized Coordinated Scheduling in LTE-Advanced Networks,” *EURASIP Journal on Wireless Communications and Networking*, vol. 2017:122, July 2017.
- [RCBP14] O. D. Ramos-Cantor, J. Belschner, and M. Pesavento, “A cooperative power control scheme for interference management in LTE-Advanced based cognitive radio networks,” in *6th International Symposium on Communications, Control and Signal Processing (ISCCSP)*, May 2014, pp. 530–533.
- [RCBP16] —, “Improved Link Adaptation with Coordinated Scheduling in non-Fully Loaded Wireless Networks,” in *IEEE 17th International Workshop on Signal Processing Advances in Wireless Communications (SPAWC)*, July 2016, pp. 1–6.
- [RCLD⁺14] O. D. Ramos-Cantor, M. Lossow, H. Droste, G. Kadel, and M. Pesavento, “A Network Simulation Tool for User Traffic Modeling and Quality of Experience Analysis in a Hybrid Access Architecture,” in *World Telecommunications Congress (WTC)*, June 2014, pp. 1–6.
- [RCP17] O. D. Ramos-Cantor and M. Pesavento, “Decentralized Coordinated Scheduling with Muting in LTE-Advanced Networks,” in *IEEE 18th International Workshop on Signal Processing Advances in Wireless Communications (SPAWC)*, July 2017, pp. 1–5.
- [rGPP04] 3rd Generation Partnership Project, “TR 25.892 v2.0.0 – Feasibility Study for OFDM for UTRAN enhancement (Release 6),” 3GPP, Tech. Rep., June 2004.
- [rGPP06] —, “TR 25.814 v7.1.0 – Physical layer aspects for evolved Universal Terrestrial Radio Access (UTRA) (Release 7),” 3GPP, Tech. Rep., September 2006.
- [rGPP10] —, “TR 36.814 v9.0.0 – Further advancements for E-UTRA physical layer aspects (Release 9),” 3GPP, Tech. Rep., March 2010.
- [rGPP11] —, “TR 36.819 v11.1.0 – Coordinated multi-point operation for LTE physical layer aspects (Release 11),” 3GPP, Tech. Rep., December 2011.
- [rGPP12] —, “TR 25.996 v11.0.0 – Spatial channel model for Multiple Input Multiple Output (MIMO) simulations (Release 11),” 3GPP, Tech. Rep., September 2012.

- [rGPP13a] —, “TR 36.872 v12.1.0 – Small cell enhancements for E-UTRA and E-UTRAN - Physical layer aspects (Release 12),” 3GPP, Tech. Rep., December 2013.
- [rGPP13b] —, “TR 36.874 v12.0.0 – Coordinated multi-point operation for LTE with non-ideal backhaul (Release 12),” 3GPP, Tech. Rep., December 2013.
- [rGPP13c] —, “TR 36.932 v12.1.0 – Scenarios and requirements for small cell enhancements for E-UTRA and E-UTRAN (Release 12),” 3GPP, Tech. Rep., March 2013.
- [rGPP16] —, “TR 36.942 v13.0.0 – Radio Frequency (RF) system scenarios (Release 13),” 3GPP, Tech. Rep., January 2016.
- [Ros10] S. M. Ross, *Introduction to Probability Models*, 10th ed. Academic Press, 2010.
- [RY10] M. Rahman and H. Yanikomeroglu, “Enhancing Cell-Edge Performance: A Downlink Dynamic Interference Avoidance Scheme with Inter-Cell Coordination,” *IEEE Transactions on Wireless Communications*, vol. 9, no. 4, pp. 1414–1425, April 2010.
- [RYW09] M. Rahman, H. Yanikomeroglu, and W. Wong, “Interference Avoidance with Dynamic Inter-Cell Coordination for Downlink LTE System,” in *Wireless Communications and Networking Conference (WCNC)*, April 2009, pp. 1–6.
- [SBT11] S. Sesia, M. Baker, and I. Toufik, *LTE - The UMTS Long Term Evolution: From Theory to Practice*, 2nd ed. John Wiley & Sons, 2011.
- [Sen06] E. Seneta, *Non-negative Matrices and Markov Chains*, 2nd ed. Springer Series in Statistics, 2006.
- [SGS⁺05] J. Salo, G. D. Galdo, J. Salmi, P. Kyösti, L. Hentilä, M. Milojevic, D. Laselva, P. Zetterberg, and C. Schneider. (2005, December) MATLAB implementation of the WINNER Phase I Channel Model ver1.5. [Online]. Available: <https://www.ist-winner.org/3gpp-scm.html>
- [SKM⁺10] M. Sawahashi, Y. Kishiyama, A. Morimoto, D. Nishikawa, and M. Tanno, “Coordinated Multipoint Transmission/Reception Techniques for LTE-Advanced,” *IEEE Wireless Communications*, vol. 17, no. 3, pp. 26–34, June 2010.
- [SMR10] S. Schwarz, C. Mehlführer, and M. Rupp, “Calculation of the Spatial Preprocessing and Link Adaptation Feedback for 3GPP UMTS/LTE,” in *6th Conference on Wireless Advanced (WiAD)*, June 2010, pp. 1–6.
- [SPK⁺13] B. Soret, K. I. Pedersen, T. Kolding, H. Kroener, and I. Maniatis, “Fast Muting Adaptation for LTE-A HetNets with Remote Radio Heads,” in *IEEE Global Communications Conference (GLOBECOM)*, December 2013, pp. 3790–3795.

- [SPM⁺12] Z. Shen, A. Papasakellariou, J. Montojo, D. Gerstenberger, and F. Xu, "Overview of 3GPP LTE-Advanced Carrier Aggregation for 4G Wireless Communications," *IEEE Communications Magazine*, vol. 50, no. 2, pp. 122–130, February 2012.
- [SYH13] L. Su, C. Yang, and S. Han, "The Value of Channel Prediction in CoMP Systems with Large Backhaul Latency," *IEEE Transactions on Communications*, vol. 61, no. 11, pp. 4577–4590, November 2013.
- [TV05] D. Tse and P. Viswanath, *Fundamentals of Wireless Communication*. Cambridge University Press, 2005.
- [WIN05] WINNER. (2005, February) D2.7 ver 1.1 - Assessment of Advanced Beamforming and MIMO Technologies. www.ist-winner.org.
- [WMMZ11] J. Wu, N. B. Mehta, A. F. Molisch, and J. Zhang, "Unified Spectral Efficiency Analysis of Cellular Systems with Channel-Aware Schedulers," *IEEE Transactions on Communications*, vol. 59, no. 12, pp. 3463–3474, December 2011.
- [Wol98] L. A. Wolsey, *Integer Programming*. John Wiley & Sons, 1998.
- [YDKS02] Y. Yoon, L. Duan, F. Khaleghi, and A. C. K. Soong, "Basic operation of the wrap-around technique for system-level simulation," 3GPP2, Tech. Rep., July 2002.
- [YRC⁺13] Q. Ye, B. Rong, Y. Chen, M. Al-Shalash, C. Caramanis, and J. G. Andrews, "User Association for Load Balancing in Heterogeneous Cellular Networks," *IEEE Transactions on Wireless Communications*, vol. 12, no. 6, pp. 2706–2716, June 2013.
- [YZSL14] Y. Yang, Q. Zhang, P. Shang, and J. Liu, "Interference Alignment based Coordinated Scheduling for Uplink Small Cell Enhancement," in *IEEE 25th Annual International Symposium on Personal, Indoor and Mobile Radio Communications (PIMRC)*, September 2014, pp. 1109–1114.
- [YZWY10] G. Yuan, X. Zhang, W. Wang, and Y. Yang, "Carrier Aggregation for LTE-Advanced Mobile Communication Systems," *IEEE Communications Magazine*, vol. 48, no. 2, pp. 88–93, February 2010.
- [ZH07] H. J. Zhu and R. H. M. Hafez, "Scheduling Schemes for Multimedia Service in Wireless OFDM Systems," *IEEE Wireless Communications*, vol. 14, no. 5, pp. 99–105, October 2007.
- [ZT03] L. Zheng and D. N. C. Tse, "Diversity and Multiplexing: A Fundamental Tradeoff in Multiple-Antenna Channels," *IEEE Transactions on Information Theory*, vol. 49, no. 5, pp. 1073–1096, May 2003.

Curriculum Vitae

Name: Oscar Dario Ramos Cantor
 Date of birth: 15 May 1986
 Place of birth: Ibagué, Colombia

Education and training

September 2012 – May 2017 Technische Universität Darmstadt,
 Darmstadt, Germany
 Doctoral candidate

October 2009 – August 2012 Technische Universität Darmstadt,
 Darmstadt, Germany
 Master of Science in Information and Com-
 munication Engineering

February 2003 – March 2008 Universidad Nacional de Colombia,
 Bogotá, Colombia
 Bachelor of Science in Electrical Engineering

Work experience

September 2012 – August 2017 Communication Systems Group
 Technische Universität Darmstadt,
 Darmstadt, Germany
 Research assistant

September 2012 – December 2015 Telekom Innovation Laboratories
 Deutsche Telekom AG,
 Darmstadt, Germany
 External cooperator (C'MON project)

June 2011 – December 2011 Telekom Innovation Laboratories
 Deutsche Telekom AG,
 Darmstadt, Germany
 Intern

February 2008 – August 2009 Banking Association of Colombia,
 Bogotá, Colombia
 Assistant of the Presidency's adviser

Other activities

February 2011 – June 2011

Fachgebiet Multimedia Kommunikation -
KOM
Technische Universität Darmstadt,
Darmstadt, Germany
Student assistant

August 2006 – August 2007

Universidad Nacional de Colombia,
Bogotá, Colombia
Fellow monitor

Additional information

Awards and distinctions

Deutscher Akademischer Austausch Dienst
(DAAD) Scholarship
Fundación para el futuro de Colombia (COL-
FUTURO) Scholarship

Andrés Bello Award in chemistry as one of
the best regional results of state test for ad-
mission to higher education (Bachelor of Sci-
ence)

List of Publications

Conference and Journal papers

1. O. D. Ramos-Cantor, J. Belschner, G. Hegde and M. Pesavento, "Centralized Coordinated Scheduling in LTE-Advanced Networks", *EURASIP Journal on Wireless Communications and Networking*, vol. 2017:122, July 2017
2. O. D. Ramos-Cantor and M. Pesavento, "Decentralized Coordinated Scheduling with Muting in LTE-Advanced Networks", in *IEEE 18th International Workshop on Signal Processing Advances in Wireless Communications (SPAWC)*, July 2017, pp. 1-5
3. O. D. Ramos-Cantor, J. Belschner and M. Pesavento, "Improved Link Adaptation with Coordinated Scheduling in non-Fully Loaded Wireless Networks", in *IEEE 17th International Workshop on Signal Processing Advances in Wireless Communications (SPAWC)*, July 2016, pp. 1-6
4. O. D. Ramos-Cantor, M. Lossow, H. Droste, G. Kadel and M. Pesavento, "A Network Simulation Tool for User Traffic Modeling and Quality of Experience Analysis in a Hybrid Access Architecture", in *World Telecommunications Congress*, June 2014, pp. 1-6
5. O. D. Ramos-Cantor, J. Belschner and M. Pesavento, "A Cooperative Power Control Scheme for Interference Management in LTE-Advanced Based Cognitive Radio Networks", in *6th International Symposium on Communications, Control and Signal Processing (ISCCSP)*, May 2014, pp. 530-533

Additional papers

6. G. Hegde, O. D. Ramos-Cantor, Y. Cheng and M. Pesavento, "Optimal Resource Block Allocation and Muting in Heterogeneous Networks", in *IEEE 41st International Conference on Acoustics, Speech and Signal Processing (ICASSP)*, March 2016, pp. 3581-3585
7. F. Bahlke, O. D. Ramos-Cantor and M. Pesavento, "Budget Constrained Small Cell Deployment Planning for Heterogeneous LTE Networks", in *IEEE 16th International Workshop on Signal Processing Advances in Wireless Communications (SPAWC)*, June 2015, pp. 1-5
8. M. Lossow, P. Arnold, H. Droste, G. Kadel and O. D. Ramos-Cantor, "Methodology to Evaluate User Experience in non-Fully Loaded Wireless Communication Systems", in *European Wireless Conference*, May 2015, pp. 1-6
9. Q. Kuang, J. Belschner, M. Lossow, H. Droste, G. Kadel and O. D. Ramos-Cantor, "Mobility Performance of LTE-Advanced Heterogeneous Networks with Control Channel Protection", in *World Telecommunications Congress*, June 2014, pp. 1-6

Patent applications

1. J. Belschner and O. D. Ramos-Cantor, "Decentralized Scheduling Method for Mobile Networks with Bursty Traffic", Public Identifier US20170181170A1, (22.06.2017)
2. O. D. Ramos-Cantor, J. Belschner and P. Arnold, "Method and System for Coordinated Radio Resource Assignment", Public Identifier WO2016150967A1, (29.09.2016)

Erklärung laut §9 der Promotionsordnung

Ich versichere hiermit, dass ich die vorliegende Dissertation allein und nur unter Verwendung der angegebenen Literatur verfasst habe. Die Arbeit hat bisher noch nicht zu Prüfungszwecken gedient.

Darmstadt, 09. Mai 2017

